

*Influence of Tackifying Resins on Properties of Polymer Blends
employed as Hot Melt Pressure Sensitive Adhesives*

Dissertation

zur Erlangung des
Doktorgrades der Ingenieurwissenschaften (Dr.-Ing.)

der

Naturwissenschaftlichen Fakultät I – Biowissenschaften –

der Martin-Luther-Universität
Halle-Wittenberg,

vorgelegt

von Frau M. Sc. Tâmara Abboud

geb. am 19. Dezember 1981 in Ribeirao Preto, Brasilien

Halle (Saale), October 23rd, 2019

Gutachter:

1. Prof. Dr.-Ing. habil. Hans-Joachim Radusch
2. Prof. Dr. rer. nat. habil. Thomas Groth
3. Prof. Dr.-Ing. Udo Wagenknecht

Öffentliche Verteidigung: July 16th, 2020

Abstract

Resins are materials largely employed in the adhesive industry and when employed in pressure sensitive adhesives they are commonly labeled as tackifiers. There are several types of adhesives and a special group is the hot melt pressure sensitive adhesive. These materials are polymer blends of thermoplastic elastomer, tackifier and, commonly, also a plasticizer. Blends are widely employed in the industry due to their properties improvement achieved for a material but with low efforts and costs involved in their development in comparison to a new designed material. Polymer blends are generally thermodynamically immiscible but they are compatible in concern to the application behavior enabling them to be extensively employed in end-use applications. Hence, understanding the compatibility between the elastomers and the tackifiers is crucial for achieving adequate adhesive performance in pressure sensitive adhesives. The influence of chemically different tackifiers is investigated in this study in order to understand its correlation with polymer blend viscoelastic properties, morphology, surface properties and adhesive performance. The effect of temperature as a processing parameter is evaluated as well since it influences the components miscibility, blend rheology and morphology. Styrenic block copolymers are classically employed in manufacturing hot melt pressure sensitive adhesives. However, developments in elastomeric field suggest the use of poly(ethylene-co-1-octene) block copolymer as an alternative for such styrenic polymers. A comparison between both thermoplastic elastomers was conducted regarding blend viscoelastic properties, morphology, surface properties and adhesive performance. The results revealed that compatibility between the thermoplastic elastomer and the tackifier highly impacts in the investigated properties and that processing temperature showed a trend of how these properties change independent of the tackifier chemistry due to processing conditions. In summary, the impact of tackifier chemistry in the polymer blends used as hot melt pressure sensitive adhesive could be demonstrated through different levels of interaction with the polyisoprene and the polystyrene contained in the block copolymer by the methods selected as well the effect of processing temperature independent of the tackifier chemistry. Tackifier chemistry also demonstrated to be relevant when olefinic block copolymer was assessed in the blends.

Kurzfassung

Harze sind Materialien, die in hohem Maße in der Klebstoffindustrie verwendet werden. Werden diese in Haftklebstoffen verwendet, werden sie üblicherweise als Klebrigmacher bezeichnet. Es gibt verschiedene Arten von Klebstoffen, von denen eine spezielle Gruppe der Haftschnelzklebstoff ist. Diese Materialien sind Polymermischungen aus thermoplastischem Elastomer, Klebrigmacher und üblicherweise auch Weichmacher. Mischungen sind in der Industrie aufgrund möglicher Eigenschaftsverbesserungen weit verbreitet, wobei im Vergleich zu einem neu gestalteten Material nur ein geringer Aufwand und geringe Kosten für deren Entwicklung anfallen. Polymermischungen sind im Allgemeinen thermodynamisch nicht mischbar, aber sie sind hinsichtlich des Anwendungsverhaltens kompatibel, so dass sie in Endanwendungen umfassend eingesetzt werden können. Daher ist das Verständnis der Verträglichkeit zwischen den Elastomeren und den Klebrigmachern entscheidend für das Erreichen einer angemessenen Klebeleistung in Haftklebstoffen. Der Einfluss chemisch unterschiedlicher Klebrigmacher wird in dieser Studie untersucht, um die Korrelation mit den viskoelastischen Eigenschaften, der Morphologie, den Oberflächeneigenschaften und der Klebeleistung von Polymermischungen zu verstehen. Die Auswirkung der Temperatur als Verarbeitungsparameter wird ebenfalls bewertet, da sie die Mischbarkeit der Komponenten, die Mischungsrheologie und die Morphologie beeinflusst. Styrolblockcopolymer werden klassisch bei der Herstellung von Haftschnelzklebstoffen eingesetzt. Entwicklungen auf dem Gebiet der Elastomere legen aber auch die Verwendung von Poly (ethylen-co-1-octen) -Blockcopolymer als Alternative für solche Styrolpolymere nahe. Ein Vergleich zwischen beiden thermoplastischen Elastomeren wurde hinsichtlich der viskoelastischen Eigenschaften der Mischung, der Morphologie, der Oberflächeneigenschaften und der Klebeeigenschaften durchgeführt. Die Ergebnisse zeigten, dass die Verträglichkeit zwischen dem thermoplastischen Elastomer und dem Klebrigmacher die untersuchten Eigenschaften in hohem Maße beeinflusst, und dass die Verarbeitungstemperatur einen Trend zeigt, wie sich diese Eigenschaften unabhängig von der Klebrigmacherchemie aufgrund der Verarbeitungsbedingungen ändern. Zusammenfassend lässt sich feststellen, dass ein signifikanter Einfluss der Klebrigmacherchemie in den Polymermischungen, die als druckempfindlicher Schnelzklebstoff verwendet werden, mit den verwendeten Methoden nachgewiesen werden konnte, was sich durch unterschiedliche Wechselwirkungen mit dem Polyisopren und dem Polystyrol im Blockcopolymer ausdrückt. Die

Klebrigmacherchemie erwies sich auch als relevant, wenn das olefinische Blockcopolymer in den Mischungen bewertet wurde.

List of symbols and abbreviations

K_b	Boltzmann constant
γ_L^-	Electron donor (base) component of surface free energy of the liquid
γ_L^+	Electron acceptor (acid) component of surface free energy of the liquid
γ_L^{LW}	Lifshitz-van der Waals component of surface free energy of the liquid
γ_{LV}	Surface free energy of the liquid
γ_L^d	Dispersive component of surface free energy of the liquid
γ_L^p	Polar component of surface free energy of the liquid
γ_S^-	Electron donor (base) component of surface free energy of the solid
γ_S^+	Electron acceptor (acid) component of surface free energy of the solid
γ_{SL}	Interfacial energy between the solid and the liquid
γ_S^{LW}	Lifshitz-van der Waals component of surface free energy of the solid
γ_{SV}	Surface free energy of the solid
γ_S^d	Dispersive component of surface free energy of the solid
γ_S^p	Polar component of surface free energy of the solid
γ_a	Free surface energy of component a
γ_{ab}	Free surface energy of the surface or interface
γ_b	Free surface energy of component b
ϕ_A, ϕ_B	Volume fraction of polymers A and B, respectively
ΔG_m	Free energy of mixing
ΔH_m	Heat or enthalpy of mixing
ΔS_m	Entropy of mixing
AFM	Atomic force microscopy
B	Bonding term
C₁	Constant
C₂	Constant
C_a	Capillary number
D	Drop size (diameter)
D	Debonding term
DMA	Dynamic mechanical analysis

DMT	Demicellization-micellization transition
DSC	Differential scanning calorimetry
EOBC	Poly(ethylene-co-1-octene) block copolymer
EOC	Random poly(ethylene-co-1-octene) copolymer
EPDM	Ehtylene-propylene-diene polymer
G*	Complex dynamic modulus
G'	Shear storage or elastic modulus
G''	Shear loss or viscous modulus
GPC	Gel permeation chromatography
HC5	Hydrogenated C5 hydrocarbon resin
HC9	Hydrogenated C9 hydrocarbon resin
HMPSA	Hot melt pressure sensitive adhesive
HRE	Hydrogenated rosin ester resin
IR	Infrared spectroscopy
LCST	Lower critical solution temperature
LDOT	Lattice disorder-order transition
N_A, N_B	Degree of polymerization of polymers A and B
NMR	Nuclear magnetic resonance
OBC	Olefinic block copolymer
P	Tack term
P₀	Intrinsic adhesion term
PHC9	Partially hydrogenated C9 hydrocarbon resin
PLOM	Polarized light optical microscopy
PSA	Pressure sensitive adhesive
RE	Pentaerythritol rosin ester resin
RFID	Radio frequency identification
S	Spreading coefficient
SAFT	Shear adhesion failure temperature
SANS	Styrene-acrylonitrile copolymer
SAXS	Small-angle X-ray scattering
SBC	Styrenic block copolymer

SBS	Polystyrene- <i>block</i> -polybutadiene- <i>block</i> -polystyrene copolymer
SEM	Scanning electron microscopy
SEPS	Poly[styrene- <i>block</i> -(ethylene- <i>alt</i> -propylene)- <i>block</i> -styrene]
SI	Polystyrene- <i>block</i> -polyisoprene copolymer
SIS	Polystyrene- <i>block</i> -polyisoprene- <i>block</i> -polystyrene copolymer
T	Temperature
tan δ	Loss tangent or loss factor
TEM	Transmission electron microscopy
T_g	Glass transition temperature
T_g^a	Glass transition temperature of component a
T_g^b	Glass transition temperature of component b
T_g^m	Glass transition temperature of mixture
UCST	Upper critical solution temperature
W_a	Work of adhesion
WAXS	Wide-angle X-ray scattering
W_c	Work of cohesion
W_a^d	Dispersive work of adhesion
W_a^p	Polar work of adhesion
X_a	Weight fraction of component a
X_b	Weight fraction of component b
$\dot{\gamma}$	Strain rate
α	Experimentally determined coefficient
β	Experimentally determined coefficient
η	Viscosity
η_d	Viscosity of the dispersed phase
η_g	Melt viscosity at T _g
η_m	Viscosity of the matrix phase
η_r	Viscosity ratio
Θ	Contact angle
σ	Shear stress
ν	Interfacial tension coefficient

γ Surface free energy, surface tension
 χ Flory-Huggins interaction parameter

CONTENTS

1	Introduction	1
1.1	General	1
1.2	Aims of the work.....	2
2	Basics and state of the art of tackifier containing adhesives	3
2.1	Tackifying resins	3
2.1.1	C9 and hydrogenated C9 hydrocarbon resins	4
2.1.2	C5 and hydrogenated C5 hydrocarbon resins	5
2.1.3	Rosin and rosin derivatives resins.....	6
2.2	Adhesives	7
2.2.1	Styrenic block copolymers.....	9
2.2.2	Olefinic block copolymers.....	12
2.2.3	Plasticizer	15
2.3	Viscoelasticity of pressure sensitive adhesives	16
2.4	Polymer blends.....	19
2.4.1	Phase diagram and phase separation.....	21
2.4.2	Mixing and morphology of polymer blends	23
2.4.3	Polymer blends interfacial tension and compatibilization	29
2.5	Adhesion phenomenon.....	30
2.5.1	Intermolecular forces	30
2.5.2	Basic concepts of surface science	31
2.5.3	Adhesion mechanisms	34
3	Experimental.....	36
3.1	Materials.....	36
3.1.1	Tackifying resins.....	36
3.1.2	Backbone polymers.....	37
3.1.3	Oils.....	37
3.1.4	Antioxidant	37
3.2	Polymer blend preparation	37
3.2.1	Polymer blend preparation for the compatibility investigation	37
3.2.2	Preparation of hot melt pressure sensitive adhesive blends.....	38

3.2.3	Hot melt pressure sensitive adhesives blends preparation for process investigation	39
3.2.4	Hot melt pressure sensitive adhesives coating.....	39
3.3	Materials characterization and instrumentation	40
3.3.1	Dynamic mechanical analysis (DMA).....	40
3.3.2	Ring and ball softening point.....	41
3.3.3	Contact angle measurements.....	41
3.3.4	Peel adhesion strength at 180°	41
3.3.5	Shear adhesion (Holding Power)	42
3.3.6	Shear adhesion failure temperature (SAFT)	42
3.3.7	Loop tack	43
3.3.8	Brookfield viscosity	43
3.3.9	Tensile properties.....	43
3.3.10	Gel permeation chromatography (GPC)	44
3.3.11	Nuclear magnetic resonance (NMR)	44
3.3.12	Differential scanning calorimetry (DSC).....	44
3.3.13	Polarized light optical microscopy (PLOM).....	45
3.3.14	Atomic force microscopy (AFM)	45
4	Results and discussion.....	46
4.1	Compatibility investigation of the thermoplastic elastomers, tackifiers and oils used in the polymer blends of hot melt pressure sensitive adhesive models	46
4.1.1	Influence of the resins chemical structure on compatibility	46
4.1.2	Influence of resin concentration on compatibility	54
4.1.3	Influence of oil on compatibility.....	55
4.2	Influence of tackifier chemical structure and concentration on properties and performance of hot melt pressure sensitive adhesive blends.....	61
4.2.1	Influence of tackifier chemical structure and concentration on viscoelastic behavior	61
4.2.2	Influence of tackifier chemical structure on morphology.....	67
4.2.3	Influence of tackifier chemical structure on adhesion and adhesive performance .	70
4.3	Influence of processing on properties and performance of hot melt pressure sensitive adhesive blends.....	76
4.3.1	Overview.....	76

4.3.2	Influence of processing conditions on viscoelastic behavior.....	77
4.3.3	Influence of processing conditions on tensile strength.....	79
4.3.4	Influence of processing conditions on morphology.....	79
4.3.5	Influence of processing conditions on adhesion and adhesive performance	81
4.4	Influence of backbone polymer on properties and performance of hot melt pressure sensitive adhesive blends	84
4.4.1	Viscoelastic properties of poly(ethylene-co-1-octene) block copolymer based blends as hot melt pressure sensitive adhesives	85
4.4.2	Morphology of poly(ethylene-co-1-octene) block copolymer based blends as hot melt pressure sensitive adhesives	88
4.4.3	Adhesion and adhesive performance of poly(ethylene-co-1-octene) block copolymer based blends as hot melt pressure sensitive adhesives	91
5	Assessment of future applications of new poly(ethylene-co-1-octene) block copolymer based pressure sensitive adhesives.....	94
6	Summary and outlook.....	98
	References.....	101
	Appendices.....	115

1 Introduction

1.1 General

Resin is a very broad term for defining organic substances with similar physical properties nevertheless with very different chemical composition.¹ They find application in many different fields, as in paints and casting but in this work, their application as tackifiers is investigated. Tackifier is a special designation for resins when their purpose is to bring stickiness to a material. It finds its utilization in a broad range of applications from adhesives for bookbinding to more demanding applications such as in transdermal drug delivery system.^{2,3}

Pressure sensitive adhesive (PSA) is a very unique type of adhesive in which the bond is formed at room temperature with either no, or light pressure.⁴ Besides, PSAs constantly present some stickiness degree. Historically, PSAs are composed of natural rubber and tackifier. Later on, with the development of the styrenic block copolymers (SBCs), these polymers are frequently applied for preparing PSAs. They present better resistance against oxidation. Recently, another class of polymer, referred as olefinic block copolymer (OBC) is also reported in the literature as a suitable polymer class for preparing hot melt pressure sensitive adhesive (HMPSA) blends but only few works have been conducted using poly(ethylene-1-octene) block copolymer (EOBC) in HMPSA mixtures.^{5,6}

PSAs can be prepared by different processes, as solvent-based, water-based or hot melt. The hot melt technology is an environmentally friendly process, since no solvent is involved since only heat is needed to bring the adhesive to a molten state in order to be mixed and further coated.⁷ Hot melt pressure sensitive adhesives are polymer blends. Blending is a common and simple practice applied in the industry in order to achieve improved final product properties to design a completely new polymer. However, due to thermodynamic reasons, miscibility among polymers is not something always possible to be achieved. In most cases, a compatible blend is obtained. A compatible polymer blend is an immiscible polymer blend, which exhibits macroscopically uniform characteristics generating satisfactory engineering properties.⁸ The compatibility among the materials in the polymer blend influences the blend morphology, which will affect its final properties. The chemical nature of each blend's component is of great relevance on the blend

compatibility level to be obtained. On the other hand, the blend morphology is also affected by processing parameters (i.e. time, temperature, shear rate), rheological properties of the materials, components concentration and interfacial properties.

There are several works in the literature investigating properties of PSAs obtained when a solvent based system is used for mixing the components as well as coating.⁹⁻¹¹ Yet, not so many studies investigate such properties using melt mixing equipment as well as melt coating.¹² Even fewer report the influence of melt mixing process parameters on PSA's properties. Therefore, this work is more precisely focused on polymer blends prepared using tackifying resins for application in a very specific class of adhesives which are pressure sensitive adhesives processed using the hot melt technology. It also explores the use of poly(ethylene-1-octene) block copolymer as part of hot melt pressure sensitive adhesive's blend. This work intends to answer the following goals described below.

1.2 Aims of the work

The aim of this work is to investigate polymer blends comprising tackifying resins differing in their chemical structures as model blends of hot melt pressure sensitive adhesives. Based on this, the following goals are part of this present study:

- Compatibility evaluation of the materials employed in the blends by means of dynamic mechanical analysis method.
- Investigating the effect of tackifying resins according to their types: hydrogenated and partially hydrogenated C9 hydrocarbon resins, hydrogenated C5 hydrocarbon resin, pentaerythritol rosin ester and hydrogenated rosin ester when blended with Poly(styrene-*block*-isoprene-*block*-styrene) and paraffinic oil utilized as HMPSA models.
- Studying the tackifier concentration effect on blends' viscoelastic properties, adhesion and adhesive performance.
- Assessment of temperature influence as a process parameter on blends viscoelastic properties, morphology, adhesion and adhesive performance.
- Formulating morphology-property relationships among HMPSA blends based on poly(ethylene-co-1-octene) block copolymers and comparing them to those based on classical poly(styrene-*block*-isoprene-*block*-styrene), having the selected tackifying resins as component of such polymer blends.

2 Basics and state of the art of tackifier containing adhesives

2.1 Tackifying resins

Resin is a very broad term for defining organic substances with similar physical properties nevertheless with very different chemical composition.¹ They have low molecular weight, ranging from about 300 g/mol to 2000 g/mol, are amorphous material and have high glass transition temperature, typically ranging from 0 °C to 70 °C.¹³

Resins can be classified according to many criteria. ISO 4618/3 categorizes them by their origin as natural or synthetic resins. Natural are those formed from vegetable or animal sources, whilst synthetic are those made from controlled chemical reactions. Further possible categorizations are based on physical aspect, reaction mechanism of their synthesis, intended modification of product properties and application. A very comprehensive natural resin is the rosin (colophony or pine resin) as well as its derivatives. From synthetic sources, the petroleum based resin is one of the most important groups. A sub-classification organizes them as C5, C9, DCPD and pure monomer. These terms are commonly used because they relate to the raw material origin. C5 and C9 hydrocarbon resins are so denominated because they are polymerized using monomers which are present in the C5 and C9 distilled oil streams. The monomers utilized for polymerizing them, comprise respectively five and nine carbon atoms per monomer.

Here, according to its application, a resin can be defined as a tackifier or a tackifying resin. It is added to an elastomer to improve tack and wettability.¹² Some important characteristics of tackifiers are their polarity, since it influences the miscibility in the polymer blend, as well as their softening point and molecular weight.^{14,15} The softening point is a well-known and a property of practical importance for selecting a resin. It is the temperature at which the material flows under load while being heated.

A lot of resin types have been applied as tackifiers in PSAs formulations, e.g. gum rosin, wood rosin, tall oil rosin, polymerized rosin, hydrogenated rosin, pentaerythritol wood rosin, glycerine-hydrogenated rosin, pentaerythritol-highly stabilized rosin, hydroabietyl phthalate, olefin, cycloaliphatic hydrogenated olefin, aliphatic petroleum hydrocarbon, modified aromatic hydrocarbon, dicyclopentadiene, mixed olefin, alpha and beta pinene,

terpene, alpha-methyl styrene-vinyl toluene, alpha-methyl styrene, styrene, terpene phenolic and coumarone-indene.¹⁶

2.1.1 C9 and hydrogenated C9 hydrocarbon resins

The C9 hydrocarbon resins are obtained by co-polymerizing mainly the monomers indene, alpha-methyl styrene and vinyltoluene. Their structures are displayed in figure 1. The term “C9” has its origin in the nine carbon atoms found in the monomers used for the copolymerization.

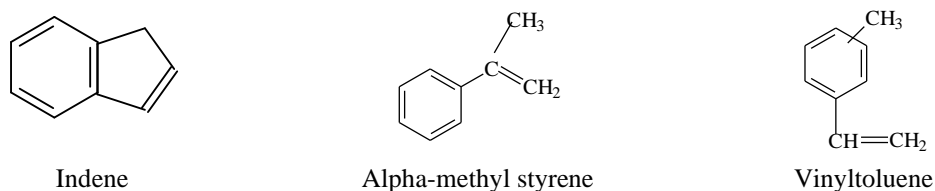


Figure 1: Structure of main monomers used for polymerizing C9 hydrocarbon resins.

Figure 2 shows the structure of the polymerized C9 hydrocarbon resin and it can be seen that the material contains many unsaturations in the final structure, which gives high aromaticity and polar character to the final material.

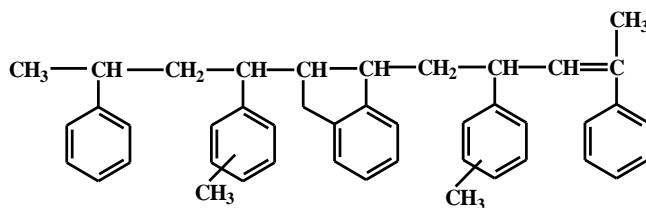


Figure 2: Representation of an ideal structure of C9 hydrocarbon resin.

The hydrogenation process of such resins is also practiced giving rise to the so-called hydrogenated C9 hydrocarbon resins.^{17,18} The structure of the hydrogenated material is shown in figure 3. It can be seen that aromatic rings are no longer present while alicyclic rings as well as saturated bonds can be seen in the polymer backbone chain. The hydrogenation reaction can be interrupted generating to the so-called partially hydrogenated C9 hydrocarbon resin.¹⁷

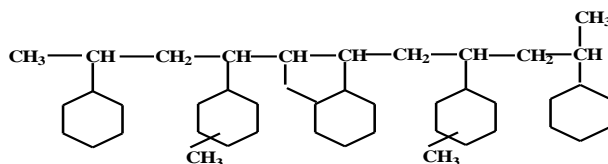


Figure 3: Representation of and ideal fully hydrogenated C9 hydrocarbon resin.

Kim et al.¹⁸ investigated the hydrogenation degree effect of aromatic hydrocarbon resins in pressure sensitive adhesives based on styrene-*block*-butadiene-*block*-styrene copolymer (SBS) and styrene-*block*-isoprene-*block*-styrene copolymer (SIS). In their first work, by measuring probe tack of a PSA based on SBS, they demonstrated that better results were achieved when the interactions between resin and polybutadiene were at the highest level, namely when the hydrogenation degree of the hydrogenated hydrocarbon resin was 70 %. In a following work, they concluded that the miscibility between tackifier and either end-block or midblock of the block copolymer correlated to viscoelastic properties of the adhesive. At lower hydrogenation degree, there was an association of hydrocarbon resin and styrenic part and the influence in tack was negligible. When there was an association with midblock, the tack properties were affected. For SBS, an optimum hydrogenation degree of 70 % was identified, while for SIS, the hydrogenation degree increased as the tack properties increased.¹⁷

2.1.2 C5 and hydrogenated C5 hydrocarbon resins

The main monomers which are co-polymerized for producing C5 hydrocarbon resins are 2-methyl-1,3-butadiene, 1,3-pentadiene, 2-methyl-2-butene and cyclopentadiene; and their structures are displayed in figure 4.

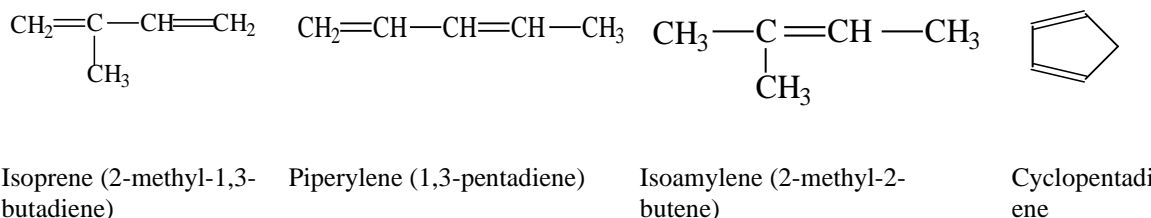


Figure 4: Structure of the main monomers used to prepare C5 hydrocarbon resins.

C5 hydrocarbon resins can also be hydrogenated and a possible structure is shown in figure 5.

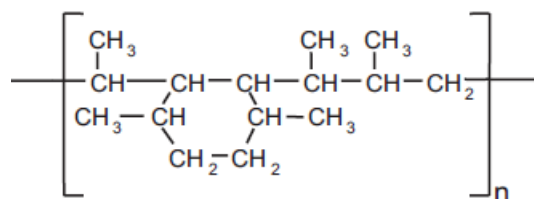


Figure 5: Representation of ideal structure of aliphatic C5 hydrocarbon resin.¹⁹

2.1.3 Rosin and rosin derivatives resins

Rosin and its derivatives are historically employed as tackifiers. They are obtained from wood by-product such as gum rosin, wood rosin and tall oil.²⁰ Gum rosin is obtained by tapping pine trees to extract pine oleoresin. The purification method, which involves filtration and water washing, and a distillation process, generates gum rosin. Rosin is composed of several different acids. The main component of rosin is the abietic acid (figure 6).²¹

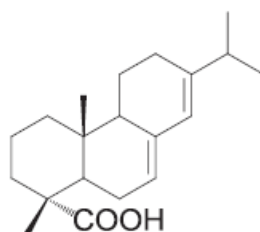


Figure 6: Structure representation of abietic acid, which is the main component of rosin resins.²⁰

Since its structure contains conjugated double bonds and a carboxyl acid, many further chemical reactions are possible giving rise to the so-called rosin derivatives.²² Among these derivatives are the rosin esters, which can further undergo a hydrogenation reaction. For the esterification reaction, mainly the alcohols glycerol and pentaerythritol are utilized to produce resins with appropriated softening points.²³ Figure 7 presents the structure of pentaerythritol rosin ester resin.

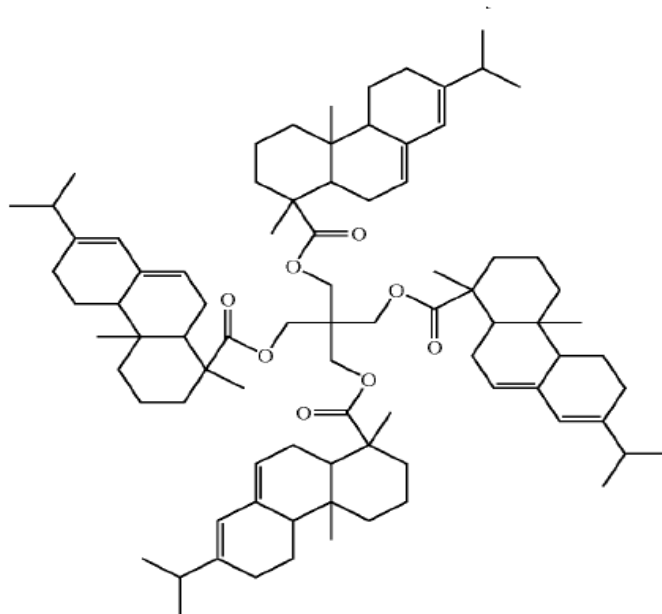


Figure 7: Structure representation of pentaerythritol rosin ester resin.²⁴

The effect of tackifiers in hot melt pressure sensitive adhesives has been studied by several researchers.^{12-14,17,18,25}

2.2 Adhesives

Adhesives are materials that promote the adhesion between two different bodies.²⁶ Some typical raw materials employed for adhesives are vinyls, natural and synthetic rubber, acrylics and modified acrylics, polyurethane, block copolymers, epoxy, silicones, polysulfide, urea-formaldehyde, polyolefin, polyester and polyamide.^{23,27-29}

Adhesives can be classified according to their production, application and their adhesion effect.²⁷ The solvent-borne system involves dissolving the adhesive and applying the solution on the substrate. The viscosity is low enough to promote a good contact between the adhesive and the substrate. Afterwards, the solvent evaporates and the bond is established.⁵ The water-borne systems are similar to the solvent-borne one; however, water is utilized to prepare the solutions. This leads to a much more ecologically friendly technology.³⁰ There are also the so-called reactive systems that can be further subdivided into one and two component systems. A chemical reaction takes place and it results in the cure of the adhesives. The one-component systems are cured, for example, by heat or UV-radiation. The two-component systems are cured via a chemical reaction which starts by the time the two components are mixed.³¹

Hot melts are adhesives that require heat to be melted. The material is applied in the molten state and the bond is formed as soon as it cools.³² There are several advantages since only heat is needed for processability, for example, costs reduction, environment friendly material and elimination of further steps in process.^{12,33} The present work is focused on this system.

Adhesives can also be classified according to their application or market segments²⁷, as listed below:

- Construction or building
- Transportation
- Woodworking
- Bookbinding
- Converting/ Packaging
- Disposables
- Flexible Packaging/ Laminates
- Footwear
- Pressure Sensitive Adhesives
- Consumer Adhesives
- Product Assembly
- Others

Pressure sensitive adhesives are able to establish a bond between two materials at room temperature with either no or light pressure.⁴ They are permanently tacky at room temperature, i.e. despite no chemical reactions or temperature variations, they are able to establish a bond.^{34,35} Their performance as adhesives is commonly measured by means of tackiness, peel strength and shear resistance.¹⁶ The output of the tackiness measurement is the force required to debond a PSA, which was virtually bonded without pressure. Peel strength measurements provide, as result, the force needed to remove a PSA which was previously bonded under standard conditions (i.e. properly brought into contact with the substrate). Shear resistance measurements provide either the temperature or the time interval in which the adhesive fails (i.e. debonds) under shear forces.³⁶ All the mentioned tests were conducted under standard conditions since parameters such as geometry, coat thickness, testing rate, room temperature, humidity, substrate, substrate contaminations, bonding pressure can all impact on the bonding and debonding processes since they are not only related to bulk properties but also to surface characteristics.

Zosel³⁷ investigated the influence of viscoelastic properties and surface properties on tack and on adhesion by means of adhesive failure energy by studying different polymers. He observed that the mean molecular weight between entanglements, M_e , influenced the

failure energy. Besides, a maximum in tackiness was obtained about 50 °C to 70 °C above the polymer glass transition temperature. Further on, he investigated the surface properties by determining the surface tension between the adherents and adherends involved. He could observe that there was a relation amid work of adhesion and adhesive failure energy. An important condition for high tack is the wetting of the adherent by the adhesive.

Historically, natural rubber has been utilized in pressure sensitive adhesives but, due to its tendency to oxidize, other materials were also introduced.^{23,38} Nowadays, together with natural rubber, acrylics and block copolymer based pressure sensitive adhesives are the most common types.^{23,39}

2.2.1 Styrenic block copolymers

Block copolymers, especially styrenic block copolymers as polystyrene-*block*-polyisoprene-*block*-polystyrene copolymer (figure 8) and polystyrene-*block*-polybutadiene-*block*-polystyrene copolymer, do not have to be chemically crosslinked to perform well as PSAs due to their physical crosslinks. Nevertheless, they need to be formulated with resins, which are substances with a low molecular weight and high glass transition temperature, in a process called tackification.⁴⁰ Hence, the resins employed for formulating PSAs are called tackifiers. The main purpose of them is to bring tackiness to the PSAs.

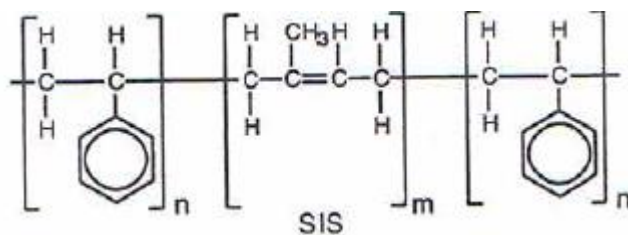


Figure 8: Polystyrene-*block*-polyisoprene-*block*-polystyrene copolymer chemical structure.⁴¹

From a chemical point of view, styrenic block copolymers are composed of polystyrene, which has a glass transition temperature of about 100 °C and an elastomer for which, in the case of polyisoprene, a glass transition temperature of about -60 °C is typically observed. Further on, polystyrene and polyisoprene have different solubility parameter values. In summary, due to these relevant differences regarding the copolymers chemistry, the

chemical nature of the other components used for preparing hot melt pressure sensitive adhesive blends will influence the blends properties differently according to the affinity of each material to polystyrene and polyisoprene segments.

Figure 9 schematically represents the morphology of SIS. The red lines represent polyisoprene segments connecting the polystyrene domains. Blue lines represent polyisoprene segments, which form loops and green lines represent polyisoprene segments ending in the polyisoprene phase.⁴²

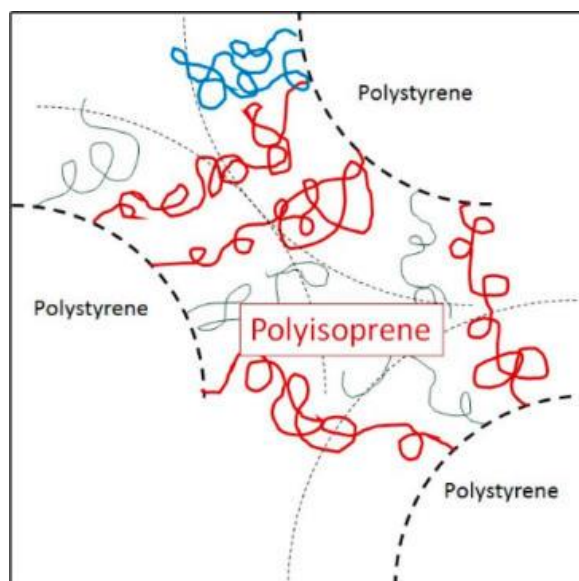


Figure 9: Proposed morphological model for Kraton D1161, where polystyrene domains are connected by polyisoprene segments (red lines). Blue lines represent polyisoprene segments forming loops and green lines are polyisoprene segments ending in the matrix phase.⁴²

The elastomeric polymer segments form the continuous phase chemically connected to the glassy phase formed by polystyrene, which organizes itself in domains acting as physical cross-links.⁴³

The morphology of such styrene block copolymers can be modified depending on different factors, such as the volume fraction of each copolymer.^{44,45} The morphology is a result of system phase behavior, which tries to minimize the system Gibbs free energy according to thermodynamic principles.^{46,47} This same principle acts in a polymer blend. However, it must be highlighted that in a block copolymer, the species are covalently bonded.⁴⁸ The isoprene and the styrene blocks forming the SIS triblock copolymer employed in this work

were completely amorphous. The different blocks presented phase separation already in the melt and finally, with glass transition of polystyrene, microphase separation occurred, resulting in elastomeric and glassy domains formation.

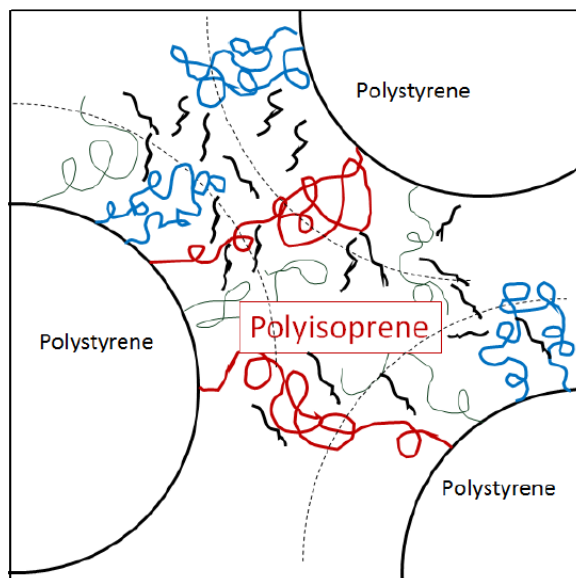


Figure 10: Morphological model of a blend comprising SIS and tackifier. Black segments represent tackifier molecules, while red, green and blue represent segments of polyisoprene segments.⁴⁹

Figure 10 represents a morphological model for a blend containing SIS and tackifier proposed by Dixit.⁴⁹ He reported that up to a concentration of 30 wt% tackifier, the mobility of polyisoprene chains were increased since the tackifier acted as a solvent for polyisoprene. However, as of a concentration of 50 wt% tackifier, the tackifier molecules could saturate the available free volume and swell the Polyisoprene-rich phase. Consequently, the polystyrene domains were pushed apart.

Very often polystyrene-*block*-polyisoprene-*block*-polystyrene copolymers of commercial grades used in PSAs are blends of triblock and polystyrene-*block*-polyisoprene copolymers. Several works have been published dealing with this topic.^{9,50-54} The morphology of triblock copolymers of type ABA and diblock copolymers AB are very different since ABA type is able to tether both ends of the polymer, which leads to possible physical crosslinks formation and very different mechanical properties.^{55,56} Blending ABA triblock copolymers/AB diblock copolymers results in a decrease in the number of

physical crosslinks.⁴² From a practical point of view, for PSAs application, pure SIS is too hard and shows lower interfacial adhesion.⁹

Commercially available polymers may have a styrene content varying from 15 wt% to 50 wt% and diblock content varying from 0 wt% to 100 wt%. Sasaki et al.⁹ studied systems of SIS/SI containing 15 wt% of styrene and varying the SI content from 0 wt% to 100 wt%. They could observe that mechanical and adhesion properties were significantly influenced by the SI amount while the morphology was not strongly affected. The polystyrene domains were still dispersed in the polyisoprene matrix; however, fracture stress significantly decreased as the diblock amount increased in the blend and the molecular mobility increased with it.

2.2.2 Olefinic block copolymers

Another kind of elastomeric copolymer not yet extensively used in PSAs is olefinic block copolymer of ethylene and octene.⁵⁷⁻⁵⁹ It is produced by a technique called chain shuttling polymerization.⁶⁰⁻⁶² In comparison to the random poly(ethylene-co-1-octene) copolymer (EOC), the Poly(ethylene-co-1-octene) block copolymer presents a higher operating temperature, improved scratch resistance as well as crystallization rates when compared to EOC.⁶³

Polyethylene is one the most produced polymers. It refers to multiple polymers and copolymers derived from ethylene.^{63,64} Polyethylene is a semi-crystalline polymer,⁶⁵ which means that due to some level of ordering in its structure, it is able to crystallize. Crystalline materials present a first-order transition, i.e. melting; the enthalpy of fusion or melting can be determined for such constituents.⁶⁶ Some models were proposed to explain the structure of crystalline polymers: the fringed micelle model, the folded chain model and the switchboard model.⁶⁷ Kinetics of crystallization is an important field of study which deals with the crystals growth rate.⁶⁸ The final structure of a semi-crystalline block copolymer cooling from the melt shall be determined by two concomitant processes which are crystallization kinetics and thermodynamic microphase separation.⁶⁹

From a chemical point of view, the segments forming the poly(ethylene-co-1-octene) are synthesized only from olefinic monomers. The ethylene segments in the copolymer chain have similar solubility parameters as the octene segments, i.e. are non-polar. Therefore,

when preparing a blend containing poly(ethylene-co-1-octene) and a tackifier, similar chemical affinity occurs between the tackifier and either the ethylene segments in the copolymer chain or the octene segments in it. From a morphological point of view, poly(ethylene-co-1-octene) is a semi-crystalline material able to develop higher or lower crystalline degree according to the polymerization parameters (e.g. comonomer amount). Figure 11 depicts a scheme for classifying block poly(ethylene-co-1-octene) copolymers.

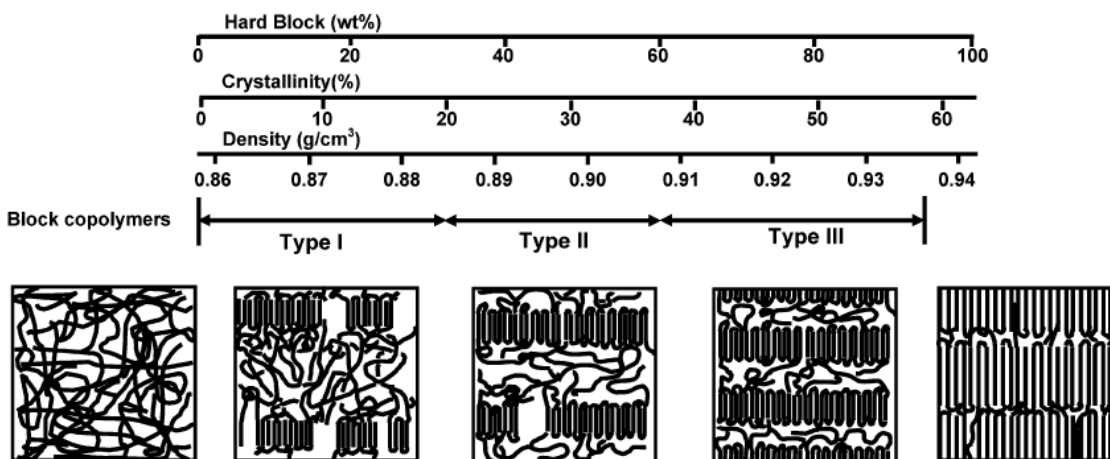


Figure 11: Classification schemes of poly(ethylene-co-1-octene) (adapted from ref.⁶¹).

The EOBC material used in this present work can be classified as Type I. i.e., a low crystalline degree as well as low percentage of the so called “hard” block. Hard blocks are copolymer segments containing high amount of ethylene and low amount of octene and soft blocks are those containing high concentration of octene. The morphology of the hard and soft blocks develops due to a crystallization process and it is originated from a miscible melt, which has the soft non-crystallizable blocks expelled to the interlamellar region.⁶¹ Auriemma et al.^{57,58} investigated the structure of EOBCs in a nanometric length scale as well as the structure-property relationship. Their proposed model of the structural organization is schematically shown in figure 12.

Auriemma et al.⁵⁷ reported that EOBCs are multiblock copolymers, which have a statistical distribution of block length and of blockiness. They present a non-uniform constitution of the chains. They concluded that the mechanical properties are highly influenced by the average molecular mass of soft and hard blocks as well as the number of blocks/chain (blockiness), even for materials with the same octene concentration.

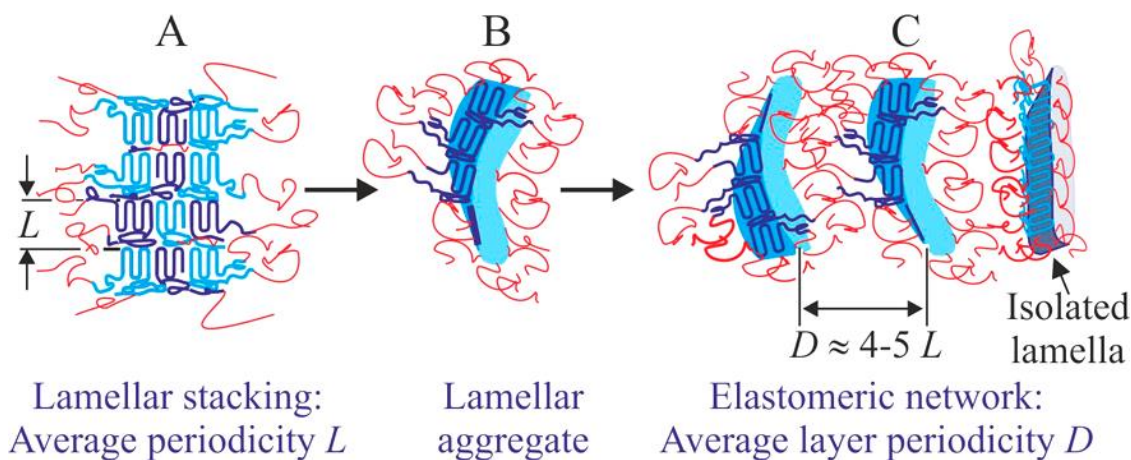


Figure 12: Structural organization representation of the EOBC chains arrangement in the solid state. The thick blue lines represent the hard blocks while the thin red lines represent the soft blocks.⁵⁸

Wang et al.⁶¹ characterized poly(ethylene-co-1-octene) block copolymers according to their thermal behavior, dynamic mechanical relaxation, crystal structure and solid state morphology. Sharp melting and crystallization peaks were reported. By increasing the comonomer amount, the heat of melting decreased proportionally to the hard block content while the melting peak temperature of the hard block decreased only slightly. There was an evident phase separation of hard and soft segments concluded by the linear decrease of crystallinity as the amount of soft segment increased.⁷⁰ Hard and soft blocks could be proved to be present since evident alpha- and beta- relaxations were identified. The morphology was reported to consist of space-filling spherulites and radially oriented lamellae.⁶¹

As Shan et al.⁷¹ highlighted in their work, the reason for the high melting point temperature measured for olefinic block copolymer is due to the presence of the semi-crystalline hard segments which form spherulitic domains. In contrast, in SBCs the glassy domains formed by polystyrene are the responsible for providing a high glass transition temperature in the styrene based part of the copolymer.

Among the applications, block poly(ethylene-co-1-octene) can be used for production of elastic films as thermoplastic elastomers since flexibility, heat resistance and elastic recovery properties are present. Their performance is comparable to styrenic block copolymers. Raja et al.⁶ evaluated blends of olefin block copolymers and amorphous

polyolefin polymers. As a compatibilizer, hydrocarbon resins were used. Nevertheless, they acted as tackifying resins as well for the pressure sensitive adhesive. The influence of resins on the morphology and viscoelastic behavior of the blends was investigated. Among the results, it was established that ternary phase morphology was observed when highly aromatic unsaturated hydrocarbon resins were used. The system employing saturated aliphatic hydrocarbon resins presented better miscibility. Further on, they could obtain satisfactory results when employing blends composed of poly(ethylene-co-1-octene) block copolymers and hydrocarbon resins tackifiers for preparing hot melt pressure sensitive adhesives for application in diapers.⁷²

2.2.3 Plasticizer

Plasticizers are small molecules which have the function of softening a polymer. They are able to accomplish it because they lower the glass transition temperature of a polymer or reduce the crystallinity or melting temperature, in the case of crystalline polymer.⁴³ A plasticizer is also employed in formulating PSAs since it improves the processability, ease polymer chains mobility and reduce product costs. Regarding the molecular structure, it decreases the polymer glass transition temperature and reduces crystallinity and melting temperature.⁴³ It has been reported that the morphology of block copolymers was influenced by the oil since it affects segmental interactions.⁷³ In investigated systems, containing polystyrene-*block*-polybutadiene-*block*-polystyrene copolymer mixed with mineral oil, the oil was preferentially located in the butadiene phase and the SBS morphology was affected. It was concluded that the polystyrene cylindrical domains evolve to spherical domains in a rubbery matrix.⁷⁴ Laurer et al.⁷⁵ studied the influence of aliphatic oils in the morphology and rheology of SIS and poly[styrene-*block*-(ethylene-*alt*-propylene)-*block*-styrene] (SEPS) copolymers. It was concluded that the compatibility between the oil and the elastomeric block (midblock) influences the copolymer morphology and plays an important role in the final properties of the copolymer leading to differences in the application. Galán et al.⁷⁶ studied ternary systems based on SBS, aliphatic and aromatic tackifiers as well as paraffinic and naphthenic oils employed as hot melt pressure sensitive adhesives. The effect of oil and tackifier regarding chemical nature as well as concentration were correlated to peel strength and tackiness by thermal transition measurements and viscoelastic relaxations determination. They observed that the

loss factor peak temperature increased as the paraffinic character of the oil decreased. However, the storage modulus at around 20 °C was basically the same for all the different mixtures produced with different oils. Higher tackiness was observed for those mixtures with higher loss factor peak temperature. Although not investigated by Galán et al.⁷⁶, they state that aromatic oils are not preferred for HMPSAs blends because they interact with the polystyrene domains causing a severe strength reduction.

2.3 Viscoelasticity of pressure sensitive adhesives

Three kinds of deformation can be identified in a body when a force is applied: elastic deformation, which is characterized by an instantaneous response and completely reversible; viscous deformation, in which the response is time-dependent and irreversible, and finally the viscoelastic deformation, which is time-dependent and reversible. Polymeric materials behave in all described ways at the same time depending on temperature and deformation rate, i.e. frequency or time.

By conducting an oscillatory measurement, for example by varying the temperature and keeping the frequency measurement constant, in a polymeric material, four important zones and transition regions can be identified.⁷⁷ Below glass transition temperature, the polymer chains are frozen and it can be assumed that no segmental movement occurs; this is the glassy zone. As the material is heated up, segments of the molecule are able to move because there is an increase in free volume, i.e. the space available for a molecule to develop internal movements. Thus, local motions, bending, stretching of the main chain and side groups become active characterizing the β and γ transitions (or secondary relaxations). These transitions are associated to mechanical properties of the material in the glassy state. The next transition zone is the α -transition. For amorphous polymers it corresponds to the glass transition temperature (T_g) where the storage modulus decreases by some orders of magnitude. The glass transition is a second-order transition and not a first-order transition as crystallization.⁴³ The mechanical properties of the polymer change severely when it goes from the glassy to the rubbery state. Therefore it is important to determine the operating range of the polymer according to this transition. As the temperature continues to increase, the rubbery plateau is reached where there is high mobility of the whole chains. The length of this zone is dependent on the molecular weight between the entanglements or cross-links. Finally, the melting takes place ending on the

terminal zone. At this point, the material is completely molten and there is a strong relation to the molecular weight of the polymer. Chemically cross-linked materials do not present this region since such state is characterized by slippage of molecules through each other, however due to chemical bonds between the chains it cannot occur.

The glass transition has not yet been explained on a molecular basis and several theories exist attempting to explain it. A commonly accepted theory is the free volume theory.^{78,79} The principle can be explained based on the presence of holes or vacant positions. The polymer segment can move towards a new position only if this new position is vacant, in other words, only in the case free volume being available. The free volume temperature related and at a certain temperature (about -52 °C of the polymer T_g), no free volume is available. Based on Doolittle`s work, Williams, Landel and Ferry developed a relation, which correlates viscosity and temperature for polymeric materials (equation 1):

$$\mathbf{Log} \left(\frac{\eta}{\eta_g} \right) = - \frac{C_1(T-T_g)}{C_2+(T-T_g)} \quad (1)$$

Where: η is the melt viscosity, η_g is the melt viscosity at T_g , T is temperature and T_g is glass transition temperature. C_1 and C_2 are constants which values for linear amorphous polymers are 17.44 and 51.6.

An important and vastly studied topic is the correlation between viscoelastic properties of blends used as adhesives and their performance.^{22,28,29,35,77,80-96} The immense amount of work dealing with viscoelastic properties correlation to adhesive performance is probably due to high relevance and application of the results as a predictive tool when designing adhesives, especially pressure sensitive adhesives. As further explained in this study, the work of adhesion is certainly a property which contributes to the adhesive performance (for example, for peel strength). However, the order of magnitude of the viscoelastic properties contribution, especially when considering the adhesion separation process, is much bigger than the work of adhesion magnitude. It is worth to remind that the work of adhesion is not less important than the viscoelastic properties, especially in the bond formation. Additionally, the dissipation energy (loss factor) effect in the debonding process is extremely relevant for the adhesive performance.

Aubrey et al.¹¹ investigated the viscoelastic behavior of natural rubber and two different tackifiers, namely poly(beta-pinene) and pentaerythritol ester of hydrogenated rosin. They observed that both of them change the viscoelastic behavior of natural rubber in a similar manner. In a frequency sweep measurement, there was a reduction of rubbery plateau width; the transition zone shifted to lower frequencies while the terminal zone shifted to higher ones. Chu et al.^{13,14,97} explored the viscoelastic properties of a rubber and resin mixture regarding resin structure, molecular weight and concentration. It was observed that when there was compatibility between rubber and resin, there was a significant shift in loss factor peak and a decrease of storage modulus in the rubbery plateau region. Even for expected compatible systems, there was a superior limit for resin molecular weight. Otherwise the system would become incompatible. A prediction of the blend loss factor peak temperature and rubbery plateau modulus can be achieved due to a relationship based on plateau modulus of the pure rubber and of one typical blend. Kraus et al.⁹⁸ developed a criterion for calculating compatibility of the polydiene midblock and resins since it is known that a satisfactory compatibility between midblock and resin is essential for tackiness in pressure sensitive adhesives.

Figure 13 illustrates a typical viscoelastic behavior of a hot melt pressure sensitive adhesive.

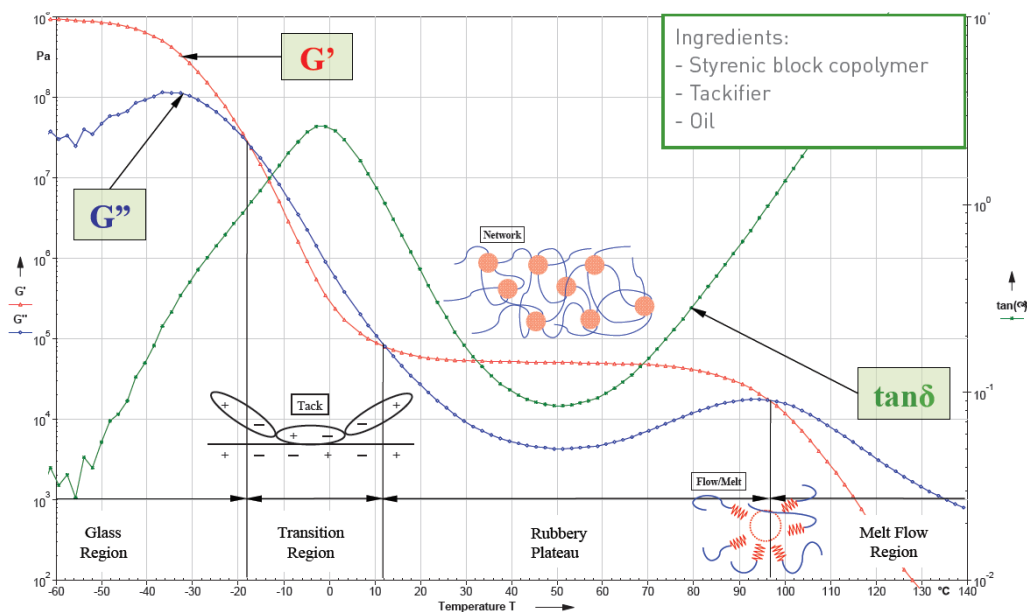


Figure 13: Typical viscoelastic behavior for a hot melt pressure sensitive adhesive .⁹⁹

2.4 Polymer blends

Mixing different polymers together in order to achieve certain mechanical, thermal, optical and other properties, which are not possible by using a single material is a common practice.^{82,100–103} Despite being very convenient, such practice is not always so simple or even possible due to components miscibility.¹⁰⁴ A miscible polymeric blend is characterized as a polymeric mixture obeying the thermodynamic criteria of miscibility. An immiscible polymeric blend is defined when more than one phase is observed. Thermodynamic relationships also describe immiscibility.^{8,105} A compatible polymer blend is said of an immiscible polymer blend, which exhibits macroscopically uniform properties generating satisfactory engineering properties.⁸

Miscibility in polymer blends can be measured by several methods which can be direct or indirect.⁷ A classical direct method is the turbidity measurement. It consists in preparing the blends, heating up / cooling down the system temperature in order to go from a one phase system to a phase separated system. The temperature at which phase separation occurs is the so-called cloud point. The identification of this point can be done by several methods from naked eyes to much more precise and sophisticated ones.¹⁰⁶

An indirect and commonly used method for determining miscibility (or better saying compatibility) in polymer blends is by measuring the glass transition temperature. The method is controversial and it cannot be understood as a measure of thermodynamic miscibility of the blend but as a measure of state of dispersion.¹⁰⁶ To consider that a blend is compatible by glass transition temperature approach is to consider that the domain size is between 2 and 15 nm.¹⁰⁶

Fox equation (Equation 2) is one of the empirical formulas proposed to calculate the glass transition temperature of a mixture.¹⁰⁷

$$\frac{1}{T_g^m} = \frac{X_a}{T_g^a} + \frac{X_b}{T_g^b} \quad (2)$$

Where: T_g^m is the glass transition temperature of the mixture containing component a and b; T_g^a is the glass transition temperature of component a; T_g^b is the glass transition temperature of component b; X_a and X_b are the weight fraction of components a and b, respectively.

The thermodynamic relationship, which rules the phase behavior of a substance mixture, is given by equation 3:¹⁰⁸

$$\Delta G_m = \Delta H_m - T\Delta S_m \quad (3)$$

Where: ΔG_m is the free energy of mixing; ΔH_m is the heat or enthalpy of mixing; T is temperature and ΔS_m is the entropy of mixing. In order to achieve a miscible system, free energy of mixing must assume a negative value, $\Delta G_m < 0$.

For low molecular weight materials, the contribution of the combinatorial entropy of mixing is an important factor, which is generally significant. Hence, the requirement of a negative value for the free energy of mixing is fulfilled, leading to many miscible mixtures of them.

For polymers, most mixtures are not miscible. It was experimentally observed that the combinatorial entropy of mixing, which considers mole fraction, is not valid. In this case, the theory developed independently by Flory¹⁰⁹ and Huggins^{110,111} is applied for polymer mixtures. The Flory-Huggins theory was developed for a binary polymer mixture assuming an incompressible lattice. It is expressed as described in equation 4.⁴⁸

$$\frac{\Delta G_m}{K_b T} = \frac{\phi_A}{N_A} \ln \phi_A + \frac{\phi_B}{N_B} \ln \phi_B + \phi_A \phi_B \chi \quad (4)$$

Where: K_b is the Boltzmann constant; ϕ_A and ϕ_B are the volume fraction of polymers A and B, respectively; N_A and N_B are the degree of polymerization of polymers A and B, respectively; T is the temperature and χ is the Flory-Huggins interaction parameter. The temperature dependence of the interaction parameter, χ , can be expressed as shown in equation 5.^{48,44}

$$\chi_{AB} = \alpha T^{-1} + \beta \quad (5)$$

Where α and β are experimentally determined coefficients.

Specific interactions, as hydrogen bonds, acid-base, dipole-dipole, are important in polymer blends since they give a considerable contribution to the enthalpy of mixing.⁴⁸

The concept of solubility parameter first developed by Hildebrand and Scott to characterize liquids interactions can also be applied to polymers.¹¹²⁻¹¹⁴

Based on the explanations exposed above, it is important to consider the phase behavior, i.e. miscibility and compatibility, among the tackifiers and polymers used when preparing PSAs.¹¹⁵ As mentioned before, styrenic block copolymers are generally employed in PSAs blends and the compatibility between each block and the tackifiers employed may be different. Aromatic tackifying resins have a solubility parameter similar to polystyrene, which means that the compatibility between them is favored in comparison to the compatibility expected between aromatic resins and the polyisoprene block. The polystyrene phase would thus be plasticized by the resin giving a negative effect to the adhesive performance.²³

2.4.1 Phase diagram and phase separation

Theoretical phase diagrams for polymer blends are illustrated in figure 14 (a). For the case of a so-called upper critical solution temperature (UCST), a phase-separated system is found as the temperature decreases. For the so-called lower critical solution temperature (LCST), phase separation occurs as the temperature is increased. It is not always that a phase diagram can be drawn for polymer blends.

Phase separation occurs by two different mechanisms, namely nucleation and growth and spinodal decomposition. Nucleation and growth occur in the metastable region. First, a nucleus must be formed and only when the necessary energy barrier for creating a nucleus with a critical radius value is reached, the particle will continue to grow. Its main characteristic is that a constant concentration is maintained and the particle increases in size with time.¹⁰⁵ Spinodal decomposition occurs in the unstable region due to composition fluctuations and is characterized by a varying composition as time increases.¹⁰⁵ The morphology developed for each phase separation mechanism is schematically represented in figure 14 (b) for a binary homopolymer blend. It can be seen that a more ordered structure is found for the nucleation and growth mechanism. Both systems evolve to coarser structures in an attempt to reduce interfacial energy by decreasing interfacial area.⁴⁸

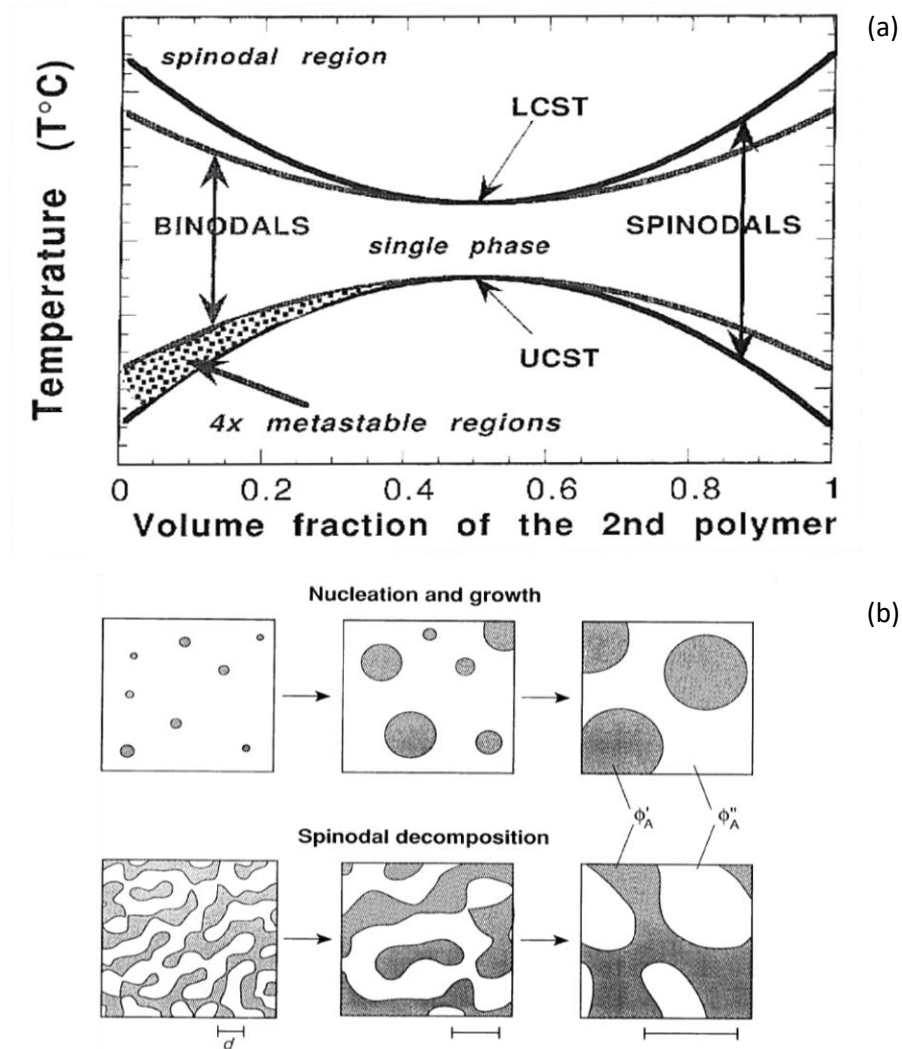


Figure 14: (a) Theoretical phase diagram for polymer blends (adapted from reference¹¹⁶) and (b) blend morphology development for nucleation and growth and spinodal decomposition mechanisms.⁴⁸

Kawahara et al.¹¹⁷ studied phase separation of poly(vinyl ethylene-co-1,4-butadiene) blended with rosin resin in solvent based system and correlated it with adhesive property. They reported that the system exhibited LCST behavior and could detect spinodal decomposition. In conclusion, they predicted that the adhesive property was related to the phase dispersed structure induced by jumping temperature over the LCST. Han et al.¹¹⁸ studied phase equilibria of solvent based PSA containing SIS and an end-block-associating tackifier having two different molecular weight tackifier grades analyzed by means of hot stage microscopy and light scattering method. They could observe that for blends containing low molecular weight tackifier, no macrophase separation occurred for

concentrations ranging between 10 % and 90 % of tackifier (when analyzed by means of light scattering method). For higher molecular weight tackifier containing blends, they observed macrophase separation at about 200 °C for 50:50 blends. They could not construct a phase diagram for this sample since thermal degradation of the blend occurred at the needed temperature. By this study, firstly, it could be observed that it is not always possible to construct a phase diagram for a polymeric mixture. Secondly, the influence of molecular weight on blend morphology could also be investigated. Finally, as concluded by the authors, an end-block associating resin which forms separate domains (macrophase separation) in the blend does not improve adhesive performance in HMPSAs.

Crystallinity and crystallization kinetics of the semi-crystalline polymer are influenced by the blend's phase behavior. This effect is more pronounced in miscible systems and it is dependent on the glass transition temperature of the added polymer.¹⁰⁵

2.4.2 Mixing and morphology of polymer blends

The structural organization of polymers and their blends is an important factor affecting their final and application properties.¹¹⁹ By studying particle size and distribution as well as dispersion and agglomeration of one component in another by creating a blend can be very helpful in understanding their final properties.^{120,121} A wide spread method for studying morphology is via microscopy¹²² and a summary of the methods suitability is presented in figure 15 regarding domain size range.

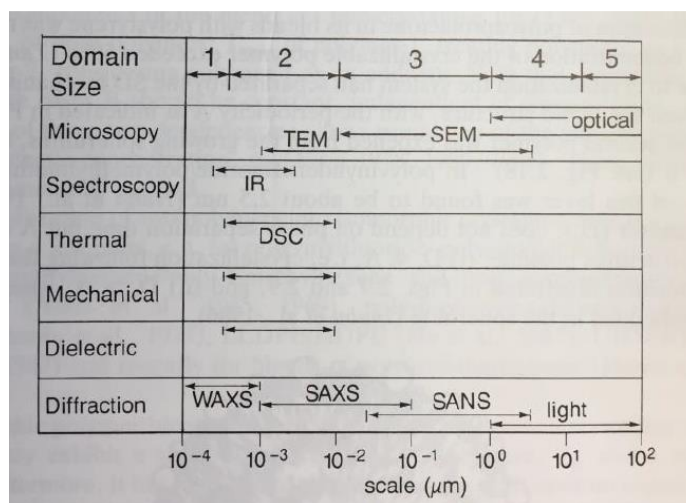


Figure 15: Experimental methods for studying polymer and polymer blends morphology.¹⁰⁶

The preparation of a polymer blend can be carried out by several methods. Among them, there is the solvent mixing method, which consists in finding a common solvent for the polymers involved.¹⁰⁵ Another possibility is the mechanical melt mixing.¹²³ Both methods may be employed for preparing pressure sensitive adhesives.

Polymer blends preparation considerably affects their morphology. For example, preparing a blend by solvent or by mechanical mixing may lead to a miscible or immiscible system. As exposed, miscibility is achieved when certain thermodynamics conditions are fulfilled, thus such behavior is explained by equilibrium process.¹⁰⁶ Mechanical blending can be conducted in different types of equipment and the equipment's relevance in the final blend morphology will depend whether the blend is miscible or immiscible. For immiscible blends, the phase separation occurs too fast leading to an irrelevant influence on the blend morphology regarding the type of mixing equipment and it is explained due to a balance between drop break up and coalescence.^{106,124}

The PSAs coating method is also an important process step, which can also be conducted by preparing a solution or by melting it. O'Connor and Macosko¹² analyzed the effect of both methods in coating PSAs which were prepared by melt mixing and they observed that the adhesive properties measured by peel, tack and shear holding power were superior regarding peel and tack for hot-melt coated adhesives while shear holding power were superior for solvent coated adhesives. They demonstrated that these differences arose from disparities in the degree of physical crosslinking and composition gradients within the solvent coatings. Since the cooling rate in hot-melt coated adhesives is very high, a microstructure that is further from the equilibrium is obtained for them in comparison to the solvent coated adhesives.

When blending polymers in the molten state, two mechanisms can be identified when a dispersed and a matrix phase are present. The dispersive mixing, which is responsible for breaking the particles into smaller ones and the distributive mixing, which is responsible for spreading the particles uniformly through the matrix, homogenizing it. Dispersive mixing involves application of stress and distributive mixing involves application of strain.¹¹⁶ Figure 16 schematically shows such mechanisms in order to illustrate the difference on how they affect the mixture. Such mechanisms occur simultaneously in a

mixture along with a third mechanism acting against the mixture of the components which is the coalescence process.

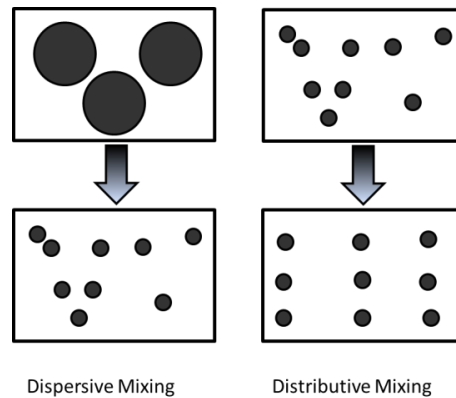


Figure 16: Theoretical illustration of dispersive mixing and distributive mixing.

The capillary number is a way of understanding whether dispersive or distributive mixing is predominant. It is the ratio between shear stress and interfacial tension and it is expressed in equation 6:

$$C_a = \frac{\sigma d}{v} \quad (6)$$

Where C_a is the capillary number, σ is the shear stress, d is the drop diameter and v is the interfacial tension coefficient. The shear stress in the mixing process acts in a way of deforming the drops whilst the interfacial tension (of the dispersed and matrix phases in the blend) acts against it. If shear stress dominates, droplet breaking becomes possible, i.e. dispersive mixing occurs. If interfacial stress dominates, distributive mixing occurs.¹²⁵ The viscosity ratio of the components is mainly responsible for the distributive mixing and it is described in equation 7:

$$\eta_r = \frac{\eta_d}{\eta_m} \quad (7)$$

Where: η_r is the viscosity ratio; η_d is the viscosity of the dispersed phase and η_m is the viscosity of the matrix phase.

Only if $\eta_m > \eta_d$ the deformation of the dispersed particles, i.e. distributive mixing, becomes possible.

It is important to remind that for polymer melt, two factors are affecting its viscosity, namely shear rate and temperature, which relation was shown by WLF equation (eq. 1). At lower processing temperature, dispersive mixing is favored since a condition of higher viscosity exists. At higher processing temperature, distributive mixing is aided since lower viscosity is achieved. In polymer blends, it is more difficult to mix a system composed of a high viscosity dispersed phase to a low viscosity matrix phase than the other way around.¹²⁶ Morphology development of polymer blends in the molten state as well as their final morphology depend on factors like rheological properties of the components (melt elasticity, viscosity ratio), components concentration, interfacial properties and processing parameters (time, temperature, shear rate).^{125,127–129}

Since the study of polymer blends is challenging, a common approach is to study known systems.¹⁰⁶ For miscible polymer blends, a model considering a mixture of low molecular weight liquids (solutions) and a model considering mixtures of polymer fractions or homologous polymer blends are used. For studying immiscible polymer blends, suspensions, emulsions and block copolymers systems are used respectively for blends with a low concentration of a more viscous polymer, a general model of blends with dispersed morphology and for well compatibilized blends and/or blends with co-continuous morphology. In these systems, a common effect is observed, i.e. they all present flow induced morphological changes.

Blends flow induced morphology is not simple to be investigated for real mechanical mixing devices due to the complex deformation field which occurs during processing. Generally many assumptions are made and systems having either shear or extensional deformation field are used for such researches.¹³⁰

Taylor¹³¹ studied the viscosity of a fluid containing small drops of another fluid. For this, he started from the expression of the viscosity of a fluid containing solid spheres in suspension. Since liquid spheres are able to deform, the expression would be very complex and he proposed some assumptions to his system. The expression is valid, if the surface tension is high enough to keep the drops shape approximately spherical. He also proposed an expression for the limit of the size which such drops can achieve in the other fluid. The drops tend to break up when either the rate of distortion of the fluid or the radius of the drop is large enough.

Wu¹³² proposed an extension of Taylor's criterion for the critical condition for drop break to the case of a viscoelastic drop in a viscoelastic matrix. He could show the interfacial and rheological effects on of the dispersed phase particle size in his systems by showing a parallel of the interfacial tension between the blends components and the correlation with viscosity ratio of them. He stated that particle size in a blend can be effectively controlled by adjusting interfacial tension of the blend components (equation 8).

$$d = \frac{4v\eta_r^{\pm 0.84}}{\dot{\gamma}\eta} \quad (8)$$

If $\eta_r > 1$; +0.84 ; If $\eta_r < 1$; -0.84

Where: d is the drop size; v is the interfacial tension; η_r is the viscosity ratio; $\dot{\gamma}$ is the strain rate and η is the viscosity.

Sundararaj et al.¹²⁴ investigated the equilibrium between drop break up and coalescence in polymer blends by studying the effects of compatibilizers and reactive polymers. The influence of shear rate was also discussed and a critical shear rate for finest dispersion was proposed. Contrary from the expected behavior of a decrease in particle size as shear rate increased, for polymer blends, i.e. viscoelastic materials, the matrix viscosity decreased and the drop elasticity increased meaning that a higher resistance against deformation occurred.

Favis et al.¹³³ studied the effect of viscosity ratio and torque ratio on the morphology of polypropylene and polycarbonate blends during processing. The size and size distribution of the minor phase in polymer blends have significant impact on final properties, e.g. impact strength. In polymer-polymer systems, differently from composite, the minor phase particles are deformable. Hence, controlling the parameters influencing particles deformation will have an impact on blend morphology and consequently in its final properties. Some of these parameters are composition, viscosity ratio and interfacial tension. Favis et al.¹³³ concluded that the viscosity ratio has an influence on the morphology of the dispersed phase. A minimum particle size was observed for a viscosity ratio at ca. 0.15 and the existence of upper and lower limits for viscosity ratio at which the deformation became too difficult.

Sundararaj et al.¹³⁴ studied the morphology development of polymer blends in a twin screw-extruder. They concluded that the break up mechanism involved was the sheeting mechanism and most of the significant morphology changes occurred during the melting and softening stages (for twin screw-extruder within 30 mm of the first point of melting and for batch mixer within 1 min). They reported that other authors also concluded that the major portion of the morphology development occurred during the pellets melting.

Some authors studied the blends morphology of the main polymer in pressure sensitive adhesives, however in solvent based systems. Nakamura et al.^{19,10} studied the effect of tackifier compatibility with the backbone polymer, namely SIS, for solvent based systems. Tackifiers with satisfactory compatibility with the polyisoprene block, showed influence in adhesion as its content increased. At low content, it was assumed it was dissolved in the polyisoprene matrix and as its content increased, agglomerates formed improving cohesion strength. Slightly differences were observed with the tackifier content increase when an end-block compatible resin was used. From small-angle X-ray scattering (SAXS) measurements, it was determined that the agglomerates were about 15 nm apart from each other. In the end-block compatible resin's system, the agglomerates were not confirmed.

Hock¹³⁵ studied the morphology of solvent borne pressure sensitive adhesives by electron microscopy on mixtures of rubber (either natural or synthetic) and natural resins. He attempted to correlate tack results with morphology observed in micrographs and he observed an optimal tack value for systems containing between 40 wt% and 60 wt% of resins. He described a two-phase system in such concentration, which he attributed to one consisting of low molecular weight rubber dissolved in resin being responsible for tack due to its more viscous-like character and one consisting of rubber (matrix) saturated with resin and being responsible to the adhesive strength.

Nakamura et al.¹³⁶ evaluated the influence of rosin based tackifier concentration and molecular weight on blends based on polyacrylic block copolymer in solvent based systems. When employing tackifier with a molecular weight of 2160 g/mol, they observed micrometer-sized agglomerates while for tackifiers with a molecular weight between 650 g/mol and 890 g/mol nanometer sized agglomerates were identified. Besides, they could also identify that compatibility decreases with molecular weight increase. By these observations combined with tack and peel strength measurements as well as viscoelastic

properties, they noticed better adhesive performance for blend containing tackifier of 890 g/mol (intermediate compatibility), hence they assumed that the nanometer sized tackifier agglomerates was connected to such performance.

Dixit⁴⁹ studied the microphase separation kinetics of pressure sensitive adhesive blends comprising commercial SIS and commercial C5 aliphatic tackifier (Piccotac 1095) by means of SAXS and rheology. He could acknowledge a decrease in the extent of ordering of polystyrene domains and from 30 wt% tackifier on, no ordering was identified for polystyrene, remaining in a liquid-like disordered state because as the tackifier amount increased, lattice disorder-order transition (LDOT), i.e. order-disorder transition assigned to the breakdown of the body-centered cubic-ordered polystyrene domains and demicellization-micellization transition (DMT), i.e. dissolution of the polystyrene spheres in the polyisoprene matrix, were reduced. The ordering process is dictated by two competing effects, namely thermodynamic driving force and polymer chain mobility. Polystyrene chain mobility is reduced as the amount of tackifier increases. Further on Dixit⁴⁹ investigated the effect of tackifier compatibility with the polystyrene block in a commercial styrene-(isoprene-co-butadiene)-styrene copolymer in this blend phase behavior. He could observe different transition temperatures for a given blend composition but containing different tackifiers. Dixit highlighted that the impact of processing temperature and final blend morphology on the adhesive properties of the blends has not yet been studied and an attempt to cover this topic is done in the present study for the systems encompassed here.

2.4.3 Polymer blends interfacial tension and compatibilization

Compatibilization of polymer blends is a common technique applied to improve blends final properties when they are immiscible or even incompatible.^{137,138} When adding a compatibilizer, which acts on the surface of the polymers, the interfacial tension between them is decreased leading to a lower free energy state of the system.^{139,140} A better contact between the polymers is achieved, leading to wetting. Hence, it can be stated that compatibilizer is a kind of surfactant in polymer blends. Blends containing block copolymers are frequently studied due to the important application as compatibilizer, as long as the block compositions are equal or similar to the components of the blend.^{141,105} In Sundararaj's et al.¹²⁴ work, they point out that diblock copolymers used as compatibilizers

contribute to interfacial tension reduction in polymer blends but they mainly play a role to the decrease of particles coalescence in mechanical mixed blends.

Harkins spreading coefficient (S) can be used to evaluate if a liquid will spread on the other, or whether component A will wet component B spontaneously or not.^{142,143} For positive values of the coefficient, a spontaneous process occurs. The background for this spreading coefficient is based on surface thermodynamics. The expression to estimate, if b spreads upon a, is described in equation 9:

$$S = \gamma_a - \gamma_b - \gamma_{ab} \quad (9)$$

Where S is the spreading coefficient, γ_a is the free surface energy of component a, γ_b free surface energy of component b and γ_{ab} is the free surface energy of the surface or interface.

Based on Dupré's equation, the spreading coefficient can be written in terms of work of adhesion (W_a) and cohesion (W_c) (equation 10):

$$S = W_a - W_c \quad (10)$$

Thus, spontaneous spreading occurs if the adhesion between a and b is larger than the cohesion of the component to be spread.

2.5 Adhesion phenomenon

Adhesion can be defined in a macroscopic level as the work transferred from one body to the other after the formation of an interface between them; and in a microscopic level as the molecular forces resisting separation as soon as an interface is established.¹⁴⁴ The adhesion phenomenon is very complex and there are many theories proposed to explain the mechanism of adhesion.¹⁴⁵

2.5.1 Intermolecular forces

The intermolecular forces involved in adhesion are the fundamental forces that hold together atoms and molecules.¹⁴⁵

Electrostatic forces act when atoms or molecules with opposite electrical charges interact. In the same manner, they repel each other when they have equal electrical charges.¹⁴⁶ Electrostatic forces are crucial to the formation of ionic bonds.

Van der Waals forces are all those deviating from the perfect gas law. These interactions are further classified as dipole-dipole interactions, dipole-induced dipole interactions and dispersion forces (or London forces).

Dipole-dipole interactions. Electrons can be unevenly distributed in a molecule due to the different electronegativity of the existing atoms. Such molecules are known as dipoles.

Dipole-induced dipole interactions. Molecules with symmetrical distribution can develop a dipole moment due to the interaction with a dipole.

Dispersion forces. Given that there is the probability that the electrons in an atom or molecule are all in one side of the atom or molecule in a moment in an atom or molecule with symmetrical distribution, there is the possibility of an instantaneous dipole being created. The dispersion forces are weak but they appear in every material and are crucial for polymeric materials.

Interactions through electron pair sharing. They comprise covalent bonding, which is formed when molecules share a pair of electrons from their external layer.

Acid-base interactions are part of the so-called donor-acceptor interactions. According to the definition for Lewis acid-base reactions, Lewis acids are those that are electron deficient and Lewis bases are those that have an unbounded electron pair.²³

Repulsive forces. When the atoms or molecules come too close, a repulsive force acts. This force is of a very short range.

In systems where no chemical reaction occurs, intermolecular dispersion forces are very important for the adhesion. Such highly localized intermolecular dispersion forces between different phases result in a physical bonding.^{26,147}

2.5.2 Basic concepts of surface science

Some basic concepts relating to surface science are necessary to be introduced prior to explaining some proposed theories of adhesion.

Surface tension is the resistance to the deformation of the surface of a liquid.¹⁴⁵ It can also be defined as the necessary work to generate a new area in the liquid. This concept does not apply for solids, thus surface energy concept is used. Surface free energy can be

defined as the necessary energy to form a unit area of new surface, or the necessary energy to move a molecule from the bulk to the surface.¹⁴⁸ Surface tension and surface energy are numerically identical for liquids.¹⁴⁹

A bond between two bodies is properly formed when they come into intimate contact with each other. The ability of a material to act so can be described as wettability. Wetting is achieved when the substrate has a higher surface energy than the adhesive.^{37,150}

The thermodynamic work of adhesion is the work required to separate the unit area of two bodies in contact. It can be expressed by Dupré's equation¹⁵¹ (equation 11):

$$W_a = \gamma_{SV} + \gamma_{LV} - \gamma_{SL} \quad (11)$$

Where: W_a is the thermodynamic work of adhesion; γ_{SV} is the surface free energy of the solid; γ_{LV} is the surface free energy of the liquid; γ_{SL} is the interfacial energy between the solid and the liquid. This equation considers that only reversible work is done during the separation of the bodies. Thus, energy dissipated during the breaking process is not considered.¹⁵¹ Surface free energy/ tension can be simply determined for liquids, however, it is not possible to be directly determined for solids. A common approach to overcome this limitation is to determine the contact angle between a solid and a liquid. A drop lying on a perfectly smooth solid surface in thermodynamic equilibrium is schematically shown in figure 17:

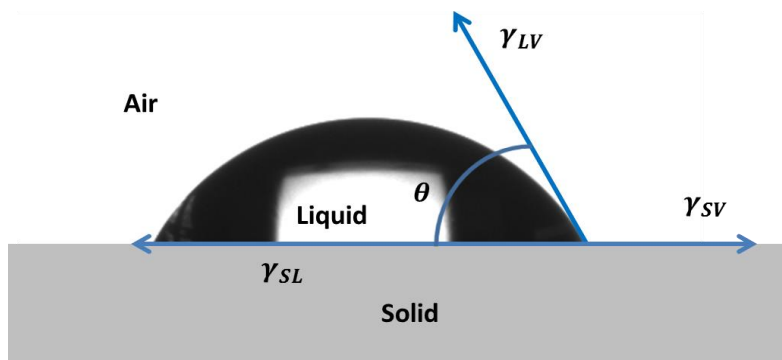


Figure 17: Representation of a drop of a known surface tension lying in equilibrium on a solid surface to measure the solid surface energy by applying Young's equation.

Young's equation (equation 12) demonstrates a correlation among surface free energy of the solid, liquid and vapor for such a drop:

$$\gamma_{SL} = \gamma_{SV} + \gamma_{LV}\cos\theta \quad (12)$$

Where: θ is the contact angle for the solid, liquid and vapor phase.

If equation (12) is substituted in equation (11), work of adhesion can be written as:

$$W_a = \gamma_{LV}(1 + \cos\theta) \quad (13)$$

Equation 13 is known as Young-Dupré equation and the work of adhesion can be determined by simply measuring the liquid surface tension and the contact angle θ .

Contact angle analysis is a very simple, fast and inexpensive method for determining the work of adhesion.¹⁵² However, it should be noticed the existence of contact angle hysteresis due to surface roughness and non-homogeneous surface chemistry.

Several theories have been proposed to determine the thermodynamic work of adhesion and surface free energy. Some of them are presented here.

- a) *Fowkes theory*: Fowkes proposed in his work that the total surface tension can be separated into 2 components for the surface free energy. The first component being the dispersive force, which embraces all the London forces. The second one being the polar force component, which includes short-range non-dispersive forces such as hydrogen bonding.¹⁵³ Surface free energy and work of adhesion, according to Fowkes work, are described in equation 14 and 15, respectively.

$$\gamma_{SL} = \gamma_S + \gamma_L - 2\sqrt{\gamma_S^d \gamma_L^d} \quad (14)$$

$$W_a = W_a^d + W_a^p \quad (15)$$

Since Fowkes considered only dispersive component, the model can be applied particularly for simple systems.

- b) *Geometric mean theory (OWRK)*: Further development was done based on Fowkes theory and the geometric mean theory was proposed considering also the contribution of the polar term, as described in equation 16.¹⁵⁴

$$\gamma_L(1 + \cos\theta) = 2\sqrt{\gamma_S^d\gamma_L^d} + 2\sqrt{\gamma_S^p\gamma_L^p} \quad (16)$$

This theory is also known as OWRK since their authors are Owen, Wendt, Rabel and Kaelbe.¹⁵⁵

- c) *Acid-base theory (Van Oss, Good and Chaudhury)*: Van Oss and Good proposed an equation, and later extended by themselves and Chaudhury, where the polar component is described in terms of acid-base interactions in order to consider the chemical nature of the phases (equation 17).¹⁵⁶

$$\gamma_L(1 + \cos\theta) = 2\sqrt{\gamma_S^{LW}\gamma_L^{LW}} + 2\sqrt{\gamma_S^+\gamma_L^-} + 2\sqrt{\gamma_S^-\gamma_L^+} \quad (17)$$

2.5.3 Adhesion mechanisms

The adhesion mechanisms or theories were proposed to try to explain the adhesion phenomenon based on the intermolecular forces.^{144,148} Since it is a complex and interdisciplinary subject, there is no unified theory explaining adhesion phenomena. Some of the mechanisms currently proposed are briefly explained in this chapter.

Thermodynamic adhesion mechanism. The thermodynamic adhesion mechanism relates to an equilibrium process at the interface for good adhesion to occur. It is accepted by many authors.^{26,151,153,157–160}

Mechanical interlocking. The mechanical interlocking mechanism is based on the fact that the adhesive keys in the substrate due to its roughness, porosity and surface irregularities.¹⁴⁸

Some authors stated that it should not be considered as a theory explaining adhesion phenomena itself, but as a contribution to it, since molecular level aspects are not considered.^{148,153}

Weak boundary layer. If a weak boundary layer is formed in the bond, an adhesive will not act properly, displaying a lower cohesive strength.²³ Bikerman proposed that, due to the presence of a low cohesive strength material, a weakness zone is formed between the adhesive and the adherend. When a force is applied, the bond rupture will occur in this

zone.¹⁶¹ Consequently, an adhesive will act properly, if such weak boundary layer is absent.

Electrostatic theory of adhesion. This theory proposes that the adhesive strength between two materials bonded exists due to opposite electrical charges interacting. An interface between an electropositive material layer and an electronegative material layer is formed.^{23,148,153}

Diffusion theory of adhesion. The diffusion adhesion theory explains that the adhesion between two materials occurs due to the molecular diffusion between them, if they are miscible and enough molecular mobility exists. It can be described by Fick's law. It is generally difficult to explain adhesion in polymers, since they are generally immiscible. An example where this theory may apply is on welding of polymers.¹⁴⁸

Molecular bonding (or chemical bonding) theory. Molecular bonding is broadly accepted and it considers the intermolecular forces between adhesive and substrate, e.g. Van der Waals forces.

In the adhesive systems investigated, no chemical reaction is involved. Thus, secondary valence forces are crucial in such systems.

The addition of tackifying resins to the polymer in the blend affects their morphology. Resins are relatively small molecules which are able to improve the polymer chains segments mobility. Thus, improved intimate contact of the adhesive and the substrate is achieved and adhesion is promoted. The surface energy of the polymer is reduced when tackifying resins are added. However, it only occurs if there is a certain degree of chemical affinity between the resin and the polymer chain segments.

3 Experimental

3.1 Materials

3.1.1 Tackifying resins

Hydrogenated C9 hydrocarbon resin (Arkon P-100) and partially hydrogenated C9 hydrocarbon resin (Arkon M-100) were provided by Arakawa Europe GmbH, Böhlen, Germany. Pentaerythritol rosin ester resin (Pensel GA 100) and hydrogenated rosin ester resin (Pinecrystal KE-311) were provided by Arakawa Chemical Industries, Ltd, Osaka, Japan. Hydrogenated C5 hydrocarbon resin (Eastotac H-100L) was produced by Eastman Chemical Company, Kingsport, USA. Properties of the resins used in the present work are shown in table 1.

Table 1: Properties of resins employed in the polymer blends.

Code	Comm. Name	Classification acc. to origin/process	R&B Soft. Point ^a	T _g ^b	M _w ^c	M _n ^c	Aromaticity ^d	Surf. Ener. dispe. ^e	Surf. Ener. Polar ^e	Surf. Ener. Total ^e
			°C	°C	g Mol ⁻¹	g Mol ⁻¹	%	mN/m	mN/m	mN/m
HC9	Arkon P-100	Hydrogenated C9 hydrocarbon resin	102	48	930	530	2.9	39.2	0.7	39.9
PHC9	Arkon M-100	Partially hydrogenated C9 hydrocarbon resin	101	48	935	535	6.1	39.6	1.5	41.1
HC5	Eastotac H-100L	Hydrogenated C5 hydrocarbon resin	103	42	930	380	0.9	40.6	0.4	41.0
RE	Pensel GA 100	Pentaerythritol rosin ester resin	104	58	1130	700	5.0	41.3	1.4	42.7
HRE	Pinecrystal KE311	Hydrogenated rosin ester resin	96	53	730	700	5.5	41.2	1.6	42.8

^a Ring & ball softening point determined as described in 3.3.2.

^b Glass transition temperature determined as described in 3.3.12.

^c Molecular weight determined as described in 3.3.10.

^d Aromaticity determined as described in 3.3.11.

^e Surface energy disperse, polar and total determined as described in 3.3.3.

3.1.2 Backbone polymers

Poly(styrene-*block*-isoprene-*block*-styrene) Kraton™ D1161PT (Kraton Polymers LLC, Houston, USA) with 15 wt% styrene and 19 wt% Polystyrene-*block*-polyisoprene copolymer diblock was used.^{15,162}

Poly(ethylene-co-1-octene) block copolymer from Infuse™ type (Dow Chemical Company, Midland, USA) was used as well. Properties of the polymers are shown in table 2.

Table 2: Properties of copolymers used in the blends.

Polymer	T _g (elast. part) ^a (°C)	T _m (crystal. part) ^b (°C)	Diblock ¹⁵ (wt%)	Styrene ¹⁵ (wt%)	Surface Energy disper. ^c (mN/m)	Surface Energy polar ^c (mN/m)	Surface Energy total ^c (mN/m)
SIS	-60	-	19	15	29.3	3.8	33.1
EOBC	-62	123	-	-	24.1	1.6	25.7

^a Glass transition temperature determined as described in 3.3.12.

^b Melting temperature determined as described in 3.3.12.

^c Surface energy disperse, polar and total determined as described in 3.3.3.

3.1.3 Oils

Paraffinic oil (Shell Deutschland Oil GmbH, Hamburg, Germany) with a kinematic viscosity of 108 mm²/s at 40 °C and a refractive index of 1.478 at 20 °C (manufacturer literature) and naphthenic oil with a kinematic viscosity of 129 mm²/s at 40 °C and a refractive index of 1.495 at 20 °C (manufacturer literature) (Shell Deutschland Oil GmbH, Hamburg, Germany) were used.

3.1.4 Antioxidant

4,6-bis((octylthiomethyl)-o-cresol), Irganox 1520 produced by BASF (Ludwigshafen, Germany) was used as antioxidant.

3.2 Polymer blend preparation

3.2.1 Polymer blend preparation for the compatibility investigation

The samples were prepared in metal beakers containing a total of 100 g of materials. They were mixed using a stirrer at 50 rpm RW 28 W (Janke & Kunkel, VWR International GmbH, Darmstadt, Germany) for 40 min at 170 °C. For compatibility study between styrenic block copolymer and resins, samples containing 20 / 30 / 50 / 70 parts by weight

of SIS, 80 / 70 / 50 / 30 parts by weight of resin were prepared. In order to reduce thermal degradation, 1 part by weight of anti-oxidant was used. For compatibility study between olefinic block copolymer polymer and resins, blends were prepared containing 50 parts by weight of EOBC and 50 parts by weight of resin. Here, also 1 part by weight of anti-oxidant was added.

Resins used were hydrogenated C9 hydrocarbon resin (*I. HC9*), partially hydrogenated C9 hydrocarbon resin (*II. PHC9*), hydrogenated C5 hydrocarbon resin (*III. HC5*), pentaerythritol rosin ester resin (*IV. RE*) and hydrogenated rosin ester resin (*V. HRE*). A comprehensive table of the formulations prepared for compatibility investigation of base polymers and tackifiers is disclosed in appendix A, table A-1.

For compatibility study between polymers and oil blends comprising 80 wt% SIS and 19 wt% oil as well as 80 wt% EOBC and 19 wt% oil were prepared. Paraffinic and naphthenic oils were used. 1 wt% anti-oxidant was added. A comprehensive table of the formulations prepared for compatibility investigation of base polymer and oils is disclosed in appendix A, table A-2.

For compatibility study between oil and resins 30 parts by weight of paraffinic oil and 70 parts by weight of resins were prepared. The employed resins were hydrogenated C9 hydrocarbon resin (*I. HC9*), partially hydrogenated C9 hydrocarbon resin (*II. PHC9*), hydrogenated C5 hydrocarbon resin (*III. HC5*), pentaerythritol rosin ester resin (*IV. RE*) and hydrogenated rosin ester resin (*HRE*). 1 part by weight of anti-oxidant was added. A comprehensive table of the formulations prepared for compatibility investigation of tackifiers and oil is disclosed in appendix A, table A-3.

3.2.2 Preparation of hot melt pressure sensitive adhesive blends

The blends intended to be hot melt pressure sensitive adhesives models were prepared using a laboratory kneader LUK 1.0 (Werner & Pfleiderer, Stuttgart, Germany) with sigma blades operating at 55 rpm. The set temperatures ranged from 180 °C to 190 °C, which corresponds to a final internal temperature of 149 °C and 155 °C, depending on the processed polymer. The total mixing time was 80 minutes. The samples comprised SIS in three concentrations (64 wt% / 25 wt% / 16 wt%), resins in three concentrations (16 wt% / 55 wt% / 64 wt%), 19 wt% paraffinic oil and 1 wt% anti-oxidant. For the investigation of

EOBC effect the samples comprised 25 wt% poly(ethylene-co-1-octene), 55 wt% resin, 19 wt% paraffinic oil and 1 wt% anti-oxidant. In both cases the resins used were: hydrogenated C9 hydrocarbon resin, partially hydrogenated C9 hydrocarbon resin, hydrogenated C5 hydrocarbon resin, pentaerythritol rosin ester resin and hydrogenated rosin ester resin. Details are displayed in appendix A, table A-4.

3.2.3 Hot melt pressure sensitive adhesives blends preparation for process investigation

The blends intended to be hot melt pressure sensitive adhesives models for investigating process effects were also blended using a laboratory kneader LUK 1.0 (Werner & Pfleiderer, Stuttgart, Germany) with sigma blades. The same blend recipe was prepared two times: one time the set internal temperature was 140 °C and the second time the set internal temperature was 165 °C both at 55 rpm. The total mixing time was 80 minutes. The formulation comprised 25 wt% of SIS, 55 wt% of resin, 19 wt% of paraffinic oil and 1 wt% anti-oxidant. The resins were hydrogenated C9 hydrocarbon resin, partially hydrogenated C9 hydrocarbon resin, hydrogenated C5 hydrocarbon resin, pentaerythritol rosin ester resin and hydrogenated rosin ester resin.

Details of the formulations are displayed in appendix A, table A-5.

3.2.4 Hot melt pressure sensitive adhesives coating

The tapes were prepared on Nordson Meltex® Hot Melt Laboratory Coater CL 2018 S (Nordson Engineering GmbH, Lüneburg, Germany) operating in the temperature range of 120 °C to 170 °C and a coating speed of 3 m/min using a gear pump operating at 18 rpm. A slot die was used to coat the molten blend on polyester film and further supported by double-side siliconized paper. Films of $35 \text{ g/m}^2 \pm 2$ coating weight were produced.

For the process investigation chapter, the coater operated either at 140 °C or at 165 °C according to the mixing temperature used.

3.3 Materials characterization and instrumentation

3.3.1 Dynamic mechanical analysis (DMA)

In a dynamic experiment, in which a sinusoidal oscillatory stress is applied, a perfectly elastic solid will respond with a strain wave in phase (phase angle 0°).

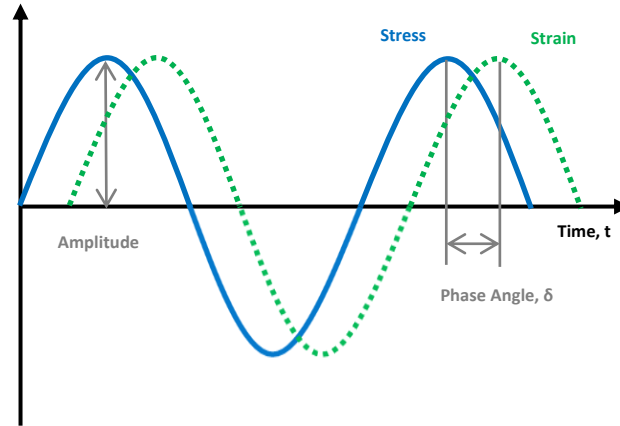


Figure 18: Principle of oscillatory measurement. As a sinusoidal strain is applied (green dotted line curve), a sinusoidal stress response occurs (blue full line).

In the same situation, a Newtonian liquid will generate a strain wave 90° out of phase and for a viscoelastic material the strain wave will be situated in between. Figure 18 schematically shows this principle. If a material shows a linear viscoelastic behavior, i.e. strain and rate of strain are infinitesimal, then the ratio of stress to strain is only a function of time and not of the stress magnitude. Using complex notation, complex modulus can be written and related to complex stress strain as described in equation 18:¹⁶³

$$G^* = G' + iG'' \quad (18)$$

Thus,

$$\tan\delta = \frac{G''}{G'} \quad (19)$$

As presented in equation 19, the real part, G' , is called shear storage modulus or shear elastic modulus and is directly proportional to the energy storage in a cycle. The imaginary part, G'' , is called shear loss modulus or shear viscous modulus and is proportional to energy dissipation in a cycle. The loss tangent or loss factor is the tangent of the phase angle, and it is the ratio between loss modulus and storage modulus, G''/G' . Hence, a relationship between the energy loss and the recoverable energy can be built.

The tests for the prepared blends were performed by a mechanical spectrometer Bohlin CVO HR120 (Malvern Instruments, Worcestershire, UK). The temperature range was -25 °C to 130 °C. The cooling run was performed and analyzed with a cooling rate of 2 °C/min at oscillation mode at 1 Hz frequency using the plate-plate geometry of 20 mm diameter. For frequency sweep, the temperature was set to 25 °C and to 150 °C with a frequency range of 0.01 rad/s to 100 rad/s using plate-plate geometry of 20 mm diameter.

The tests for the neat SIS, EOBC and their respective blends with paraffinic and naphthenic oils were performed according to ISO 6721-7 using a mechanical spectrometer MCR 501 (Anton Paar GmbH, Graz, Austria) in torsion mode at 1 Hz. The heating run was performed and analyzed in the temperature range of -100 °C to 150 °C for SIS and its blends; and from -100 °C to 90 °C for EOBC and its blends; and a heating rate of 2 K/min at torsion mode at 1 Hz and 0.05 % strain. The dimension of the samples was 30 mm x 10 mm x 2 mm made from pressed plates prepared at 160 °C.

3.3.2 Ring and ball softening point

The tests were carried out at the Petrotest RKA-2 (Petrotest Instruments GmbH & Co. KG, Ostfildern, Germany) according to ASTM E-28.

3.3.3 Contact angle measurements

Contact angle measurements were performed using a drop shape analyzer DSA 100 (Krüss, Hamburg, Germany) by the sessile drop method. A 20 µl drop was deposited on the material surface and three liquids were used for the measurements, namely water, diiodomethane and ethylene glycol. The surface energy and work of adhesion of the pure materials as well as of selected blends were determined by applying the Owens, Wendt, Rabel and Kaelbe equation (OWRK) using the DSA4 software (details in appendix B).

3.3.4 Peel adhesion strength at 180°

The samples were tested according to PSTC-1 using the tensile strength tester UPM 1446 (Zwick GmbH, Ulm, Germany). Tapes of 220 mm x 25 mm were prepared from the coated material and tested against two substrates, namely steel and polyethylene. The peeling rate was 300 mm/min. Figure 19 presents the test arrangement.

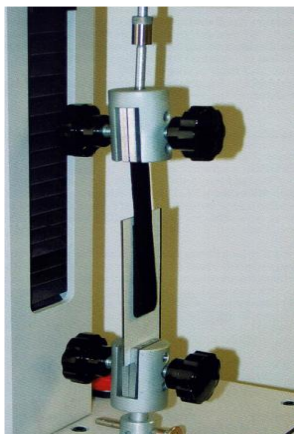


Figure 19: 180° peel test arrangement.¹⁶⁴ As the upper clamp moves up with a rate of 300 mm/min, the tape (black stripe) is detached from the substrate and this force is recorded.

3.3.5 Shear adhesion (Holding Power)

The tests were carried out on a Shear tester HT-8 (ChemInstruments, Fairfield, USA) according to PSTC-107. The sample testing area was 25 mm x 25 mm measured against steel. The samples were measured at 40 °C and 60 °C with a 1 kg weight and the falling time was recorded. Figure 20 presents the test arrangement.

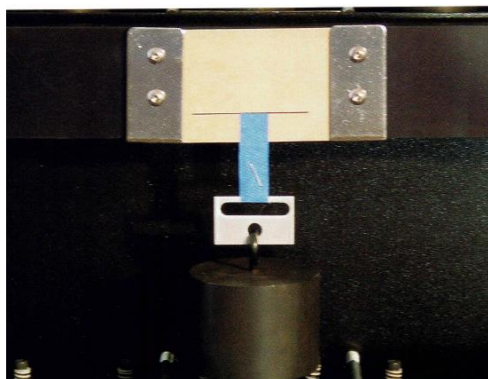


Figure 20: Holding power test arrangement.¹⁶⁴ As the 1 Kg weight is coupled to the ring, the tape (blue stripe) is submitted to shear forces and detaches from the steel panel.

3.3.6 Shear adhesion failure temperature (SAFT)

The tests were carried out on a shear tester HT-8 (ChemInstruments, Fairfield, USA) integrated in a mechanical convection oven DKN 602 (Yamato Scientific America Inc., Santa Clara, USA) according to ASTM D4498-07.

The samples testing area were 25 mm x 25 mm with a temperature ramp program of 30 °C/h using 500 g weight. The failure temperature was recorded. Figure 20 presents the test arrangement.

3.3.7 Loop tack

The measurements were conducted according to DIN EN 1719 using the tensile strength tester UPM 1446 (Zwick GmbH, Ulm, Germany). Samples of 175 mm x 25 mm were prepared and tested in a loop configuration. It was tested against steel with a peeling rate of 300 mm/min. Figure 21 shows test arrangement (left hand-side) and schematic representation of a sample being tested (right hand-side).

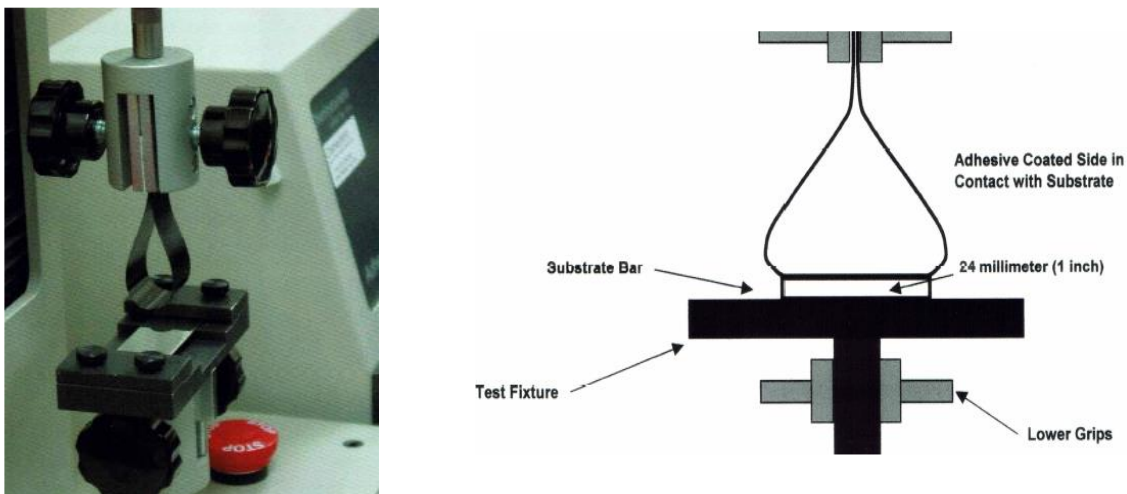


Figure 21: Loop tack test arrangement (left hand-side) and its schematic representation (right hand-side).¹⁶⁴ As the upper clamp moves up with a rate of 300 mm/min, the tape (black stripe) is detached from the substrate and the maximum force is recorded.

3.3.8 Brookfield viscosity

A Brookfield viscometer RVDV-II+ (Brookfield Engineering Lab., Inc., Middleboro, USA) with spindle 27 was used according to ASTM D-3236. The viscosity was determined at 140 °C.

3.3.9 Tensile properties

The mechanical properties were measured in the tensile tester UPM 1446 (Zwick GmbH, Ulm, Germany) at a cross-head speed of 300 mm/min. The samples were prepared using a

heated film drawer at 180 °C. A PTFE coated glass fiber fabric was used as removable support. The molten hot melt was spread on the support film by a scraper to reach a film thickness of 50 µm ± 5. Test pieces were cut from this film by a die cutter.

3.3.10 Gel permeation chromatography (GPC)

Gel permeation chromatography (SECcurity GPC system), (PSS GmbH, Mainz, Germany) was performed with a column combination of pre-column (PSS SDV 5 µm), column 1 (PSS SDV 5 µm, 1000 Å), column 2 (PSS SDV 5 µm, 100000 Å) and column 3 (PSS SDV 5 µm, 1000000 Å) and a SECcurity differential refractometer detector. 20 mg of each sample was dissolved in 5 ml tetrahydrofuran (THF) for 24 hours. The calibration was carried out based on polystyrene standards.

3.3.11 Nuclear magnetic resonance (NMR)

The ¹H nuclear magnetic resonance was performed using an Avance III 400 MHz (Bruker BioSpin GmbH, Rheinstetten, Germany) with a pulse interval of 15 s, acquisition time of 4.09 s, pulse angle of 90 °, resolution of 0.3 Hz (LB) and 0.24 Hz (FIDRES) and number of scans set at 64.

3.3.12 Differential scanning calorimetry (DSC)

The glass transition temperatures of the resins were determined using a DSC 822 (Mettler Toledo Inc., Columbus, USA) at heating and cooling rates of 10 K/min. The first heating run ranged from -60 °C to 200 °C and back to -60 °C. It was held at -60 °C for 10 min. The second heat run ranged from -60 °C to 300 °C and the glass transition temperature was determined from this second run.

The glass transition temperature of neat SIS was determined using a DSC 2041F1 Phoenix (Netzsch GmbH, Selb, Germany) at heating and cooling rates of 10 K/min. The first heating run ranged from -150 °C to 200 °C and back to -150 °C. It was held at -150 °C for 10 min. The second heating run ranged from -150 °C to 300 °C.

The glass transition temperature, the melting temperature, heat capacity and enthalpy of neat EOBC and its blends with each resin were determined using a DSC 2041F1 Phoenix (Netzsch GmbH, Selb, Germany) at heating and cooling rates of 10 K/min. The first

heating run ranged from -150 °C to 200 °C and back to -150 °C. It was held at -150 °C for 10 min. The second heating run ranged from -150 °C to 300 °C.

3.3.13 Polarized light optical microscopy (PLOM)

Images of neat SIS, neat EOBC and their respective selected blends were prepared under polarized light (crossed polarizers) using a DM 2700 M microscope from Leica (Leica GmbH, Wetzlar, Germany). The studied materials were molten directly in the microscopy slides placed on the top of a heating plate.

3.3.14 Atomic force microscopy (AFM)

The morphology of the neat SIS, neat EOBC as well as selected blends was characterized by Atomic Force Microscopy. The images were acquired using a Nanowizard 4 (JPK-Instruments AG, Berlin, Germany) under intermittent contact mode.

For the pure polymers, a preparation from the pellets using a cryo-ultramicrotome (PT-CRX LN Ultra, RMC products) (Boeckeler Instruments, Inc., Tucson, USA) using diamond knives was conducted.

For the blends, the measurements were conducted directly from samples coated using the Meltex lab coater.

4 Results and discussion

4.1 Compatibility investigation of the thermoplastic elastomers, tackifiers and oils used in the polymer blends of hot melt pressure sensitive adhesive models

Miscibility and compatibility of a polymer blend components are of great importance to understand its final properties after processing it. Systems consisting of polymer and tackifiers of different chemical nature and at different concentrations were studied in order to characterize their compatibility. Furthermore, the effects of the oil on compatibility used in PSA blends were also assessed.

4.1.1 Influence of the resins chemical structure on compatibility

The influence of the resins chemical structure on compatibility with SIS and EOBC was studied by means of dynamic mechanical analysis. The glass transition temperature for neat materials was determined by DSC whilst for the blends it was determined by the loss modulus peak temperature and compared to the calculated values predicted by Fox equation (Equation 2).

Class et al.^{13,14,97} analyzed blends of natural rubber and SBR with polystyrene resin, polyvinyl cyclohexane resin and poly(tert-butylstyrene). In their study, they concluded that the degree of compatibility of rubber-resin can be assessed by its viscoelastic properties. A system will present a good degree of compatibility with the elastomer, if both a pronounced shift in the loss factor peak (glass transition) temperature of the elastomer is achieved and a decrease in the storage modulus value in the rubbery plateau region is observed. Table 3 presents storage modulus at 25 °C, which is in the rubbery plateau region and at which further properties were determined, i.e., application temperature, loss modulus peak temperature and loss factor peak temperature for pure polymers investigated and 1:1 blends in the elastomeric region.

Further on, figure 22 (a) presents the storage modulus and loss factor curves as well as (b) loss modulus for such blends.

Table 3: Viscoelastic properties for pure SIS, pure EOBC, 1:1 blends of SIS and resins and 1:1 blends of EOBC and resins.

Sample	G' at 25°C (10 ⁵ Pa)	G'' Peak Temperature (elastomeric region) (°C)	tanδ Peak Temperature (elastomeric region) (°C)
<i>SIS</i>	8.98	-60	-51
S-HC9-50	1.76	-11	2
S-PHC9-50	1.77	-18	-5
S-HC5-50	1.97	-17	-2
S-RE-50	2.66	-7	12
S-HRE-50	1.92	-16	-5
<i>EOBC</i>	42.5	-59	-52
E-HC9-50	22.4	4	15
E-PHC9-50	21.6	-10	3
E-HC5-50	19.0	-10	3
E-RE-50	94.1	50	83
E-HRE-50	66.8	30-70	40-80

According to Class et al.^{13,14,97} criteria, all the presented systems mixed with SIS showed a certain degree of compatibility since storage moduli in the rubbery plateau region decreased for blends when compared to pure SIS; while loss factor peak temperature, corresponding to glass transition temperature of the polyisoprene phase in the copolymer, increased.

Blends containing EOBC and hydrogenated C9 hydrocarbon resin, partially hydrogenated C9 hydrocarbon resin and hydrogenated C5 hydrocarbon resin presented a decrease in storage modulus at 25 °C as well as an increase in glass transition temperature, thus, a good molecular interaction exists. Systems containing EOBC and pentaerythritol rosin ester resin as well as hydrogenated rosin ester cannot be considered compatible since an increase in the storage modulus at 25 °C was observed as well as a glass transition temperature (loss factor peak) around 80 °C for pentaerythritol rosin ester resin and a broad loss factor peak glass transition temperature around 40 °C to 80 °C for hydrogenated rosin ester.

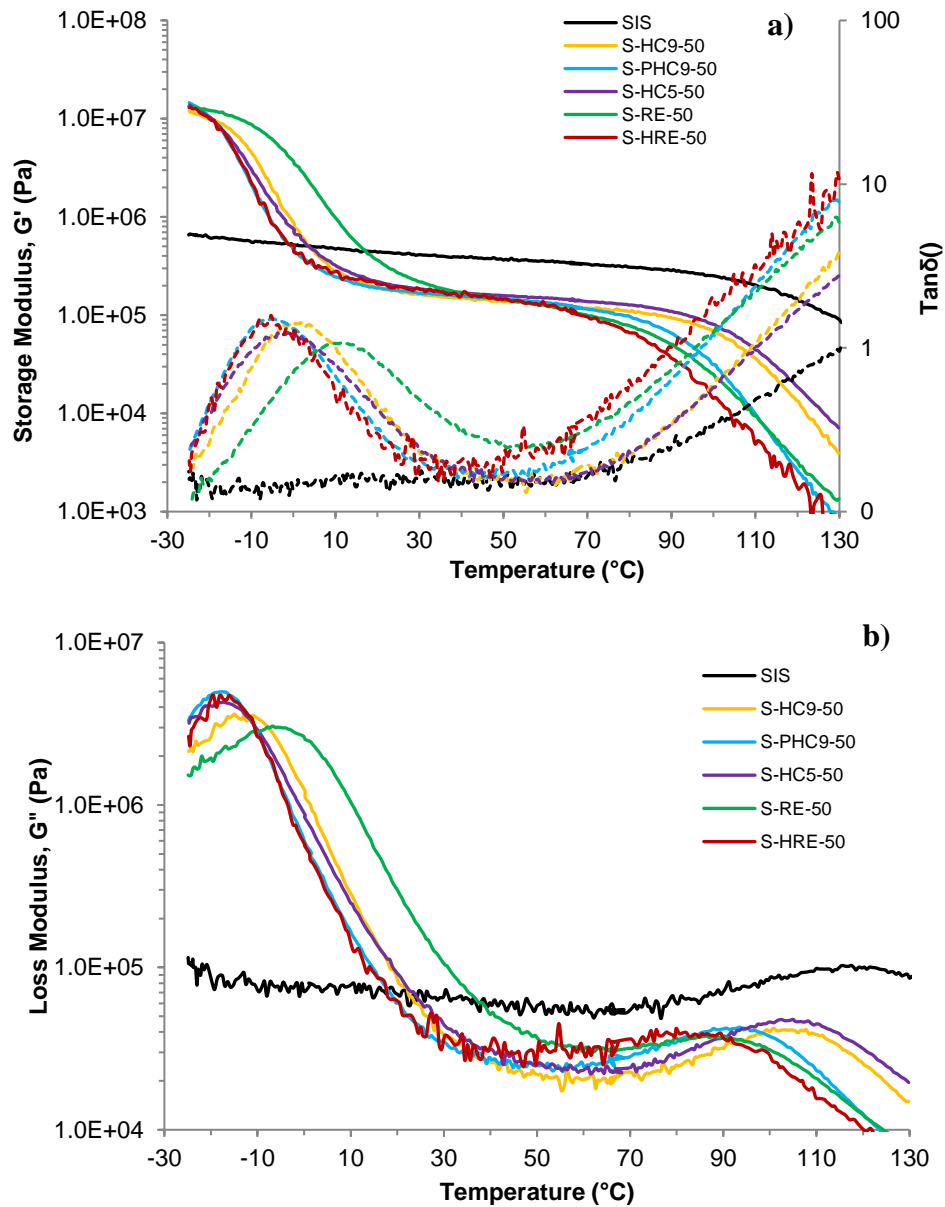


Figure 22: Storage modulus (full lines) and loss factor (dashed lines) (a); loss modulus (b) for pure SIS and 50:50 blends comprising SIS and chosen resins determined by means of Bohlin CVO HR120.

Loss factor curves for pure EOBC, blends containing EOBC and chosen tackifiers are displayed in figure 23. The measurements were performed in torsion mode from -100 °C till 100 °C in order to clearly show the two peaks identified in natural resins based blends and only one peak identified in petroleum based resins.

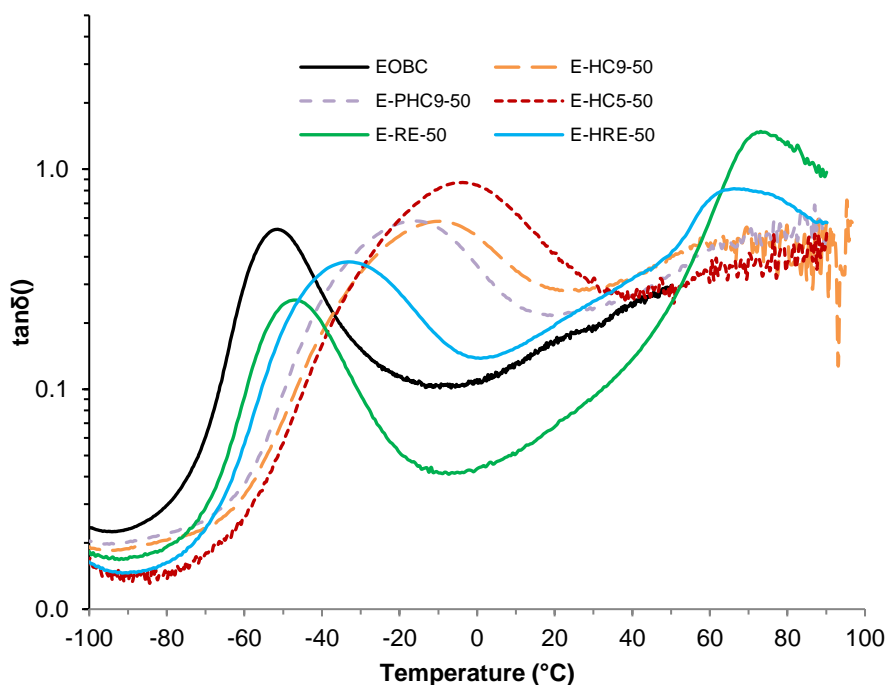


Figure 23: Loss factor for pure poly(ethylene-co-1-octene) block copolymer and 50:50 blends containing EOBC and chosen resins determined by means of MCR 501.

In an attempt to evaluate the compatibility of the employed resins and the glassy region, i.e. polystyrene, the peak temperature of the loss moduli for the neat SIS as well as for the 1:1 blends with resins are displayed in table 4. It can be observed a shift of the peak temperature toward lower temperatures for all the blends and a larger shift for the natural resins. It can be interpreted as an association indication between the resin and the glassy region. A weaker association degree is observed for the hydrocarbon resins, even weaker for the less polar hydrocarbon resins while a stronger association degree for the natural resins was found.

Table 4: Loss moduli peak temperature at the glassy (polystyrene) region for pure SIS and 1:1 blends of SIS and tackifiers.

Sample	G'' Peak Temperature (glassy region)(°C)
SIS	115
S-HC9-50	103
S-PHC9-50	94
S-HC5-50	104
S-RE-50	89
S-HRE-50	84

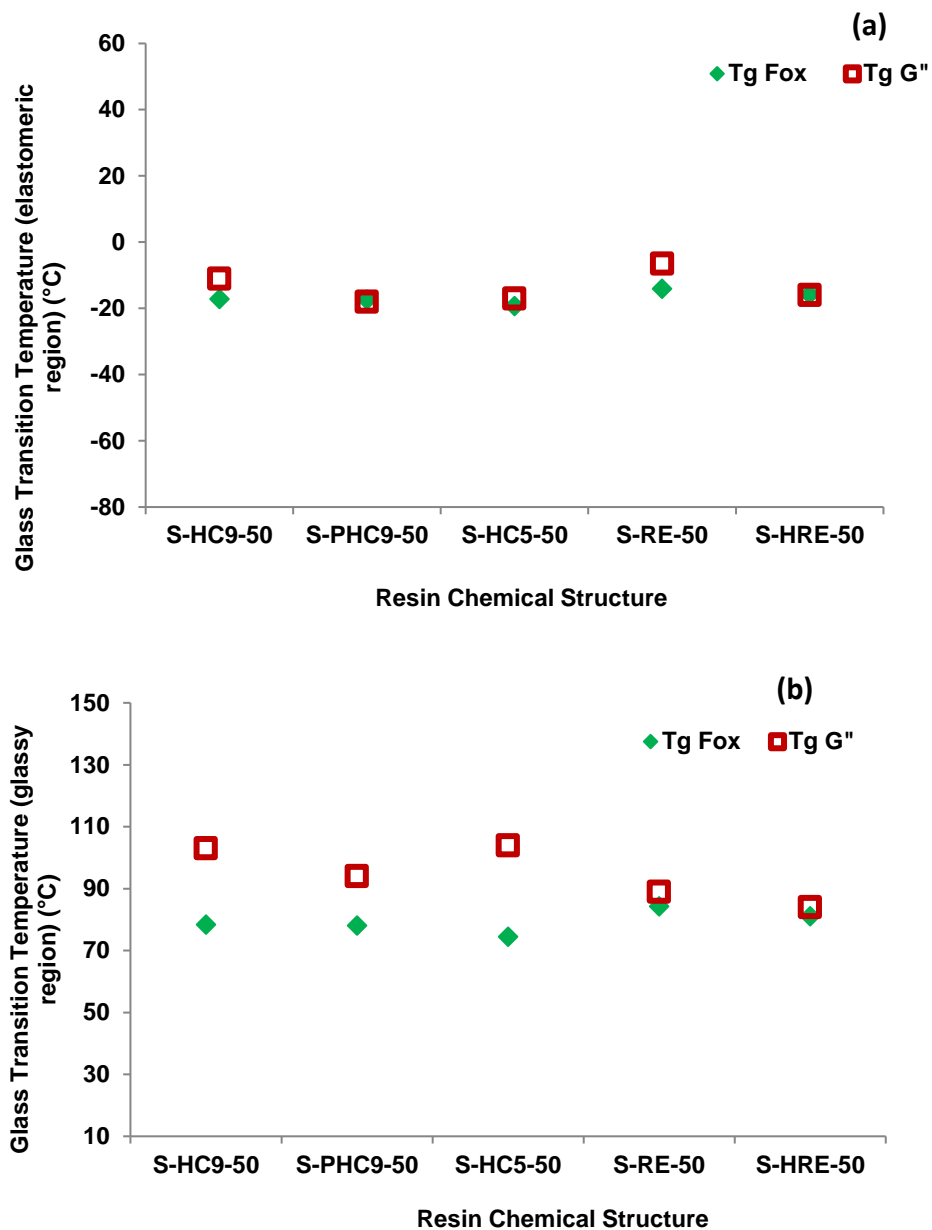


Figure 24: Glass transition temperature measured (G'' peak temperature) and predicted by Fox equation for blends with resins and SIS 1:1 for the elastomeric region (a) and for the glassy region (b).

When studying compatibility of end-block associating tackifier with SIS, Han et al.¹¹⁸ also observed a shift of glass transition temperature to lower temperatures. They hypothesized that the amount of tackifier, which does not associate with the polystyrene microdomains, may have formed a separate phase. Thus, a rubber matrix rich phase containing high amount of tackifier and a tackifier rich phase containing some polyisoprene could also be a possibility. Kamagata et al.¹⁶⁵ identified these two phases for their system when the resin

concentration was over 40 wt% by the presence of a shoulder in the loss factor curves. Such shoulders were not identified in the loss factor curves in the present study.

Figure 24 presents a comparison of glass transition temperature values measured by means of DMA and calculated values by Fox equation for mixtures for SIS: resins 1:1 blends (a) for the elastomeric region and (b) for the glassy region. A reasonable congruence can be observed for the measured and predicted values regarding hydrocarbon resins and polyisoprene while a not satisfactory congruence between these values is observed for the polystyrene. Natural resins present a good congruence between the measured and predicted values for both polymers leading to an understanding that these resins have a satisfactory association with the elastomeric matrix and the dispersed glassy phase.

Figure 25 presents the comparison of glass transition temperature values measured by means of DMA and predicted values by Fox equation for mixtures for EOBC/ Resins 1:1 blends for the elastomeric (amorphous) region. In analogy to the SIS and SIS based blends, a second peak on G'' curves could not be identified.

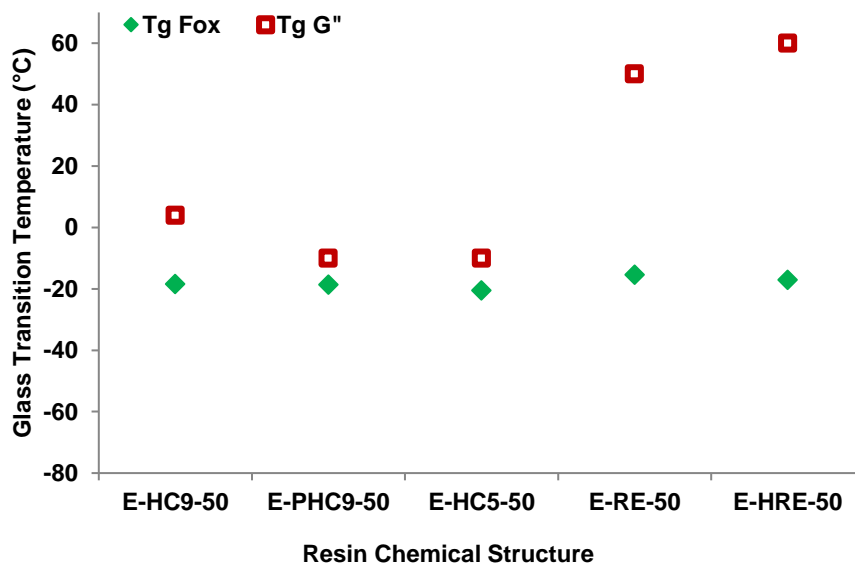


Figure 25: Glass transition temperature measured (G'' peak temperature) and predicted by Fox equation for blends with resins and EOBC.

Congruence is observed for EOBC using predicted values and G'' peak temperature measured by DMA for hydrocarbon resins HC9, PHC9 and HC5. It can be seen that for

EOBC blends containing natural resins, RE or HRE, the results strongly deviate from the predicted values by Fox equation, reassuring the poor compatibility between EOBC and these rosin-based resins.

Figure 26 presents the DSC curves for the pure EOBC and the respective 1:1 blends with the tackifiers analysed.

Poly(ethylene-co-1-octene) block copolymer can be understood under the concept of thermoplastic block copolymer since the soft and hard segments form separate domains.⁷⁰ The sharp peak with a bimodal distribution at about 120 °C characterizes the presence of well structured large crystals. The soft block melting region can be observed in the region between -50 °C and +20 °C although a sharp limit for this region is very difficult to be determined. The polymer microstructure varies strongly in this region.

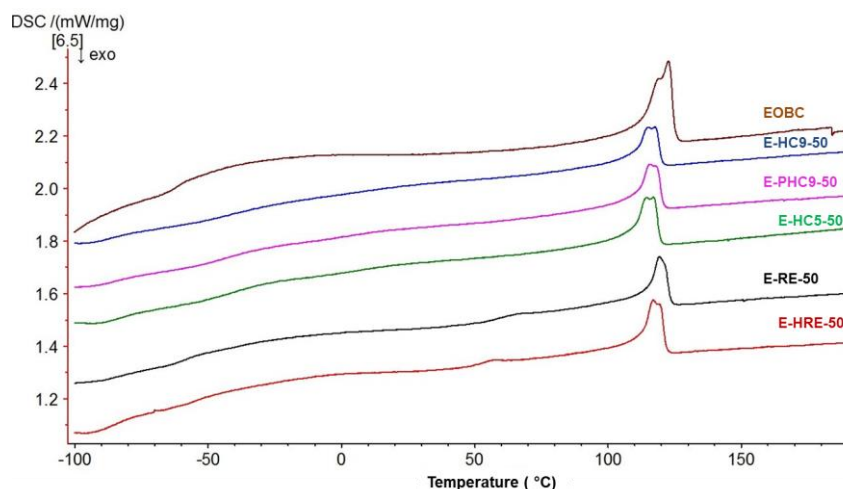


Figure 26: DSC curves for EOBC and blends of 1:1 EOBC:resin for the second heating run. For better clarity, the curves are vertically shifted.

An overview of the glass transition temperature, heat capacity, heat of fusion as well as adjusted heat of fusion for the neat EOBC and for the 1:1 EOBC:resin blends measured from the second heating run, which occurred under non-isothermal crystallization conditions, are summarized in Table 5.

Table 5: Glass transition temperature, heat capacity, heat of fusion and adjusted heat of fusion measured by DSC at a heating rate of 10 K/ min for neat EOBC and blends 1:1 EOBC:Tackifiers.

Sample	Soft Block							Hard Block			
	T _g (°C)	ΔC _p (J/(g*K))	T _{mi} (°C)	ΔH (J/g)	ΔH Adj (J/g)	T _m Peak (°C)	T _{mf} (°C)	Onset T (°C)	T _m Peak (°C)	ΔH (J/g)	ΔH Adj (J/g)
EOBC	-62.1	0.157	-50	7.98	7.98	-19.5	20	88.3	122.6	21.88	21.88
<i>Pol+ Resin</i>											
E-HC9-50	-36.9	0.143	-23	0.36	0.72	-17.8	20	109.5	117.5	12.25	24.50
E-PHC9-50	-42.2	0.161	-30	0.49	0.98	-21.9	20	110.4	115.9	13.40	26.80
E-HC5-50	-37.7	0.191	-25	-0.09	-0.17	-3.1	20	109.0	116.8	14.46	28.92
E-RE-50	-58.2	0.097	-50	5.07	10.14	-21.2	20	115.5	119.4	17.22	34.44
E-HRE-50	NI (-53.8)	0.055	-45	4.71	9.42	-8.5	20	112.9	116.8	18.79	37.58

In congruence with the glass transition temperature determined by DMA for the neat EOBC and for its blends, an increase in the T_g is observed. However, for the natural resins blends, the glass transition was not easily identified, especially for E-HRE-50. Furthermore, a second glass transition temperature can be identified for the natural resins blends at about 50 °C indicating a phase separation for these systems. In congruence with the results measured by DMA, for the hydrocarbon resins only one T_g was identified in the blends, reassuring the high degree of compatibility between these resins and the EOBC.

The hard block melting peak temperatures for all the blends slightly decrease since the addition of resin influences the crystallization behavior. Crystals, which are smaller, less perfect and with lower thickness, are preferably formed. The melting point depression theory considers that solvents, diluents, plasticizers are impurities, which contribute to this melting temperature decrease.^{43,166,167}

The adjusted heat of fusion for the hard block increases, indicating that crystalline degree is higher than for the pure EOBC. It is worth highlighting that the adjusted heat of fusion increases even more for the natural resins blends. It might be due to a higher influence on the crystallization or due to a difficulty (overlapping) in determining the baseline.

The soft block melting region is extremely broad, and an attempt to determine the initial and final melting temperatures was performed. The results of the heat of fusion can give a hint that, for the hydrocarbon resins, crystals are no longer formed in this region (or of these types) and for the natural resins blends, crystals in the soft block part are still present.

4.1.2 Influence of resin concentration on compatibility

The effect of resins concentration on compatibility with SIS was studied by means of dynamic mechanical analysis.

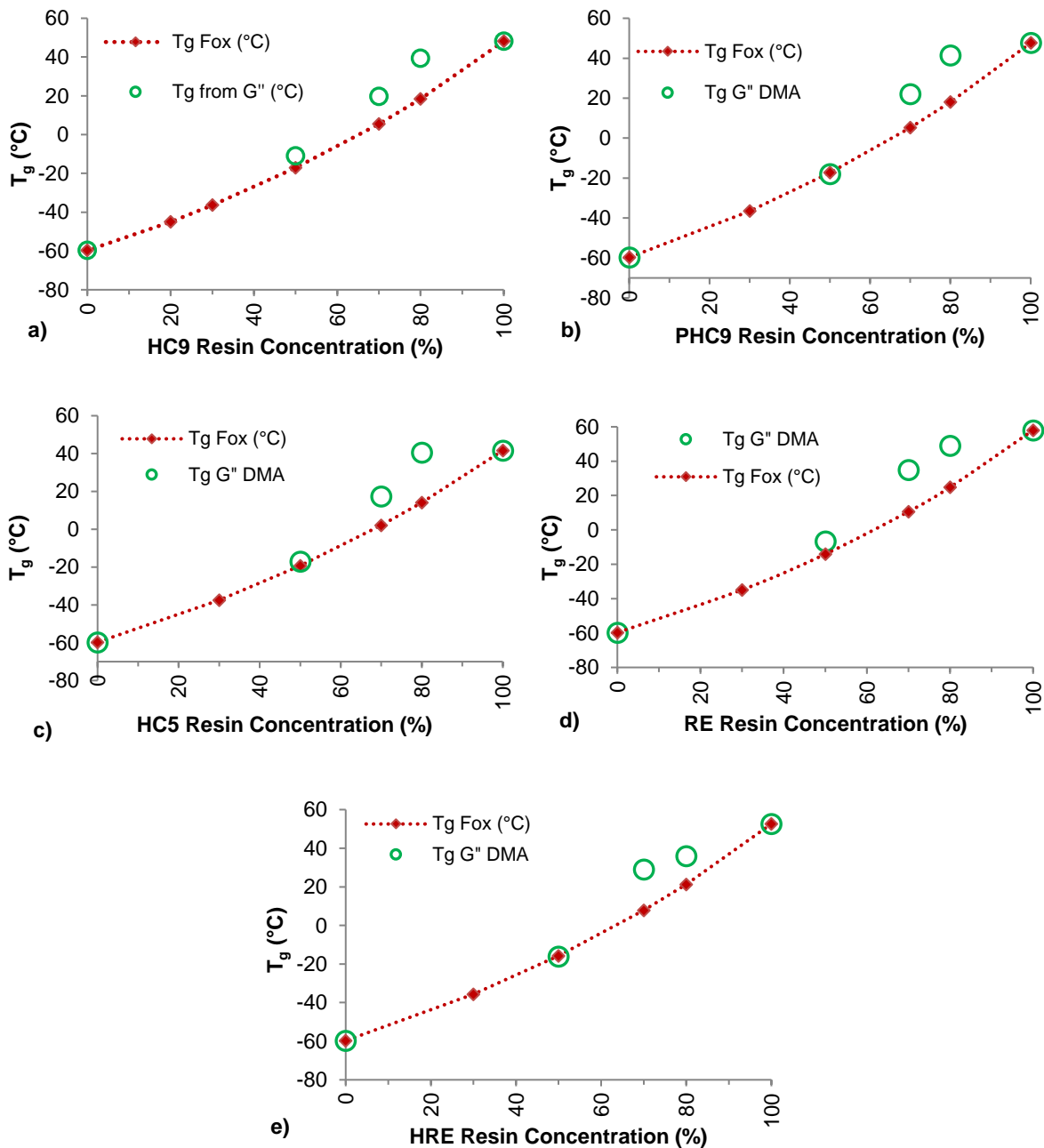


Figure 27: Glass transition temperature as function of resin content for blends of SIS/ resins (a) hydrogenated C9 hydrocarbon resin; (b) partially hydrogenated C9 hydrocarbon resin; (c) hydrogenated C5 hydrocarbon resin; (d) pentaerythritol rosin ester resin; (e) hydrogenated rosin ester resin. Open symbols are used for the experimental values from DMA, red curves represent the calculated values by Fox equation.

The glass transition temperature was determined by the loss modulus peak temperature and compared to the calculated values predicted by Fox equation, as shown in figure 27. Systems containing SIS and resins presented a better correlation with the predicted values in a concentration around 50 wt% of resin. As observed by Kamagata et al.¹⁶⁵, in systems containing pentaerythritol ester resin and natural rubber, a homogeneous phase is observed up to 40 wt% resin. For higher resin concentration systems, they state that a phase separation occurs.¹⁶⁵

4.1.3 Influence of oil on compatibility

An additional investigation considering the effect of oils, which are used as plasticizers in hot melt pressure sensitive adhesive blends, on compatibility with SIS was conducted by means of dynamic mechanical analysis and differential scanning calorimetry.

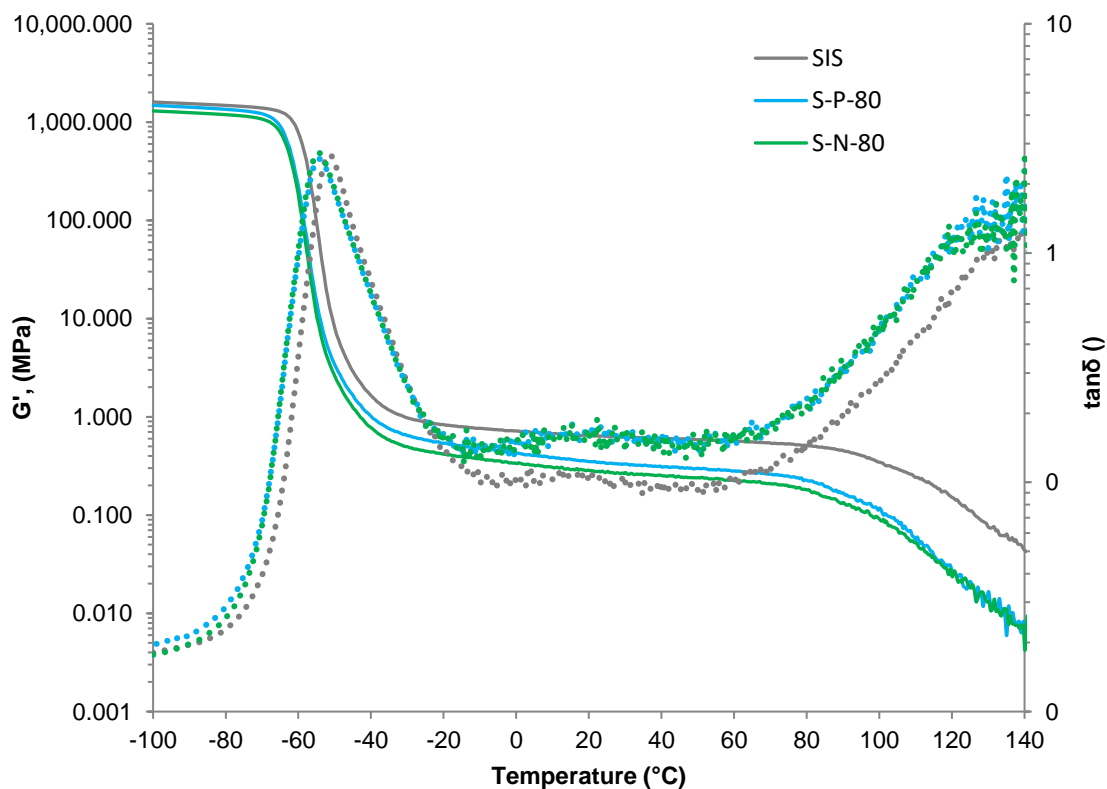


Figure 28: Storage modulus (full line) and loss factor (dotted lines) for neat polystyrene-block-polyisoprene-block-polystyrene copolymer (grey lines), blend of 80 wt% polystyrene-block-polyisoprene-block-polystyrene copolymer / 20 wt% paraffinic oil (blue lines) and blend of 80 wt% polystyrene-block-polyisoprene-block-polystyrene copolymer / 20 wt% naphthenic oil (green lines).

The storage modulus and loss factor curves are presented in figure 28 and loss modulus curves in figure 29 showing data for neat SIS, a blend of 80 wt% SIS and 20 wt% paraffinic oil as well as a blend comprising 80 wt% SIS and 20 wt% naphthenic oil. They were determined using a mechanical spectrometer MCR 501.

The general effect of oil acting as plasticizer is confirmed in the measurements. A decrease in glass transition temperature of the blend in comparison to neat SIS is observed as well as a decrease in storage modulus. Plasticizers are known to dissolve in the polymer and to ease the polymer chains mobility.⁴³

Furthermore, the glass transition temperature for blends containing paraffinic oil is lower than for those containing naphthenic oil. Similar results were reported by Galán.⁷⁶ In a comprehensive study of oils used in PSA, Carvagno et al.¹⁶⁸ described that the oil viscosity as well as its glass transition temperature correlates with adhesive performance. Further on, they observed that the glass transition temperature of PSA prepared with iso-paraffinic oil was lower than T_g of PSA prepared with naphthenic oil. However, they attributed this factor to the lower T_g of the iso-paraffinic oil and not to its composition. In the present study, the viscosity of the naphthenic oil is higher than the viscosity of the paraffinic oil. Thus, both factors may be attributed to the lower glass transition temperature identified in the blend containing SIS and paraffinic oil. In the region of the glass transition temperature of the styrene block, a shift in G'' toward lower temperature was observed for both blends, as expected. It is difficult to determine the temperature at which the viscous behavior dominates the elastic behavior in this region, however, it might occur at first to the blend based on naphthenic oil, allowing to be speculated that better interaction occurs between naphthenic oil and the styrene domains. Carvagno et al.¹⁶⁸ detected no correlation in their experiments for carbon content type and this point where loss factor is equal one. Although the glass transition temperatures of the oils were not measured, values of around $-75\text{ }^\circ\text{C}$ are reported in the literature for paraffinic oils measured by DSC.¹⁶⁸

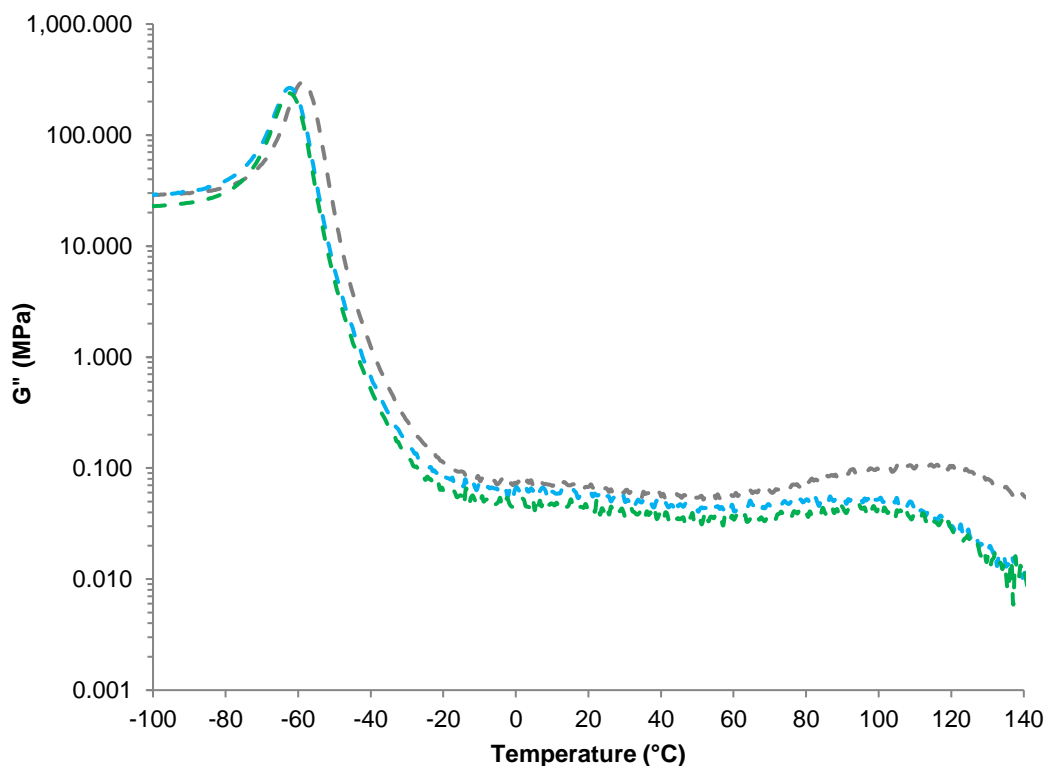


Figure 29: Loss modulus (dashed lines) for neat polystyrene-block-polyisoprene-block-polystyrene copolymer (grey lines), blend of 80 wt% polystyrene-block-polyisoprene-block-polystyrene copolymer / 20 wt% paraffinic oil (blue lines) and blend of 80 wt% polystyrene-block-polyisoprene-block-polystyrene copolymer / 20 wt% naphthenic oil (green lines).

The experimental data measured by DMA for paraffinic oil are in satisfactory correlation with the calculated ones by additive rule of mixture (equation 20), as shown in table 6.

$$T_g^m = W_a T_g^a + W_b T_g^b \quad (20)$$

Table 6: Glass transition temperature determined by loss moduli peak temperature and predicted by additive rule.

Sample	T_g from G'' (°C)	T_g additive rule (°C)
S-P-80	-63	-63
E-P-80	-64	-65

Debier et al.¹⁶⁹ investigated the compatibility between a naphthenic/ paraffinic oil and polystyrene at two concentrations, namely 50/50 and 90 % polystyrene / 10 % oil. Both blends were opaque concluding that the polystyrene and the oil may not be compatible. Based on the exposed data, it is supposed that the oil is preferentially located in the polyisoprene matrix phase.

Results of DMA for blends of EOBC and oils are presented in figure 30 and their DSC curves are depicted in figure 31. It can be observed by DSC measurements that the glass

transition temperature for both blends decreased in comparison to the neat EOBC and that for the blend with paraffinic oil the T_g is the lowest one, confirming the result reported in the literature.⁷¹ Therefore, it can be assumed that the oil associates only with the amorphous phase.

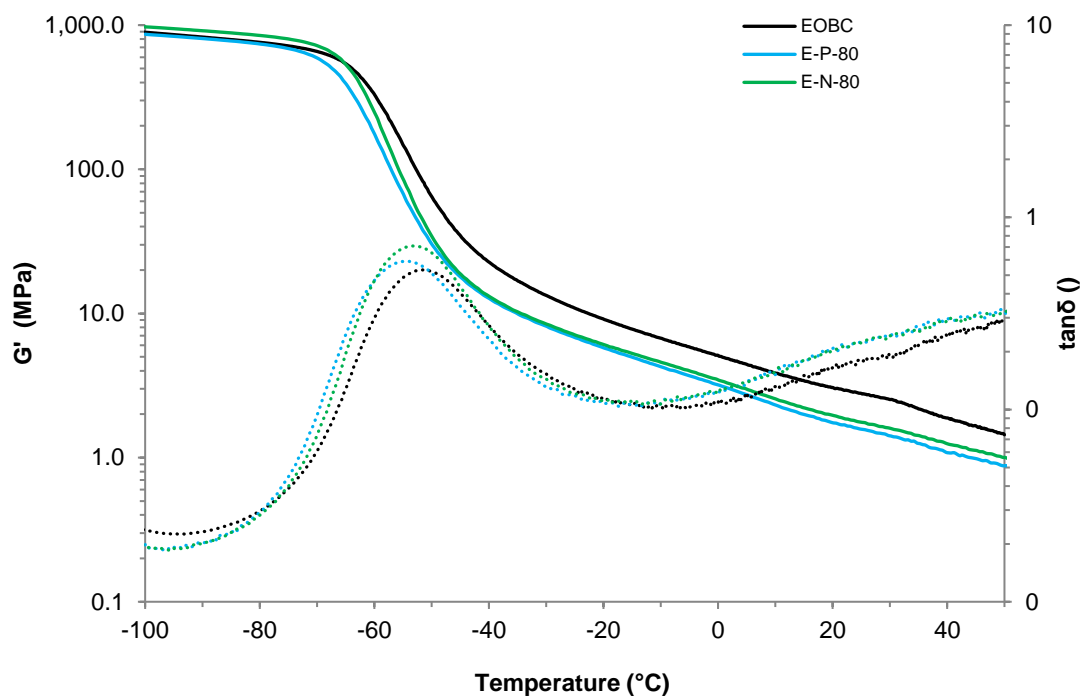


Figure 30: Temperature sweep at torsion mode for neat poly(ethylene-co-1-octene) block copolymer (black lines), 80 wt% poly(ethylene-co-1-octene) block copolymer / 20 wt% paraffinic oil (blue lines) and 80 wt% poly(ethylene-co-1-octene) block copolymer / 20 wt% naphthenic oil (green lines). Storage modulus curves and loss factor are represented by full lines and dotted lines, respectively.

The influence of oil on the crystalline structure of EOBC was also evaluated by DSC measurements. The results are summarized in Table 7.

Table 7: Glass transition temperature, heat capacity, heat of fusion and adjusted heat of fusion measured by DSC at a heating rate of 10 K/ min for neat EOBC and blends of 20 wt% Oil and 80 wt% EOBC.

Sample	Soft Block							Hard Block			
	T_g (°C)	ΔC_p (J/(g*K))	T_{mi} (°C)	ΔH (J/g)	ΔH Adj (J/g)	T_m Peak (°C)	T_{mf} (°C)	Onset T (°C)	T_m Peak (°C)	ΔH (J/g)	ΔH Adj (J/g)
EOBC	-62.1	0.157	-50	7.98	7.98	-19.5	20	88.3	122.6	21.88	21.88
<i>Pol + Oil</i>											
E-P-80	-66.3	0.189	-55	10.08	12.60	-29.9	15	113.9	119.6	21.01	26.26
E-N-80	-64.3	0.158	-55	4.69	5.86	-32.9	-4	112.8	118.8	22.29	27.86

In the hard block region, it was detected that the melting peak temperature decreased for both type of oils in correlation with the typical behavior of polyolefins when oil is added. This effect is caused by the reduced crystals size as well as their reduced perfection.⁴³ In comparison to the resin addition, it can be observed a less pronounced effect on crystallinity in the hard block region. In the soft block region, an attempt was also made for the EOBC and oils blends to define the limits at which the melting temperature would start and end. Only an indication that crystals still exist in this region could be interpreted.

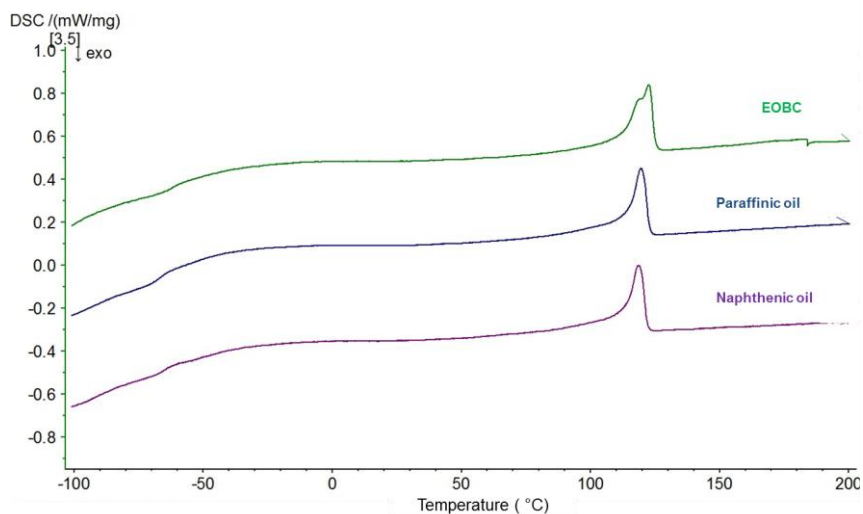


Figure 31: DSC curves for neat poly(ethylene-co-1-octene) block copolymer; 20 wt% paraffinic oil / 80 wt% poly(ethylene-co-1-octene) block copolymer; 20 wt% naphthenic oil / 80 wt% poly(ethylene-co-1-octene) block copolymer.

The investigated resins were also blended with paraffinic oil to characterize their compatibility. Figure 32 presents DMA loss modulus curves for blends containing 70 wt% resins and 30 wt% oil. It can be seen that the blends were very viscous and as expected no rubbery plateau region existed. A glass transition temperature from the loss modulus peak temperature could be experimentally determined and the determined values are summarized in table 8.

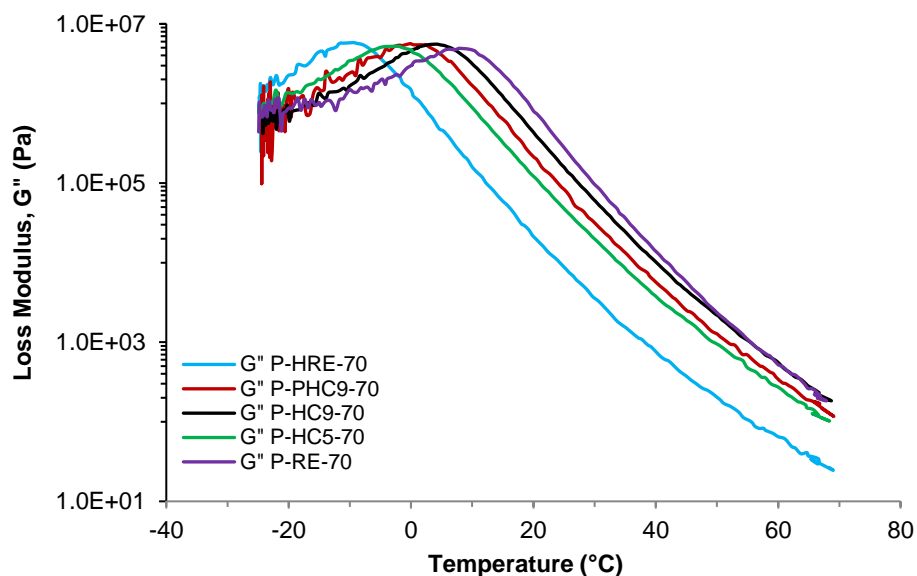


Figure 32: Loss modulus curves of blends containing 70 wt% resin / 30 wt% paraffinic oil.

The blends presented a macroscopically homogeneous behavior, which was visible by naked eyes.

Table 8: Glass transition temperature determined by loss moduli peak temperature and predicted by Fox equation and additive rule.

Sample	T _g from G'' (°C)
P-HC9-70	4.3
P-PHC9-70	1
P-HC5-70	-2
P-RE-70	9
P-HRE-70	-9

As a next step, the mixture of block copolymer, resin and oil was studied regarding its mechanical behavior. Figure 33 illustrates the effect of adding a compatible plasticizer, i.e., oil to SIS, of adding a compatible resin and of adding both to SIS. By adding a compatible resin, the rubbery plateau modulus decreased in relation to the pure SIS plateau modulus. The glass transition temperature of the blend was higher than the T_g of the pure SIS. By adding a plasticizer, the glass transition temperature was lowered (as can be seen in figure 28 and 29) and the rubbery plateau modulus decreased in comparison to pure SIS. When all the three components were mixed in a concentration typically employed in HMPSA blends, a decrease in rubbery plateau modulus was reached and this should occur in the application temperature (in this case ca. 25 °C) as well as an increase in glass transition

temperature in comparison to the pure SIS in order to obtain a blend which encompasses pressure-sensitive adhesive character.

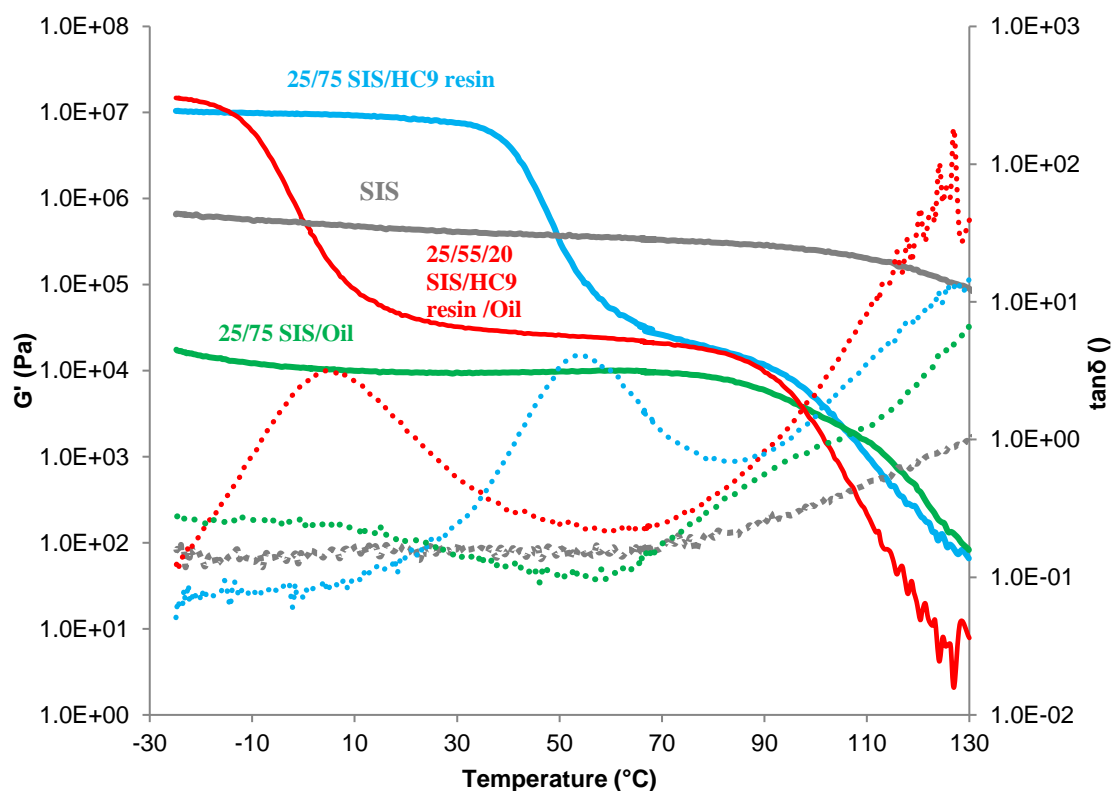


Figure 33: DMA curves for pure SIS, addition of tackifier, addition of oil and addition of oil and tackifier together to SIS. The full lines are storage modulus curves and dashed lines are loss factor curves.

4.2 Influence of tackifier chemical structure and concentration on properties and performance of hot melt pressure sensitive adhesive blends

Different classes of tackifying resins were used in the present work to understand their effect on blends of a model HMPSA as well as the effect of their concentration on such blends. Their influence on blends viscoelastic properties, morphology, adhesion and adhesion performance are discussed below.

4.2.1 Influence of tackifier chemical structure and concentration on viscoelastic behavior

Viscoelastic properties of the blends were investigated by means of dynamic mechanical analysis. In the work of Tse et al.^{86,146}, a rheological model developed by them was employed to analyze the adhesive behavior of blends containing a styrenic block

copolymer and resin (equation 21). In their study, SIS and a C5 tackifying resin were evaluated.

$$P = P_0 B D \quad (21)$$

Where P is the tack term for the PSA/stainless steel substrate interface, P_0 is the term related to the intrinsic adhesion, B is the bonding term and D is the debonding term. These two last parameters are terms related to the viscoelastic properties of the bulk PSA. The B term depends on the plateau modulus of the adhesive as well as the contact time and pressure of the bond formation during the test. The D term is related to the energy dissipation during debonding process. Tse et al.^{86,146} stated that intrinsic adhesion can be measured by means of contact angle as surface energy values. The order of magnitude of such contribution is of 10^{-1} J/m^2 , while the two other terms, which are related to the blend viscoelastic properties, present values with an order of magnitude in the range of 10^2 J/m^2 to 10^4 J/m^2 . Furthermore, they show a satisfactory correlation for the debonding term with logarithm G'' at the debonding frequency and finally to the adhesive tack values. Figure 34 shows such correlation for the blends employed at different concentrations.

As stated by Chang,⁸⁸ a frequency of 10^2 Hz corresponds to the debonding frequency of a $50 \text{ }\mu\text{m}$ thick adhesive for a tack test conducted at 5 mm/s . In the present study, a 5 mm/s loop tack test was conducted for samples with an average value of $50 \text{ }\mu\text{m}$ thickness. A very good relationship was observed for all the samples indicating that a high dissipation is connected to high tackiness of the adhesive.

It is emphasized in figure 35 the outcome when different resins are compared. Tack values are presented for blends having the same resin concentration on weight but with different chemical structure. The blends presenting higher logarithm loss modulus at 100 rad/s also exhibit higher tackiness.

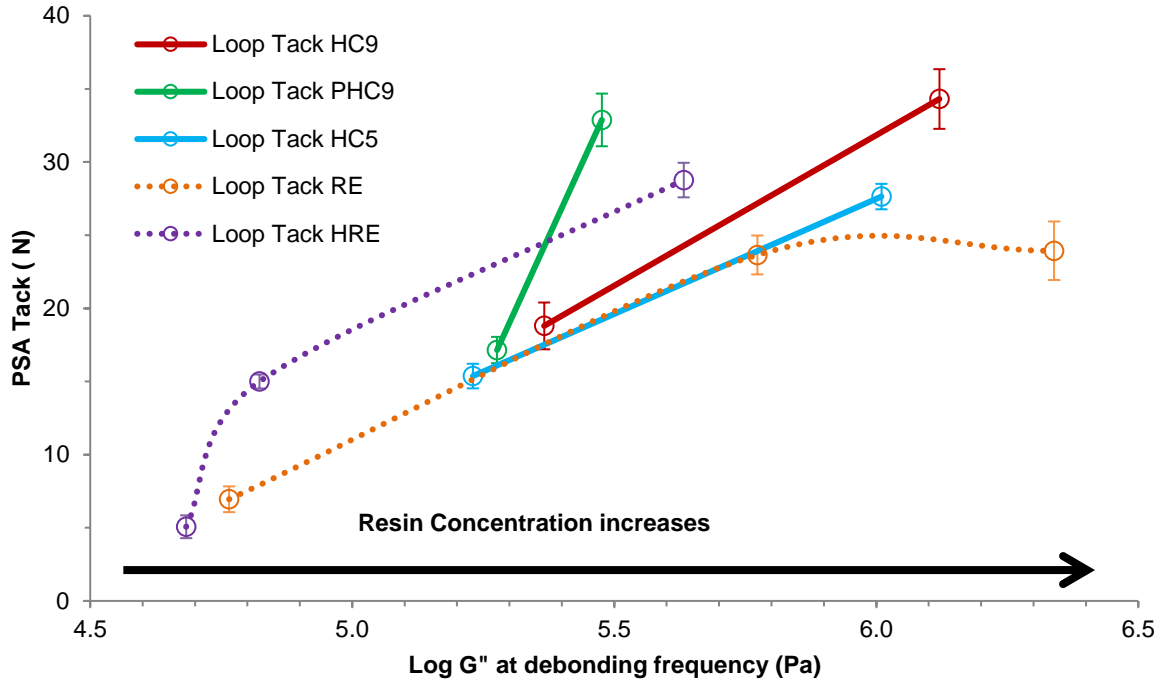


Figure 34: Loop Tack correlation with logarithm loss modulus at debonding frequency of 100 rad/s at 25 °C. Resin concentration increases in the formulation from left to right, as indicated by the black arrow.

A good compatibility between the elastomeric part of the SBC and the tackifier is important to bring pressure-sensitive characteristic to the adhesive. As previously stated, if there is a good compatibility between the polymer and the resin, a decrease in the storage modulus in the rubbery plateau region can be expected as well as an increase in glass transition temperature of the elastomeric region. Based on the results presented in section 4.1, it was assumed that a distinct compatibility degree was observed for SIS and the tackifiers investigated in this study.

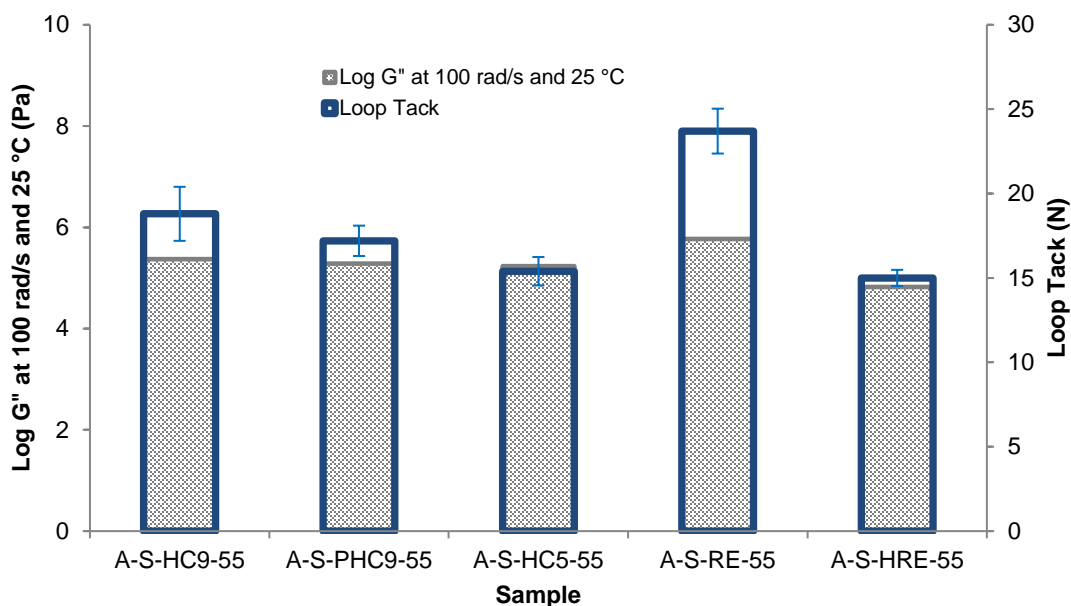


Figure 35: Logarithm of loss modulus measured at debonding frequency of 100 rad/s at 25 °C and loop tack results emphasizing the results obtained for each hot melt pressure sensitive adhesive blend containing 55 wt% of resin.

Figure 36 shows storage modulus and loss factor curves (a) and loss modulus curves (b) for neat SIS as well as for HMPSAs models containing SIS, paraffinic oil and the resins examined.

It can be seen that for all the blends, the storage modulus in the rubbery plateau region decreased to a lower level than the Dahlquist criterion value, which is highlighted by the yellow line. The yellow line is positioned in a level where G' corresponds to about 3×10^5 Pa which is known as the Dahlquist criterion.¹⁷⁰ This is recognized to be a limit modulus value for an adhesive to exhibit characteristics of a PSA at application temperature. Also, relevant shifts in glass transition temperature values are observed. As already shown, the glass transition temperature for the elastomeric part of the SIS triblock copolymer is -60 °C. Based on it, a pressure sensitive character for these blends is expected to be achieved. Further on, it can be observed from loss modulus curves in figure 36 (b) that a shift towards lower temperatures in the glass transition region of the styrenic domains occurs, which follows the same trend as observed in section 4.1. Blends containing natural resins show a higher decrease in glass transition temperature for the glassy region, followed by the partially hydrogenated C9 hydrocarbon resin and finally by the hydrogenated resins.

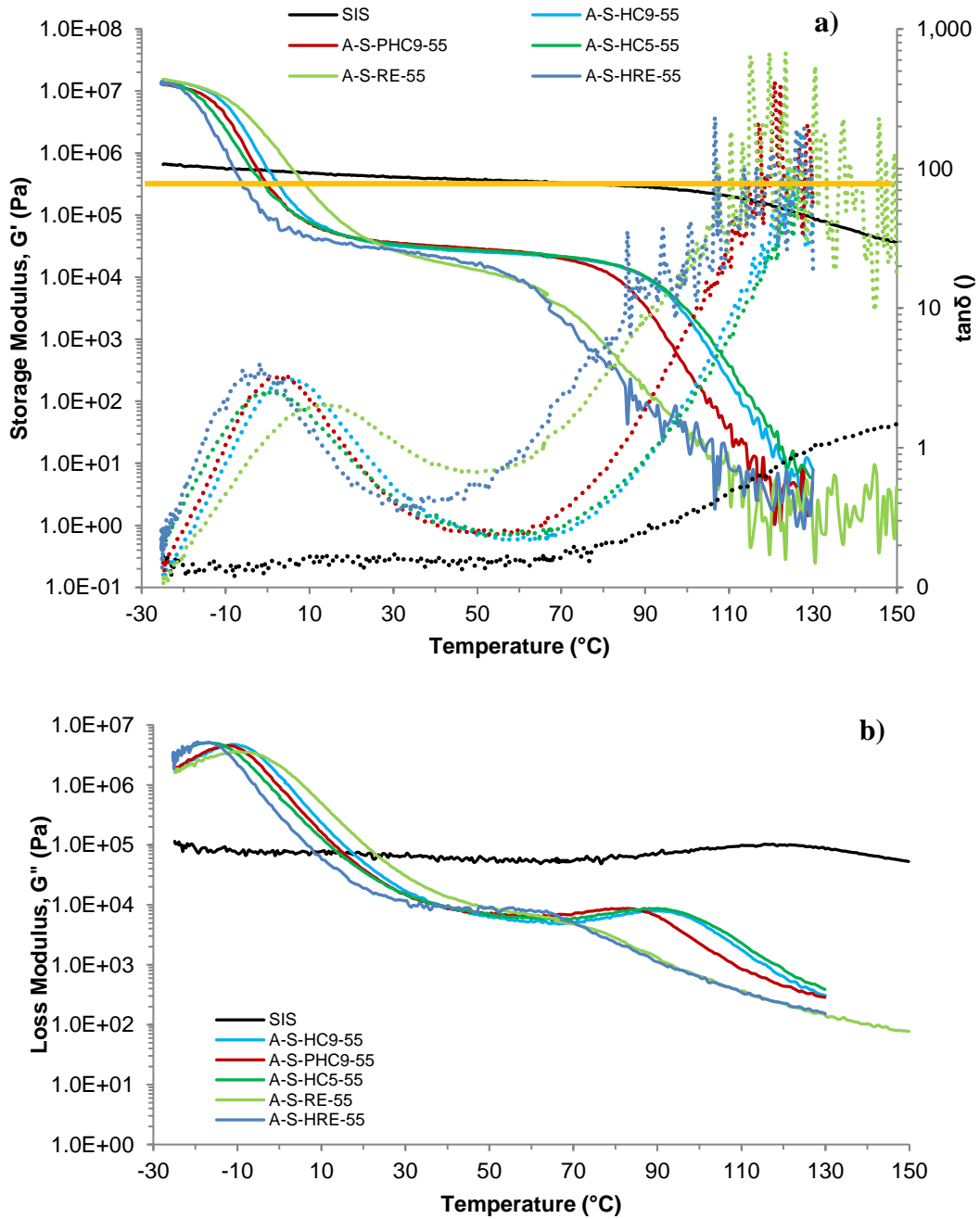


Figure 36: (a) storage modulus curves (full lines) and loss factor curves (dotted lines) and (b) loss modulus curves for hot melt pressure sensitive adhesives as well as polystyrene-block-polyisoprene-block-polystyrene copolymer. Yellow line depicts storage modulus value according to Dahlquist criterion.

Figure 37 presents the peel strength results measured against stainless steel at 25 °C for the studied blends. Indeed, all of them revealed a pressure-sensitive character with relevant peel strength values.

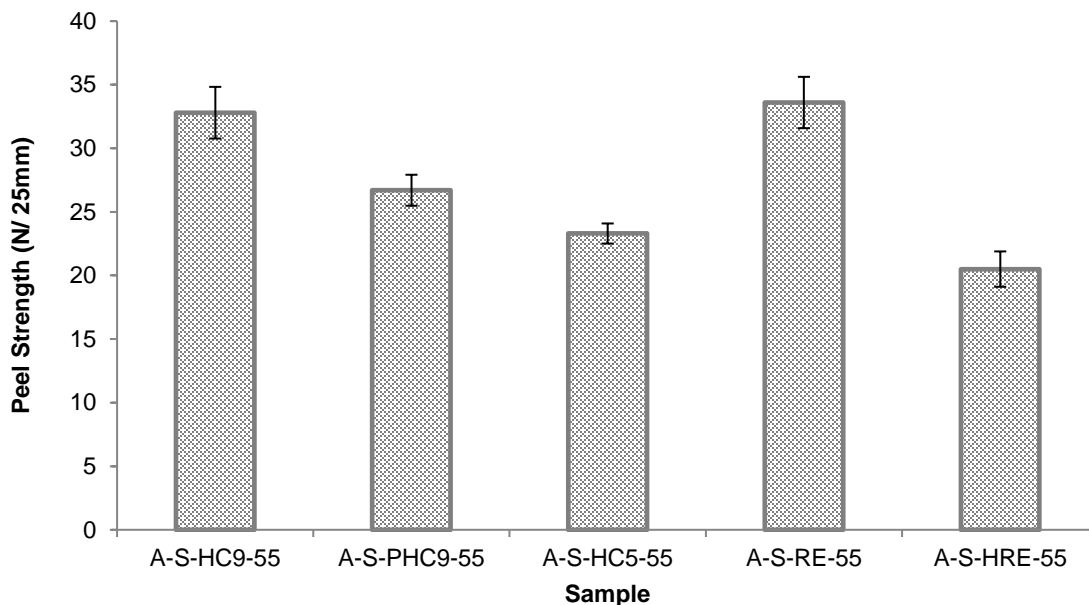


Figure 37: Peel strength results obtained for each hot melt pressure sensitive adhesive blend containing 55 wt% of resin.

As it can be expected for compatible systems, the glass transition temperatures in the elastomeric region increase with addition of a tackifying resin. Storage modulus measured at 25 °C decreases as the resin is added.

Figure 38 shows the effect of tackifier concentration in blends containing hydrogenated C9 resin in comparison to neat SIS on viscoelastic properties. The measurements were conducted between -30 °C and 130 °C, thus the glass transition temperature for the elastomeric part of neat SIS cannot be identified in these graphs. However it was demonstrated from previous measurements that the glass transition for the pure SIS is about -60 °C (figure 28). Analogous measurements were conducted for blends containing partially hydrogenated C9 resin, hydrogenated C5 resin, pentaerithritol rosin ester resin and hydrogenated rosin ester resin and are presented in appendix D.

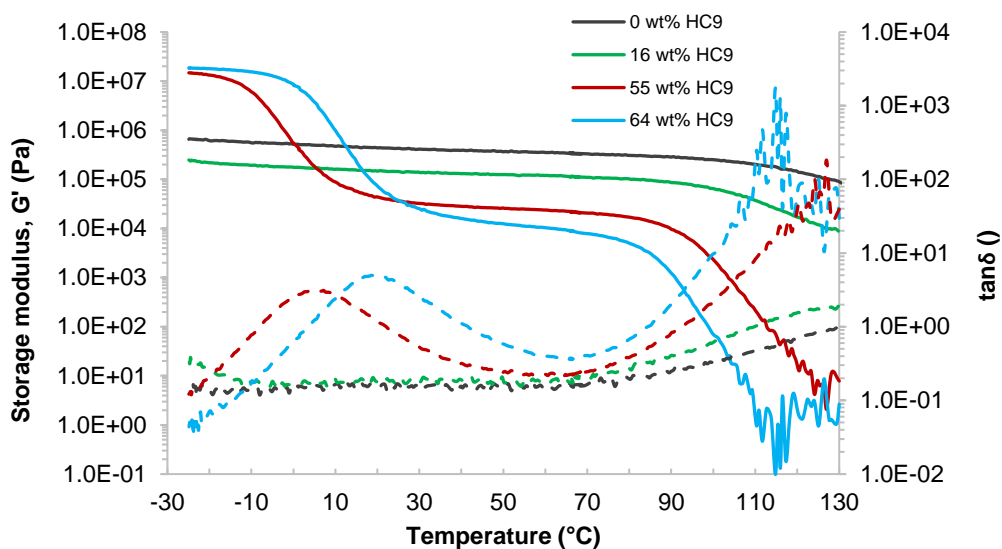


Figure 38: Storage modulus (full lines) and loss factor (dashed lines) curves for pure SIS (black curves), and 16 wt% resin (green curves), 55 wt% resin (red curves) and 64 wt% resin (blue curves) for blends comprising hydrogenated C9 hydrocarbon resin (A-S-HC9).

As seen in figure 38, a decrease in storage modulus occurred in the rubbery plateau region. Properties were determined at 25 °C. The storage moduli measured at 25 °C for all blends were lower than the G' at 25 °C of the pure SIS in the rubbery plateau region. As the tackifier concentration in the blends increased, an increase of the elastomeric glass transition temperature occurred, as can be seen by the shift in the loss factor peak temperature. The same behavior was identified for the blends containing partially hydrogenated C9 resin, hydrogenated C5 resin, pentaerithritol rosin ester resin and hydrogenated rosin ester resin (appendix D).

4.2.2 Influence of tackifier chemical structure on morphology

Morphology of the studied blends was analyzed by means of polarized optical morphology and atomic force microscopy for selected samples. Optical microscopy images are presented in figure 39 from selected samples. Figure 39 (a) shows neat SIS observed using polarized light microscope. No defined structure could be detected under optical microscopy for SIS. Figure 39 (b) presents an image for the sample HC9-140 and figure 39 (c) presents image for sample RE-140. In these two images, some particles can be identified but not the structure of the SIS. The blends were macroscopically transparent, however, it is important to bear in mind that they are not thermodynamically miscible. Such particles might be present due to an incomplete mix.

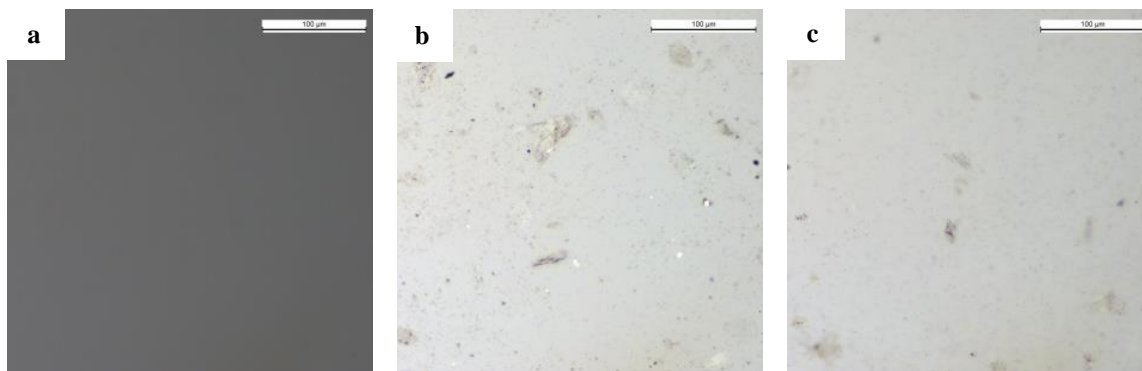


Figure 39: (a) Polarized light optical microscopy image of pure SIS; (b) Polarized light optical microscopy image of hot melt pressure sensitive adhesive blend containing hydrogenated C9 hydrocarbon resin (HC9-140); (c) Polarized light optical microscopy image of pentaerythritol rosin ester resin (RE-140). The bars in the figures represent a scale of 100 μm .

No special interpretations can be stated when comparing the polarized light optical microscopy images for the HMPSA based on hydrocarbon resin (figure 39 (b)) and the one based on pentaerythritol rosin ester resin (figure 39 (c)).

Atomic Force Microscopy images (phase mode) displayed in figure 40 present the morphology for the neat SIS (a), HMPSA blend containing 55 wt% of HC9 (b), HMPSA blend containing 55 wt% of PHC9 (c) and HMPSA blend containing 55 wt% of RE (d). In the AFM images, the darker areas correspond to softer regions in comparison to whiter/yellower areas which correspond to harder regions.

It can be observed from figure 40 (a) showing a gyroid arrangement where the lighter areas correspond to the harder styrenic domains. By investigation of blend with HC9 (figure 40 (b)), it can be seen that the styrenic domains arrange themselves in a spherical way. They can be clearly distinguished as dispersed in a matrix since the contour is very sharp. Figure 40 (c) presents a polymeric blend containing partially hydrogenated C9 hydrocarbon resin and it can be seen that the styrenic domains contour became a bit more diffuse than those in figure 40 (b). This may be understood as a better interaction between the dispersed phase and the matrix phase. This interpretation is supported by the DMA results in which it was observed that the PHC9 showed a more pronounced decrease in the glass transition temperature of the glassy region (figure 36 (b)).

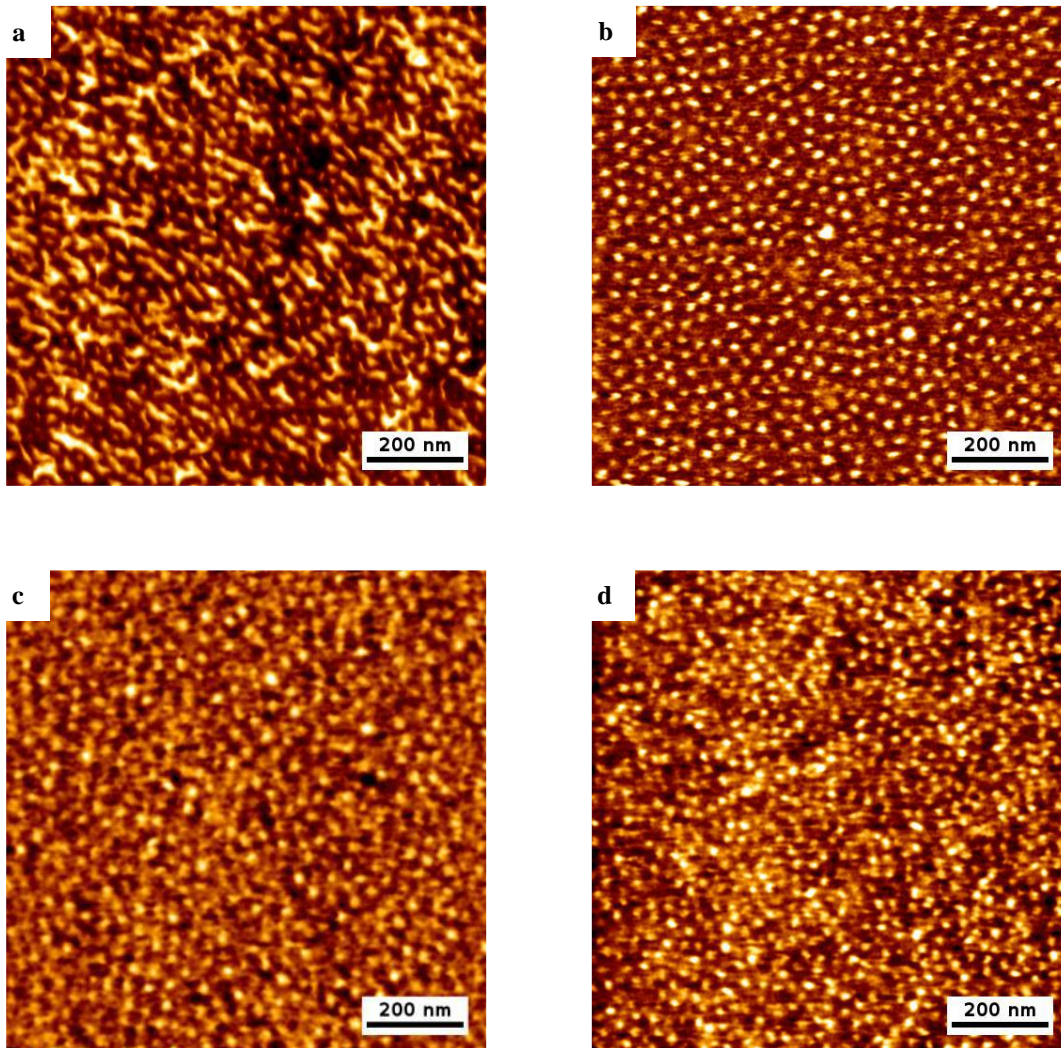


Figure 40: (a) AFM image (phase mode) of neat SIS; (b) AFM image (phase mode) of HC9-140; (c) AFM image (phase mode) of PHC9-140; (d) AFM image (phase mode) of RE-140.

In figure 40 (d) a blend containing natural resin is depicted. The styrenic domains, arranged in a spherical way, are also identified; however, the outline is somewhat less sharp in comparison to figure 40 (b). This is an indication of better interaction between the dispersed phase and the matrix. This is in line with the DMA results where a better segmental interaction between the styrenic domains and the natural resins could be observed in comparison to blends containing HC9. The observations of the AFM images are in congruence with the images displayed by O' Brien et al.¹⁵ They also investigated polymeric blends of type Kraton D1161 (SIS) and hydrocarbon resins with different aromaticity levels by means of AFM. They also observed differences in the blends morphology, especially regarding the styrenic domains, as the aromaticity level of the

resins changed. They speculated that this different morphology may be related to differences in holding power measurements performed at room temperature. They could further determine the particle's diameter size of the glassy polystyrene domains for their polymer blends and an average of 14 nm was measured for the low and intermediate aromatic containing resins while an average of 22 nm was measured for the high aromatic containing resins polymer blends.

4.2.3 Influence of tackifier chemical structure on adhesion and adhesive performance

Surface energy of both the neat materials and the blends were determined by contact angle measurements and are presented in tables 1 and 2 for pure materials. Figure 41 presents the surface energy for hot melt pressure sensitive adhesive blends containing 55 wt% of resin.

The results show that all blends possess a lower surface energy than the stainless steel plate's used as substrate for the tests. Thus, the intrinsic adhesion term P_0 is expected to be fulfilled. A direct relation between the surface energy value and the peel strength was not observed based on these data. It could only be determined that the adhesives presented a lower surface energy than the substrate's, which is a condition generally to be fulfilled for good adhesion. As previously mentioned, the viscoelastic properties of the HMPSA strongly influence the final adhesion force, here characterized by its peel strength. Nevertheless, it must be observed that the blends' surface energy is much lower than the neat components' surface energy. The combination of these components leads to a system with lower free energy than the pure components and this is helpful for the adhesion phenomenon. Thus, the thermodynamic adhesion mechanism may be one of the adhesion mechanisms occurring in such systems.

Siročić et al.¹⁷¹ studied the miscibility for a blend composed of SAN and EPDM, using high impact polystyrene as a compatibilizer.

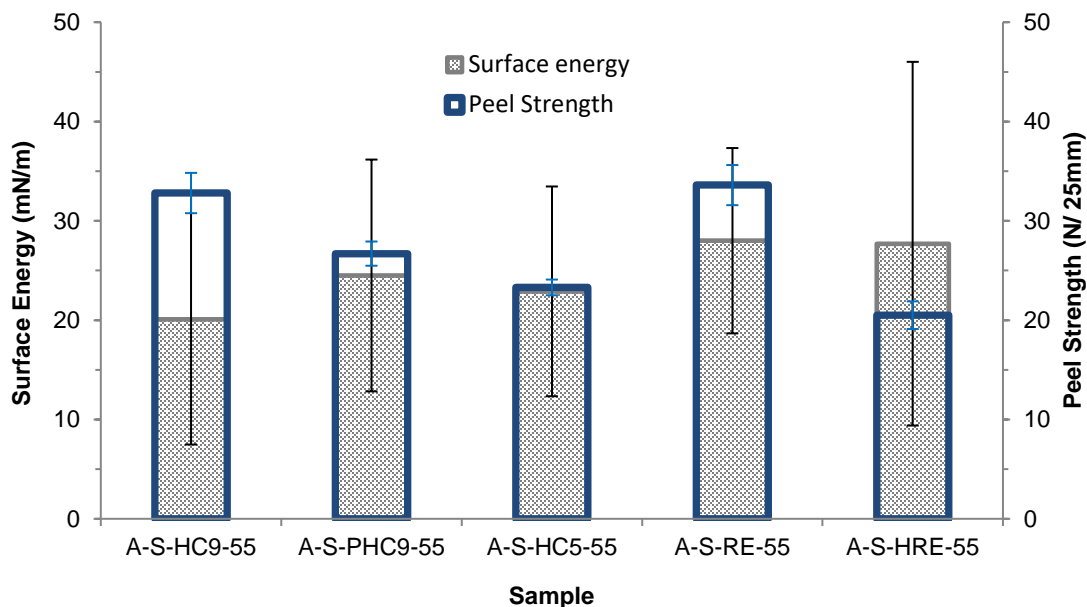


Figure 41: Surface energy and peel strength results for hot melt pressure sensitive adhesive blends containing 55 wt% of resin.

In their study, they employed the surface energy value as an indicator for the blend miscibility trend and attempted to validate what they called “minimum interfacial energy hypothesis”. The non-polar and acid-base interactions were the background for this hypothesis; when these interactions were at their highest level in a blend, the interfacial energy was at its lowest level. An attempt to illustrate this behavior is depicted in figure 42. The orange spheres represent the dispersed phase, the blue dots represent the matrix phase and the dashed blue lines represent the non-polar and acid-base interactions. According to the authors, it can be interpreted that, due to these interactions, the systems present lower surface energy values than the pure materials. These results are consistent in relation to the DMA curves which showed that these systems show a satisfactory degree of compatibility. It is also observed that the measured polar components of the surface energy values are zero or close to zero and these values are lower than the pure materials polar components. According to Siročić et al.¹⁷¹, this is an indication that the interactions between the phases present in the blends show a dispersive character.

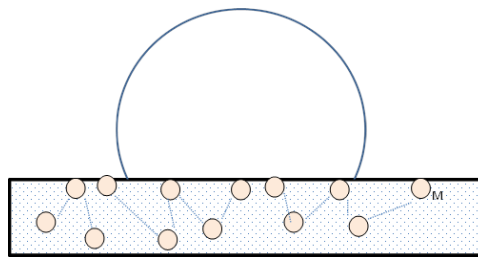


Figure 42: Schematic representation of film being measured by contact angle method. The orange spheres represent the dispersed phase and the blue dots represent the matrix phase. The connecting dashed lines represent the interactions (non-polar and acid-base) responsible for minimizing the interfacial energy of the HMPSA blend film.¹⁷¹

Figure 43 presents the surface energy measured for blends containing each analyzed tackifier as its concentration increases.

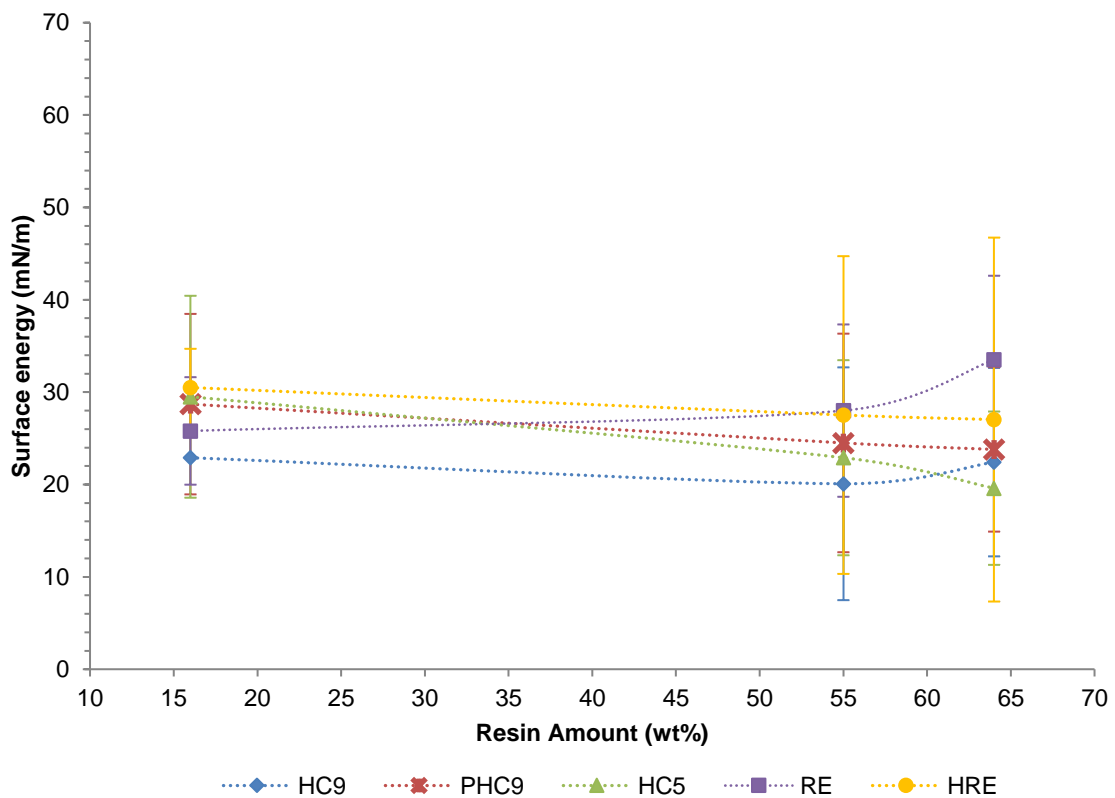


Figure 43: Surface energy of blends containing different resins as their concentration increases.

It is difficult to come to a conclusion based on these data but it might be assumed that the minimum interfacial energy for these polymer blends is achieved when a concentration of about 50 wt% of resin is present.

Adhesion shear resistance (Holding Power) is an industrial method intended to measure HMPSA shear resistance. It can be performed at room temperature or at elevated temperatures. At elevated temperatures, the failure mode (cohesion or adhesion) can be identified. However, it is not always easy to identify or to assure that only cohesive failure is happening and no adhesive (interfacial) failure is occurring. Sosson et al.¹⁷² studied the shear failure mechanism in chemically crosslinked PSAs by an own developed device in an attempt to determine in situ the PSAs failure micromechanisms. Considering the parameters analyzed, they could conclude that the crosslinking density plays an important role in the failure mechanism. For weakly crosslinked adhesive, a fluid-like behavior was observed and failure occurred due to creep. For strongly crosslinked adhesive, the results suggested a fracture failure instead of creep failure. In the present study, holding power was determined at elevated temperatures in order to accelerate the testing procedures. These temperatures were above the glass transition of the elastomeric part of SIS and below the glass transition temperature of the dispersed polystyrene domains. Thus, polystyrene domains were expected to act like physical crosslinks in the blends. It can be observed that relevant differences in holding power results were identified for natural based blends in comparison to hydrocarbon based blends, as depicted in figure 44.

From the characterization reported in section 4.1, it becomes clear that natural resins had a better interaction degree with the polystyrene, and a higher shift in the glass transition temperature occurred for polystyrene. Thus, chain mobility was aided at lower temperatures in comparison to blends using hydrocarbon resins, as seen in figure 36. The fluid-like behavior started at lower temperatures for natural resins based blends. This can be also observed in figure 36 (b) where the loss modulus curves displayed a larger shift in glass transition temperature of the glassy region for blends employing natural resins. Further on, in figure 36 (a) the entanglement density expressed by the horizontal G' values (G'_e) was higher for hydrocarbon resins based blends. This gives a contribution to the shear resistance.

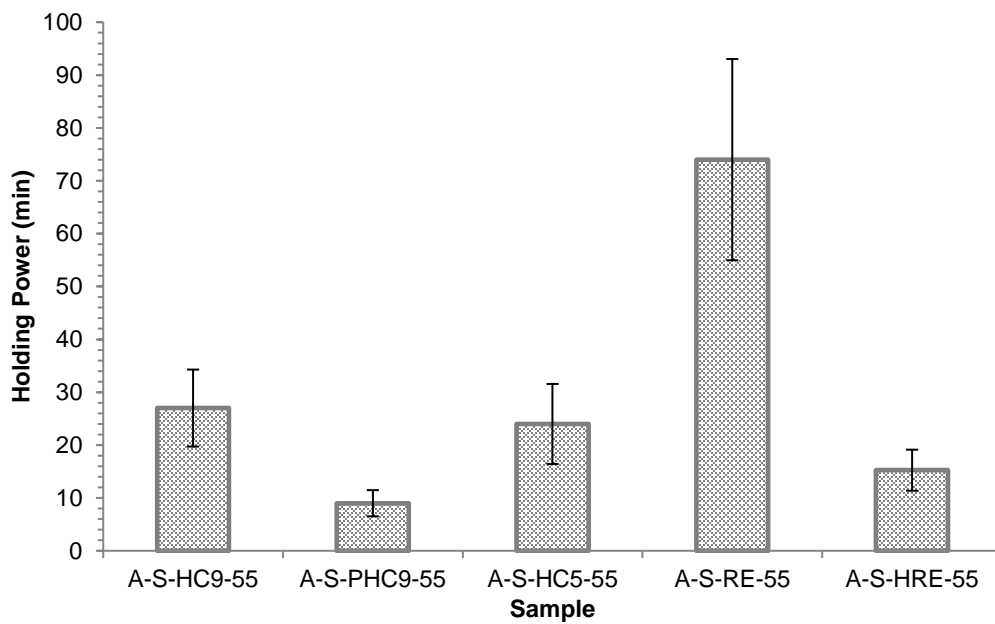


Figure 44: Shear adhesion holding power results determined at 60 °C for hydrogenated C9, partially hydrogenated C9 and hydrogenated C5 resins and at 40 °C for pentaerithritol rosin ester and hydrogenated rosin ester resins.

O' Brien et al.¹⁵ studied the effect of aromaticity degree in aliphatic hydrocarbon resins in PSAs. They stated that when observing the third cross-over point, meaning where $G' = G''$ ($\tan\delta=1$) at around 70 °C to 90 °C in the present systems, a reasonable correlation was observed between the third cross-over temperature and the shear-adhesion failure temperature test. A reasonable correlation was observed in the present study as well, as shown in figure 45, which confirmed the statement from the authors.¹⁵ The meaning of this point is that the temperature at which elastic and viscous moduli are the same and after this point for such systems, viscous behavior prevails. According to the authors, this happens as the styrene domains soften and begin to flow. From the compatibility study, this may be indeed correlated to the polystyrene domains starting to soften. Exactly those resins which showed a higher compatibility to polystyrene phase, in which a higher shift of the dispersed phase loss factor peak to lower temperatures occurs, are those, in which the cross-over temperatures are lower. Consequently, it results in lower shear adhesion failure temperature values. Shear adhesion failure temperature (SAFT) test is a measurement of material bulk cohesion and it is related to the polymer glass transition temperature. Figure 46 presents the adhesive performance results in relation to the blends resin concentration.

As it can be seen in general, as resin concentration increases peel strength increases and holding power decreases. This is a general result essentially observed overall for PSAs.

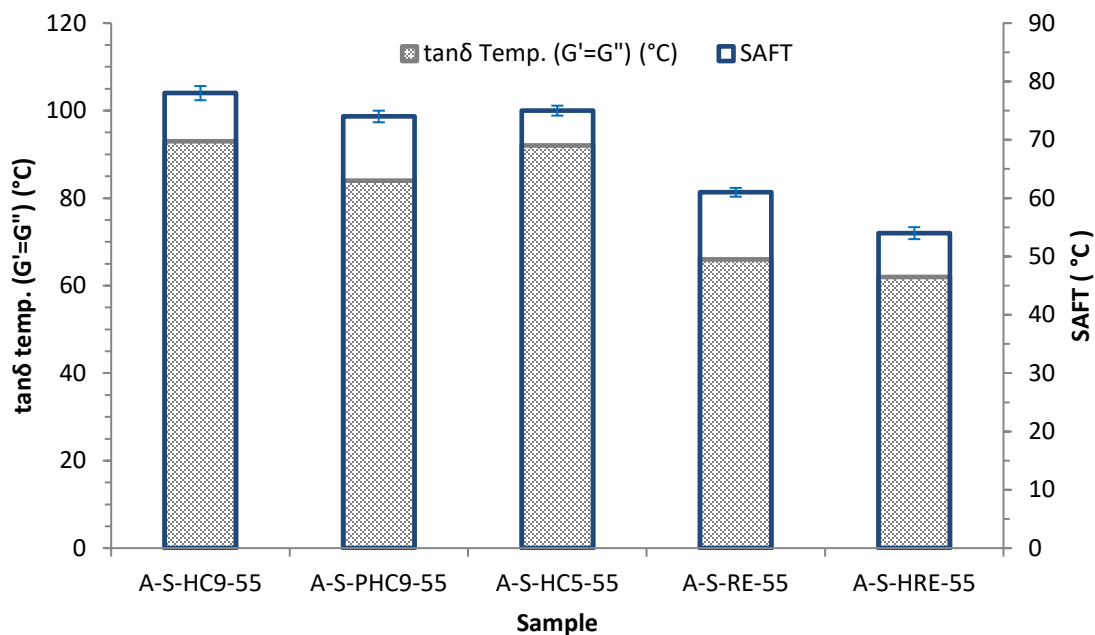


Figure 45: Loss factor temperature at the third cross-over point, i.e. at $G'=G''$ and shear adhesion failure temperature (SAFT).

As the tackifier concentration increases and the thermoplastic elastomer concentration decreases, the storage modulus in the plateau region decreases and this leads to lower peel strength.

For the holding power, it can be understood that less polystyrene is present in the formulation which means less physical cross-links and due to the interaction of polystyrene and tackifier, as the tackifier amount increases, the glass transition temperature in the glassy part shifts to lower temperatures.

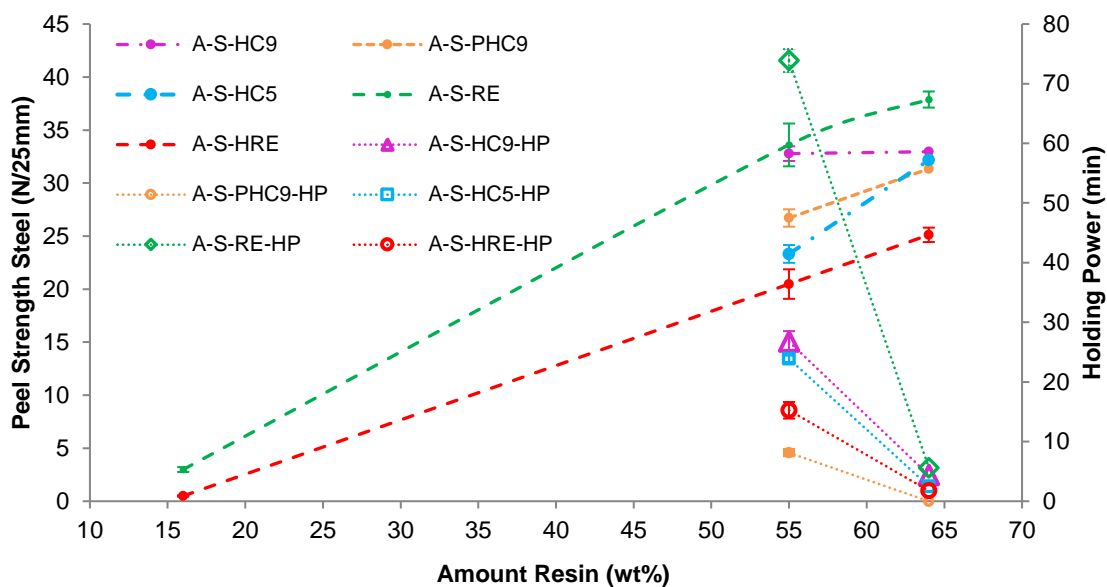


Figure 46: Adhesive performance (peel strength and shear adhesion holding power) in correlation to resin concentration.

4.3 Influence of processing on properties and performance of hot melt pressure sensitive adhesive blends

4.3.1 Overview

HMPSA's blends were prepared by following identical formulation for each investigated tackifier type. Mixing and coating were carried at 140 °C or at 165 °C. A processing parameter effect investigation, in this case the temperature, was conducted and the outcomes are discussed in this chapter. Hot melt PSAs were blended by mechanical mixing and coated using slot die coating technology, which are very different processes in comparison to solvent based PSAs. Several authors^{17,19,10} investigated morphology and final properties of solvent born adhesives but not so many investigations were conducted on mechanically blended PSAs. Some authors¹⁵ state that solvent blending of PSAs is preferred for a research when comparing materials involved in the blends due to processing effects on adhesive performance, for example temperature and shear rate. On the other hand, solvent blending influences the PSA morphology.¹² Since hot melt pressure sensitive adhesives were investigated in this present study, mechanical melt mixing and melt coating were performed and an attempt to understand process parameter influence on adhesive performance was conducted.

4.3.2 Influence of processing conditions on viscoelastic behavior

Viscoelastic properties of the blends were explored by means of DMA measurements (Figures 47 and 48).

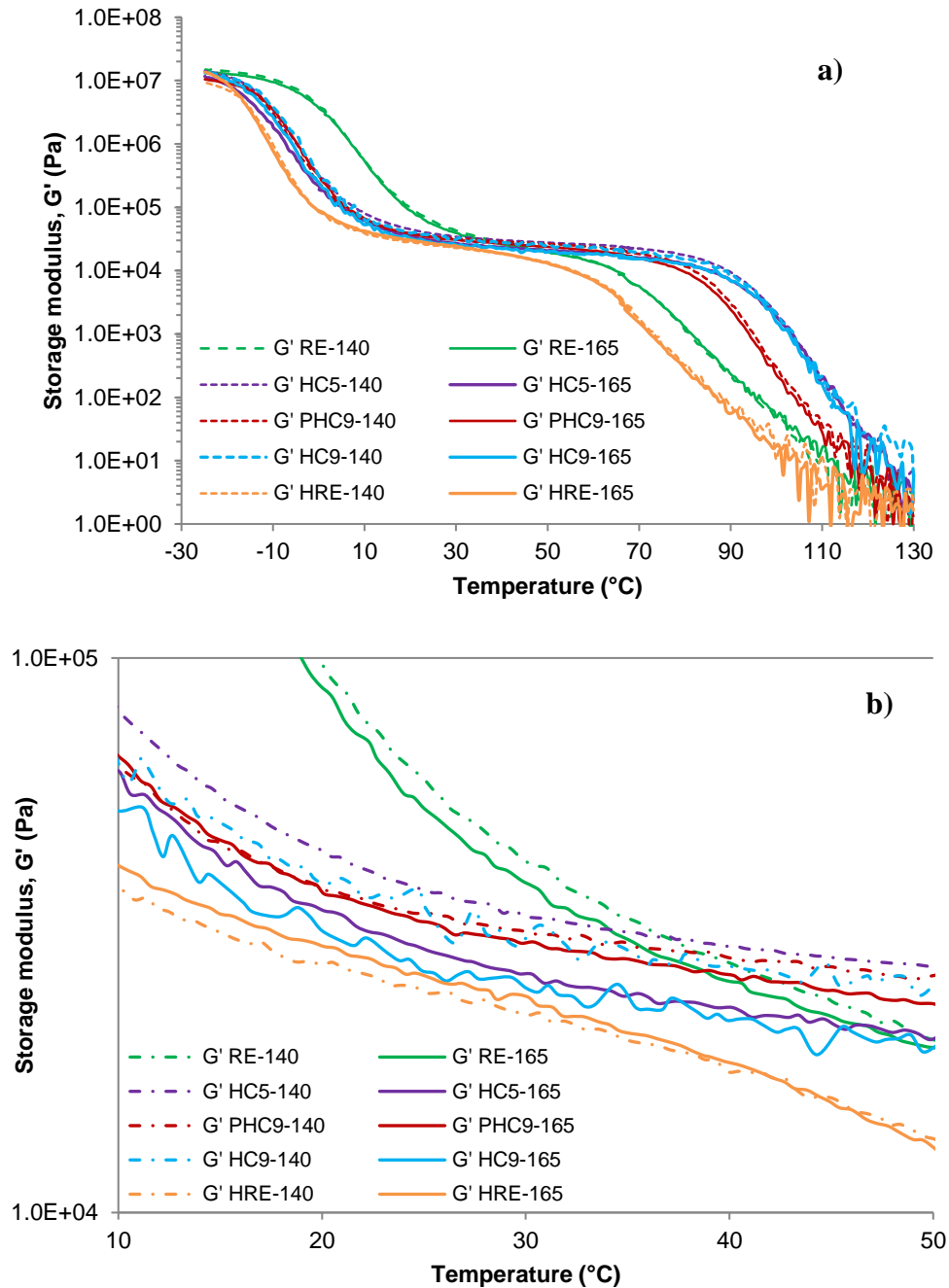


Figure 47: Storage modulus curves for blends processed at 140 °C and at 165 °C (a). A zoomed graph is shown (b) at around 25 °C, i.e. properties measurement temperature.

For most of the blends, independent on the tackifier chemistry involved, slightly higher storage moduli were obtained at 25 °C for blends processed at 140 °C. A deviation was noticed for samples involving HRE resin. The storage moduli determined for this sample at 140 °C and 165 °C were indeed very similar, however, this result was unexpected.

Loss modulus curves are shown in figure 48 and it can be observed that when comparing a pair of the same resin processed at 140 °C and at 165 °C, the elastomeric glass transition temperatures are the same. When comparing the glassy region glass transition temperature for the same situation, they are also the same. Thus, it can be understood that the interaction of the tackifier and the styrenic domains are the same for blends processed at 140 °C and at 165 °C.

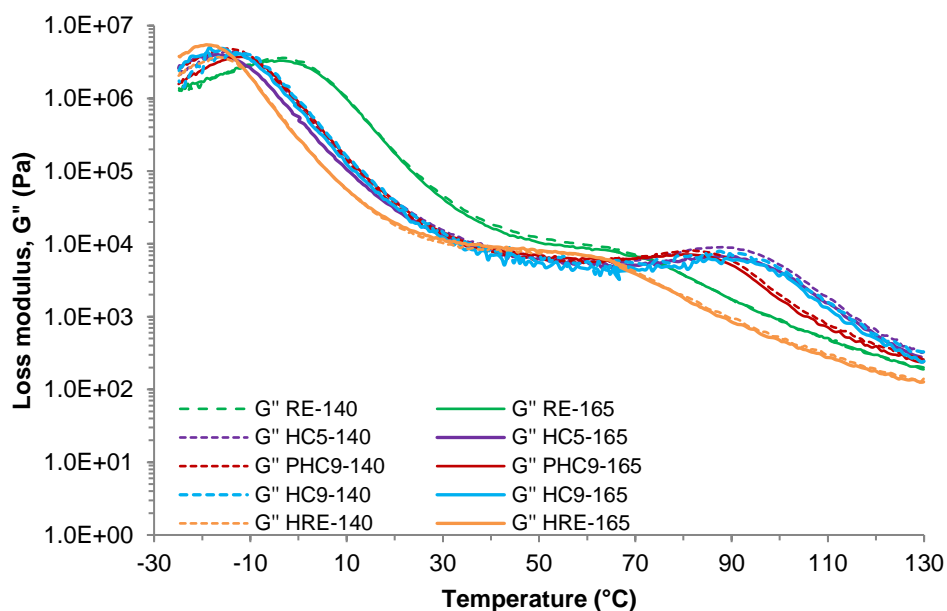


Figure 48: Loss modulus curves for blends processed at 140 °C and 165 °C.

Viscosity measurements determined by Brookfield viscometer at 140 °C (figure 49) for all samples revealed that higher viscosity values were identified for blends processed at lower temperature, independent on the chemical structure. This fact points either to a higher thermo-mechanical destruction when processing at higher temperatures or to different mixing degrees, hence resulting in different morphologies leading to different rheological behavior.

4.3.3 Influence of processing conditions on tensile strength

Mechanical properties were measured at room temperature and figure 49 presents tensile strength results of the samples involved.

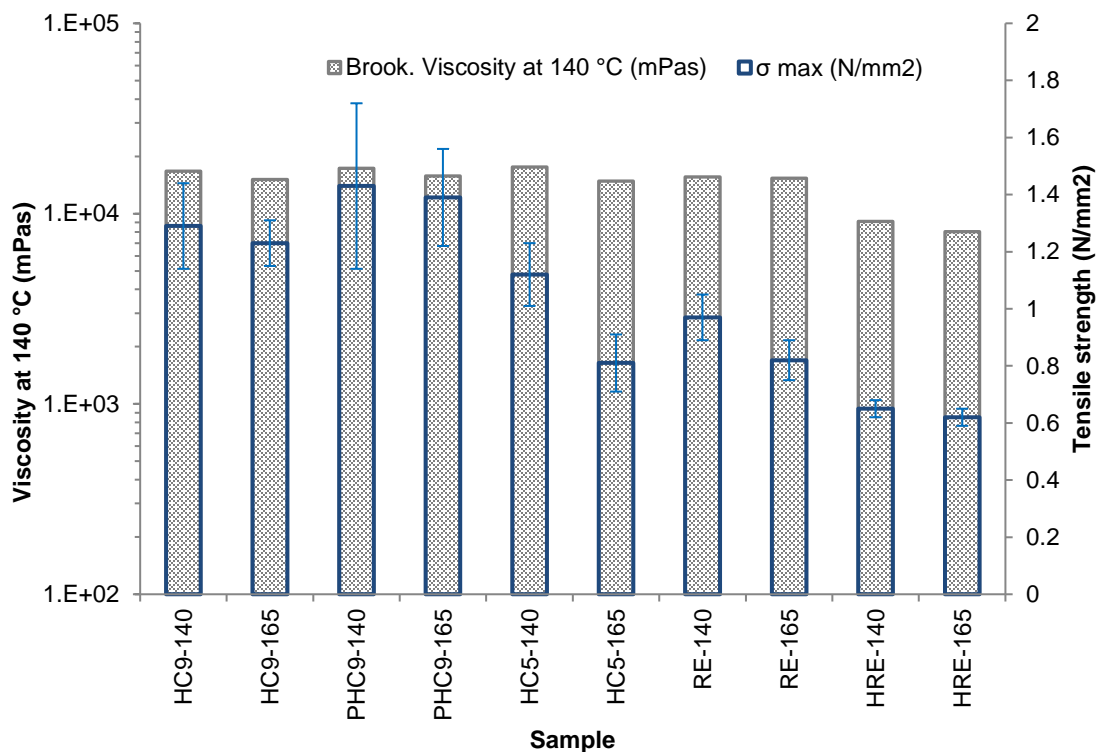


Figure 49: Brookfield viscosity measured at 140 °C and tensile strength results for blends processed at 140 °C and at 165 °C.

Although small differences in tensile strength are observed, a clear trend exists showing that for mixtures processed at lower temperatures, higher tensile strength values are identified. These results are in congruence with storage moduli determined at 25 °C. The results of storage modulus, viscosity and tensile strength for blends processed at 140 °C in comparison to 165 °C led to the conclusion that SIS chains degradation might have occurred, as discussed before concerning viscosity. From literature, such effect is also reported for HMPSAs.¹⁵

4.3.4 Influence of processing conditions on morphology

Blends of model PSA were investigated by means of atomic force microscopy.

By stress-strain test results, viscosity, DMA, peel strength and holding power, it could be confirmed that differences on properties indeed occurred when processing and coating the same adhesive formulation under different temperatures. Further on, tensile strength results supported this assumption as well as the viscosity results. Smaller particles mean higher particles surface area, helping to increase particles friction in the blend which led to a higher blend viscosity.

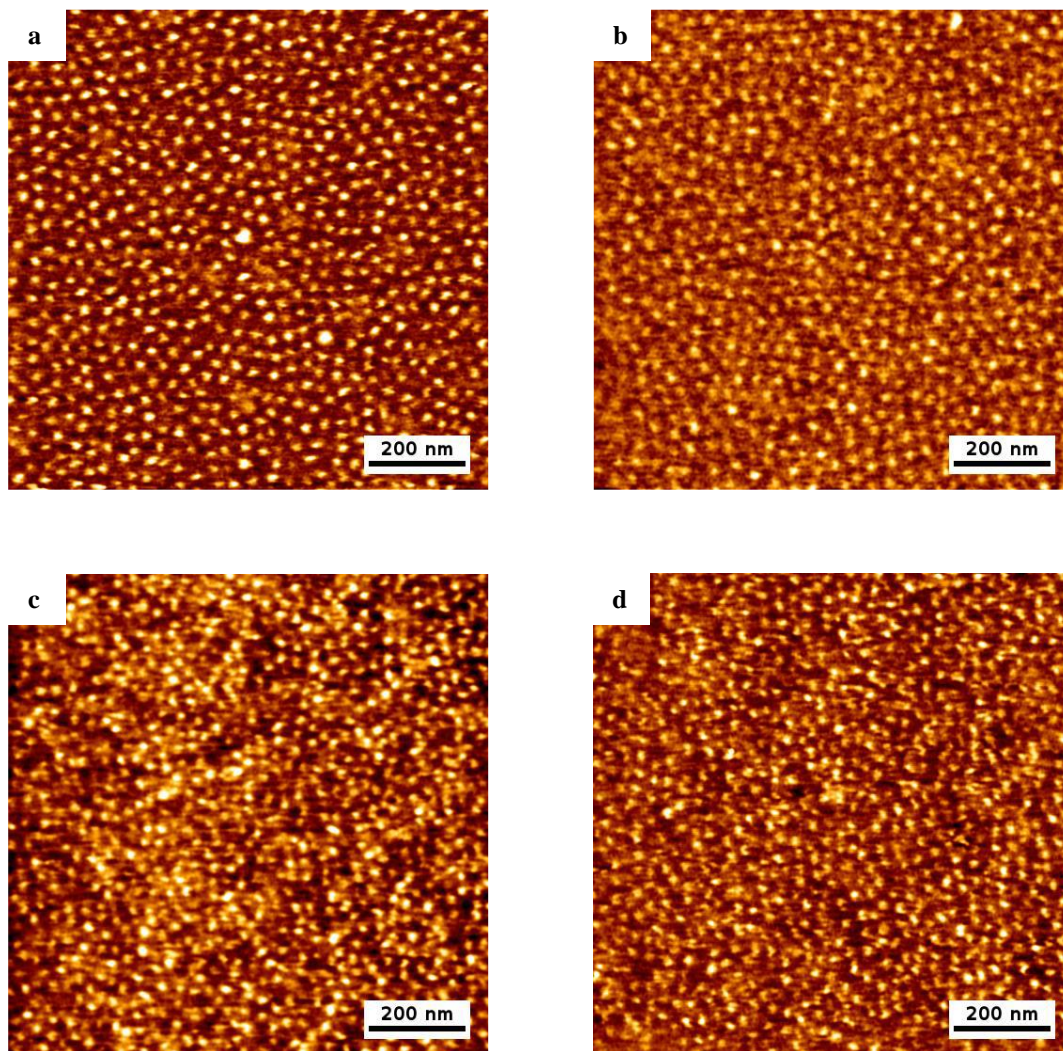


Figure 50: (a) AFM image (phase mode) of HC9-140 ; (b) AFM image (phase mode) of HC9-165 ; (c) AFM image (phase mode) of RE-140; (d) AFM image (phase mode) of RE-165

Atomic Force Microscopic images for the blends containing hydrogenated C9 resin processed at 140 °C and at 165 °C are presented in figure 50, as well as blends containing rosin ester resin processed at 140 °C and 165 °C. No essential differences can be identified

regarding the styrenic domains when comparing blends containing hydrogenated C9 hydrocarbon resins processed at 140 °C (figure 50 (a)) or at 165 °C (figure 50 (b)). In the same manner, no essential differences among the styrenic domains were observed when comparing images containing rosin ester resin blend processed at 140 °C disclosed in figure 50 (c) and processed at 165 °C shown in figure 50 (d). These observations are in congruence with the results measured by means of dynamic mechanical analysis. Although no particle size distribution or further statistical analysis by means of AFM was conducted, merely based on RE-140 image (figure 50 (c)) and RE-165 image (figure 50 (d)), a more inhomogeneous image can be identified at figure 50 (c) since larger brighter regions are found in the middle and larger darker areas in the right-hand side. This observation might be connected to different mixing degrees when processing at different temperatures. This assumption is in congruence with the results obtained by Brookfield viscosity measurements.

4.3.5 Influence of processing conditions on adhesion and adhesive performance

Surface energy results show a trend of higher values for blends processed at 165 °C than for those processed at 140 °C, except for resin HC5 as displayed in figure 51. All of the blends present lower surface energy values than stainless steel, thus a bond formation for all these materials are expected to be achieved and indeed confirmed by good peel strength results (figure 51). When a better compatibilization of the blend is achieved, a lower interfacial tension is achieved and a better adhesion between the phases is expected to occur leading to better mechanical properties. This is supported by the tensile strength values measured for such blends independent on the tackifier chemistry. Besides, it is assumed that particles present in blends processed at 140 °C are smaller than particles present in those processed at 165 °C. This also assists in decreasing the interfacial tension between the components in the blend.¹³²

Figure 52 shows the schematic explanation of the differences observed between blends processed at 140 °C and at 165 °C when their films contact angle were measured. The orange spheres represent the dispersed phase whilst the dotted blue area represents the matrix phase. Figure 52 (a) represents the situation of finely dispersed phase. Due to better interactions and compatibilization of the materials, the surface energy values were lower

than in the situation depicted in figure 52 (b). Coarser dispersed phase was expected to be identified in this situation since the surface energy values measured were higher. In this case, the measurement result was more influenced by the matrix.

When a weaker interaction occurs between the phases, it is expected the surface to be enriched by the lower molecular weight polymer due to conformational entropy of the polymer chains.¹⁷¹ This supposition could not be confirmed by the AFM, which is a suitable tool for this analysis, due to the very soft and sticky nature of the samples.

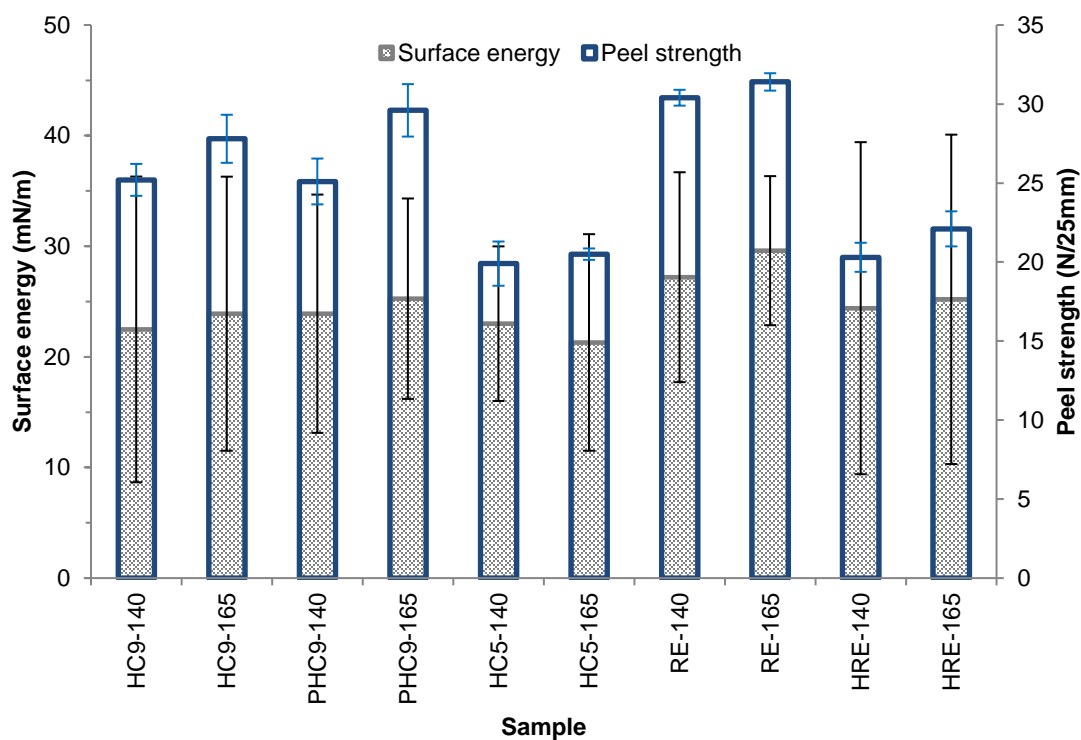


Figure 51: Surface energy and peel strength results for hot melt pressure sensitive adhesive blends containing 55 wt% of resin; mixed and coated at either 140 °C or 165 °C.

Peel strength values were higher for polymer blends processed at higher temperatures (figure 51). Considering the work of Tse¹⁴⁶, equation 21 states that peel strength is influenced by both surface and viscoelastic properties. Considering the surface energy results, the adhesion term was higher for HMPSAs processed at 140 °C. Considering viscoelastic properties such as viscosity, storage modulus and loss modulus, the B and D terms were higher for HMPSAs processed at 165 °C. As a result, it can be observed that even though only small differences in the viscoelastic properties were achieved for the

polymer blends processed at different temperatures, these differences were related to different peel strength results and it overcame surface properties effects.

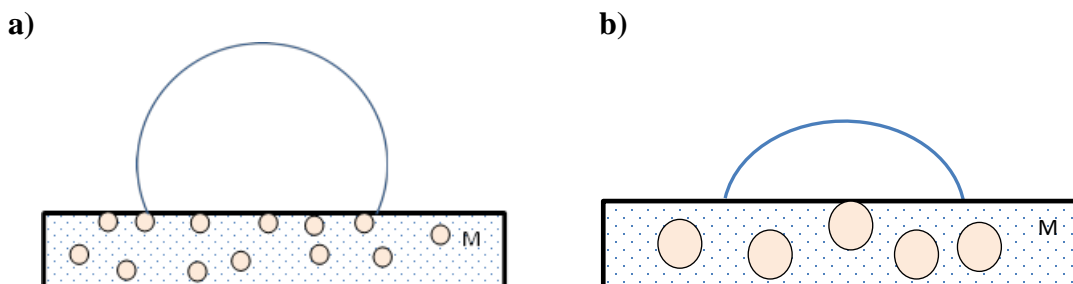


Figure 52: Schematic representation of film measured by contact angle method. The orange spheres represent the dispersed phase and the blue dots represent the matrix phase. For the system with finely dispersed phase (represented in (a)), the surface energy measured was more influenced by the better compatibilized (interacted) system and the system with coarser dispersed phase (represented in (b)), the measurement was more influenced by the matrix surface energy value.

Shear adhesion holding power measured at 60 °C (at 40 °C for HRE based blend, since values could not be detected at 60 °C) was determined for the blends studied in order to understand about blends cohesion and the results are displayed in figure 53. Holding power test is a method, in which high deviation values are detected. However, a very good congruence is identified for all samples independent on the tackifier employed. A decrease in shear adhesion is expected from practical work when blends are processed at higher temperatures and higher shear rate since a reduction of molecular weight occurs.¹⁵ Shear rate during mixing process was kept constant in this present work and indeed lower holding power values were measured for blends processed at higher temperatures. As observed from loss modulus curves, no differences in glass transition temperature were observed when comparing a pair of tackifier processed at 140 °C and at 165 °C. Further on, no differences were observed in the AFM images for the styrenic domains when comparing blends containing the same tackifier but processed either at 140 °C or at 165 °C. This supports the conclusion that the processing temperature influences the holding power results but probably not due to an effect on the physical crosslinks derived from the styrenic domains. Instead, the reason for this behavior might be connected to the molecular weight of the SIS.

In summary, no differences were observed concerning styrenic domains interaction with the tackifiers when processed at different temperatures but considering the same type and

concentration of resin. Differences which might be associated with molecular weight decrease due to SIS chain scission degradation were perceived. Differences in surface energy which might be associated with process parameters were observed. Molecular weight directly affected holding power.

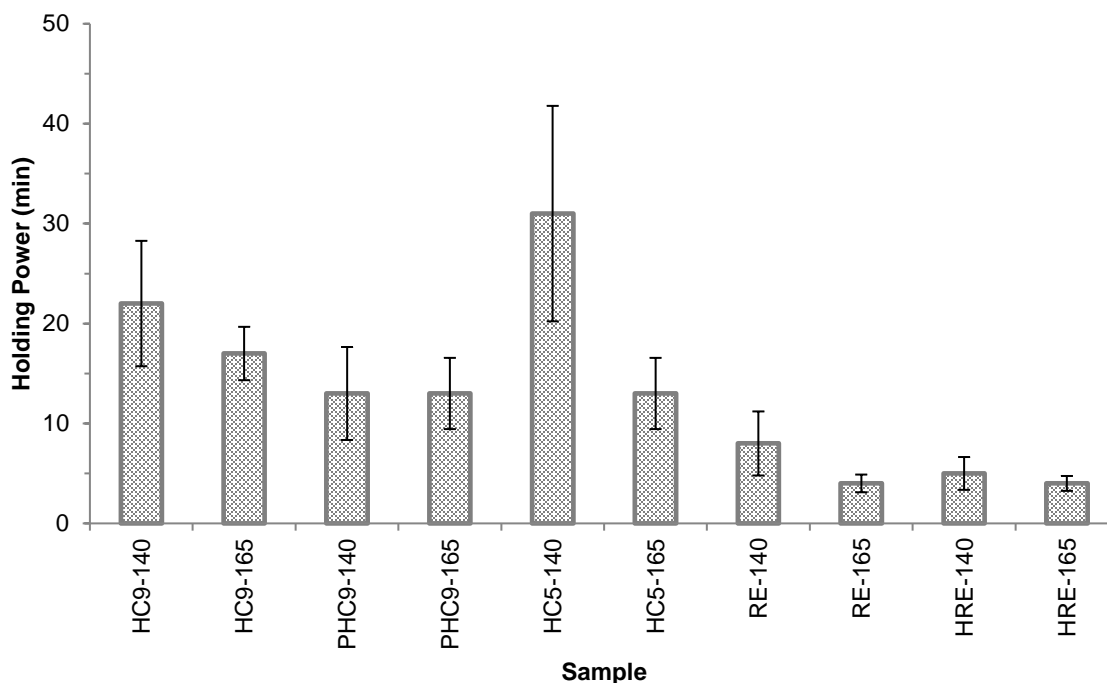


Figure 53: Shear adhesion holding power results for hot melt pressure sensitive adhesive blends containing 55 wt% of resin; mixed and coated at either 140 °C or 165 °C.

4.4 Influence of backbone polymer on properties and performance of hot melt pressure sensitive adhesive blends

Typically hot melt pressure sensitive adhesives are formulated with styrenic block copolymers being employed as the so called “backbone polymer”, as it has been shown through this work. With the introduction of the polymerization technique “chain shuttling polymerization”, synthetization of block copolymers of olefins with relevant structure and properties as well as economically encouraging production could be established.^{60,173} As shown in some works,^{5,6,71} olefin block copolymers produced from ethylene and 1-octene are suitable for HMPSAs blends due to their rheological properties, which are similar to SBCs. Figure 54 presents the storage and loss modulus curves as well as loss factor curves measured in torsion mode for neat SIS and neat EOBC employed in this work. It can be

seen that the loss modulus peaks as well as the loss factor peaks temperatures were similar for both materials evidencing a similar glass transition temperature for the elastomeric part for both of them as well as a well-defined rubbery plateau region. However, higher storage modulus was seen for the EOBC and ramp-like behavior in this region. In their study, Shan et al.⁷¹ obtained blends based on EOBC with suitable characteristics for a PSA only when high amounts of tackifier and plasticizers were used due to the high stiffness of the EOBC.

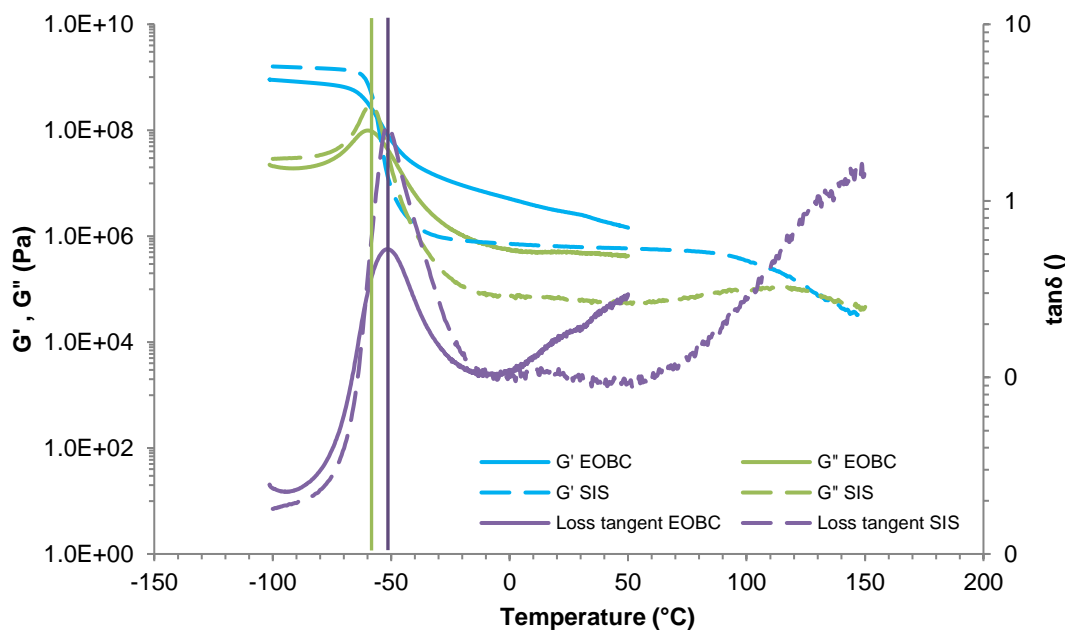


Figure 54: Temperature sweep torsion mode (MCR 501 device) for neat SIS and neat EOBC. The purple vertical line highlights the maximum of the loss factor curve at the elastomeric region of both polymers, indicating the glass transition temperature. The green vertical line indicates the maximum of loss modulus curves for both polymers at the glassy region (this peak can also be used to identify the glass transition temperature).

4.4.1 Viscoelastic properties of poly(ethylene-co-1-octene) block copolymer based blends as hot melt pressure sensitive adhesives

Viscoelastic properties of the EOBC based blends were investigated by means of dynamic mechanical analysis.

Figure 55 (a) presents storage modulus for compounds based on EOBC, oil and different classes of tackifying resins used here as well as neat EOBC; loss factor curves are shown in figure 55 (b) for the same compounds and material.

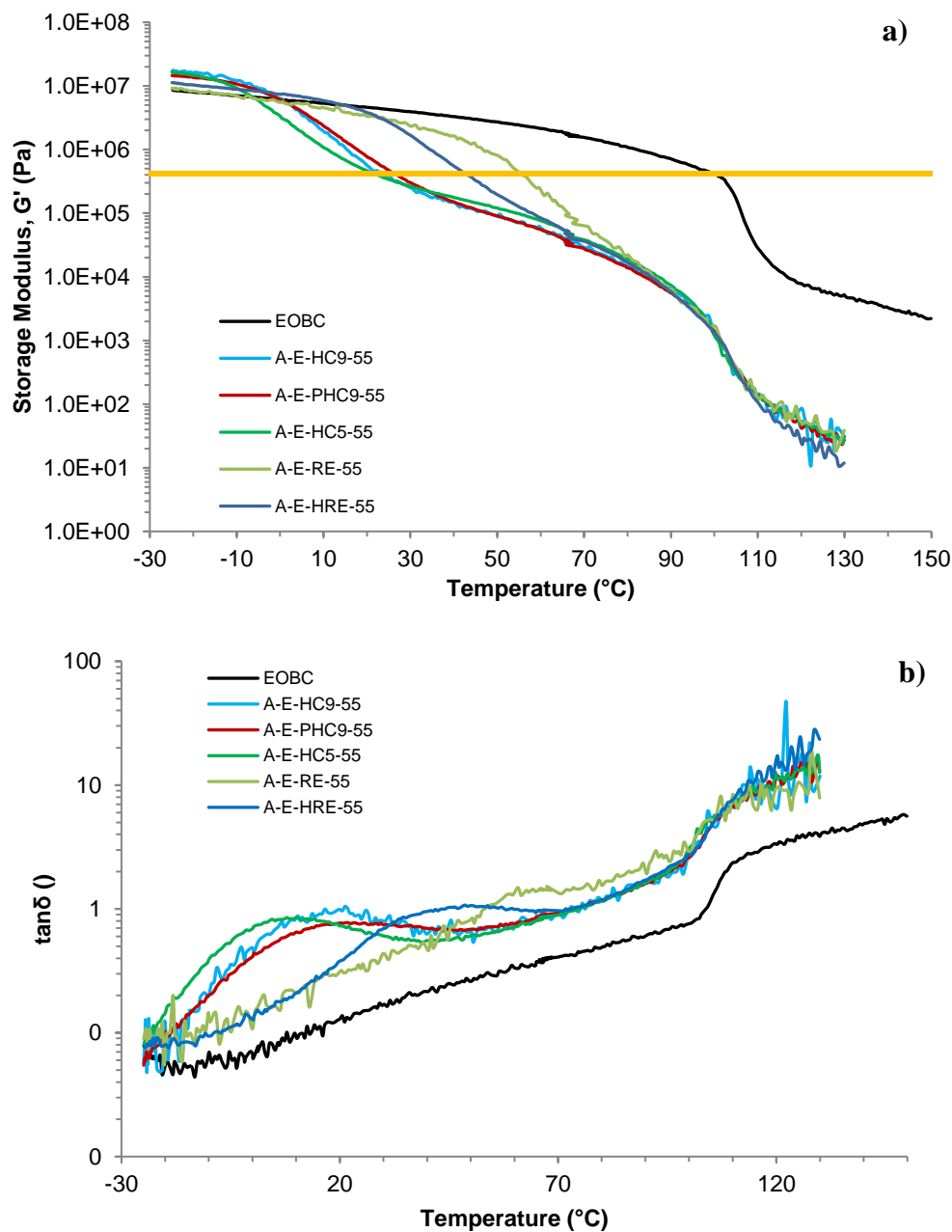


Figure 55: (a) Storage modulus curves for neat EOBC and blends based on different tackifiers. Yellow line showing modulus fulfilling Dahlquist criterion.¹⁷⁰ (b) Loss factor curves for neat EOBC and blends based on several tackifiers.

The yellow line depicted in figure 55 (a) is positioned in a level where G' corresponds to about 3×10^5 Pa, which is known as the Dahlquist criterion.¹⁷⁰ This is recognized to be a limit modulus value for an adhesive to exhibit characteristics of a PSA at application temperature. It can be seen that together with the pure EOBC compounds based on natural resins show G' at room temperature region higher than the Dahlquist criterion. Compounds

based on partially and fully hydrogenated C9 hydrocarbon resins are in a borderline region and compound based on hydrogenated C5 hydrocarbon resin presents the lowest value.

As exposed in equation 21, from Tse et al.^{86,146} work, it can be considered that the requirements to establish a bond are not achieved for polymer blends containing natural resins and fulfilled for the hydrogenated C5 hydrocarbon resin blend. Hydrogenated and partially hydrogenated C9 hydrocarbon resins are in a boundary region. Figure 56 presents values of loop tack and logarithmic loss moduli for the EOBC based blends. A conclusive correlation is difficult to state since only HC5 resin based blend presented some tackiness, and thus correlating with the debonding term, D. However, it can be understood that when the bonding was never formed, no tackiness (and debonding) was achieved.

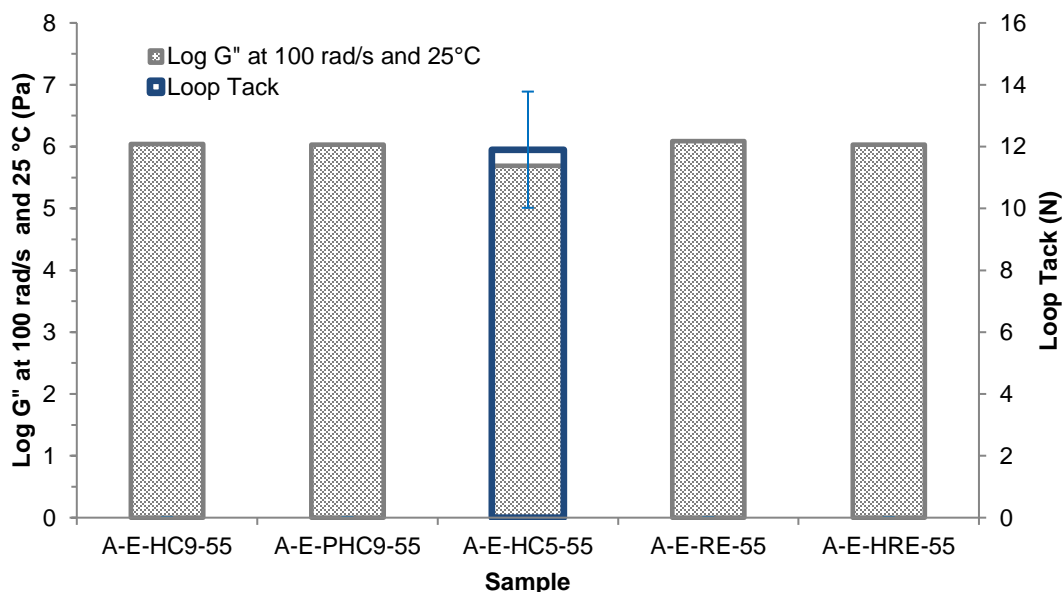


Figure 56: Logarithm of loss modulus measured at debonding frequency of 100 rad/s at 25 °C and loop tack results emphasizing the results obtained for each hot melt pressure sensitive adhesive blend containing 55 wt% of resin based on poly(ethylene-co-1-octene) blends.

These viscoelastic results reaffirm the importance of good compatibility between backbone polymer and tackifier based on the chemistry nature of the tackifier. They also highlight the importance of viscoelastic properties of the blends on the pressure sensitive adhesive strength. It is interesting to note that even for lower G'' values at high frequency and 25 °C obtained for SIS based blends (A-S-HC9-55, A-S-HRE-55, A-S-HC5-55, A-S-PHC9-55)

in comparison to EOBC-based blends (A-E-HC5-55), tackiness is higher for SIS based blends. This suggests that not only the viscoelastic properties are correlating with HMPSAs tackiness.

4.4.2 Morphology of poly(ethylene-co-1-octene) block copolymer based blends as hot melt pressure sensitive adhesives

Optical microscopy images are presented in figure 57. Selected blends were analyzed by means of this technique. Figure 57 (a) shows an image of neat EOBC under polarized light. Spherulites can be identified, as expected for this type of material. Figure 57 (b) is an image of blend containing hydrogenated C9 hydrocarbon resin. This blend is similar, regarding formulation, to those measured for SIS based HMPSA under such magnification. Dispersed particles are observed, heterophase blend, but the spherulites observed in the neat EOBC can no longer be identified. From section 4.1, it was observed that a good compatibility degree was identified for EOBC and HC9 blends. Figure 57 (c) presents a HMPSA blend containing natural resin RE. Spherulites cannot be identified and separated phases are apparently present. Furthermore, the blend was macroscopically opaque.

From section 4.1, two glass transition temperatures were detected and a poor degree of compatibility for such blend was understood.

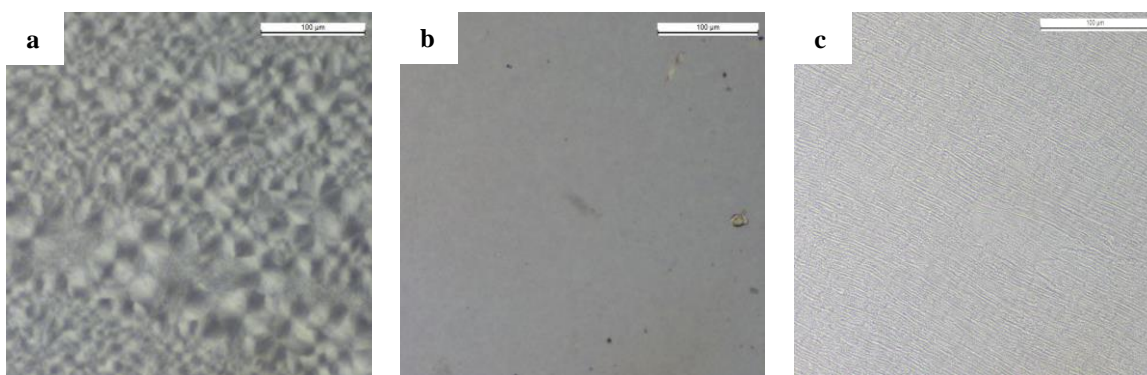


Figure 57: Polarized light optical microscopy of (a) neat EOBC; (b) A-E-HC9-55; (c) A-E-RE-55. The bar in the figure represents a scale of 100 µm.

The morphology of EOBC based blends were also investigated by means of atomic force microscopy (Figure 58).

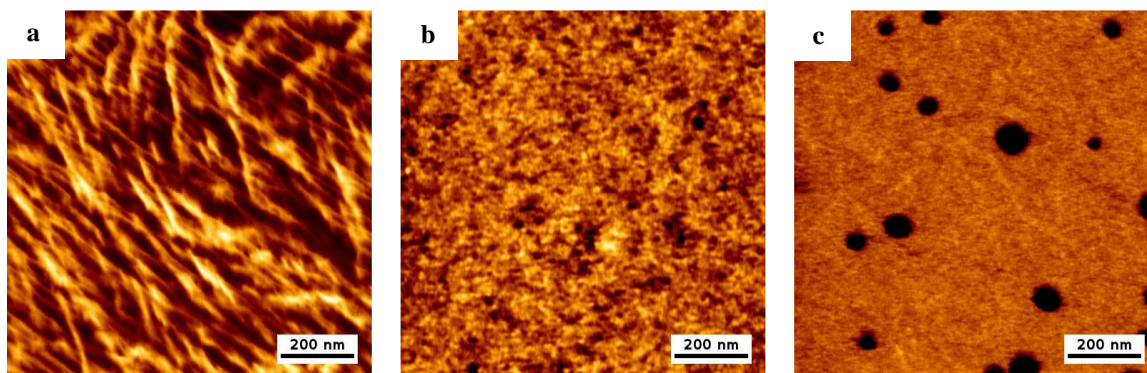


Figure 58: (a) Phase mode AFM image of neat EOBC; (b) phase mode AFM image of A-E-HC9-55; (c) phase mode AFM image of A-E-RE-55.

Figure 58 (a) presents an atomic force image of the neat EOBC (phase mode). A lamellar structure is observed and identified as the whiter regions while an amorphous region is identified in the darker region.

Figure 58 (b) depicts atomic force image of a blend containing 55 wt% of HC9. A very diffuse image is observed, showing that the well-defined lamellar structure is no longer present and that “pre-structure” of crystals (smaller crystals) appears (whiter regions). Some small, fairly well dispersed dark regions are observed and this might be the tackifier. The diffuse contour is also an indication of good interaction among the phases in the polymeric blend.

Figure 58 (c) presents a very different morphology when compared to figure 58 (b). Very well defined dark spherical phase-separated domains are observed. This is a clear hint that the soft region has a low molecular interaction with the hard region. The soft region is assumed to be the tackifier. This is in congruence with the DMA and DSC results, where two distinct glass transition temperatures were identified for the blends.

Figure 59 compares blends produced with SIS (a) and EOBC (b) having HC9 as tackifier. It can be observed that a completely different morphology is exhibited for each system.

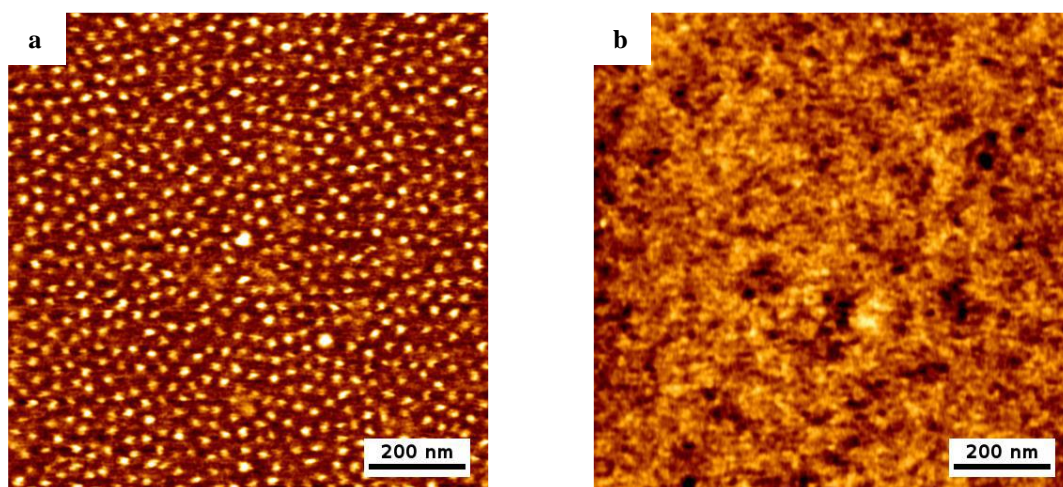


Figure 59: (a) Phase mode atomic force image of HC9-140; (b) phase mode atomic force image of A-E-HC9-55.

Figure 60 compares blends produced with SIS (a) and EOBC (b) having RE as tackifier. Also here, completely different morphology between them is observed. It should be highlighted the phase-separated domain demonstrated in figure 60 (b).

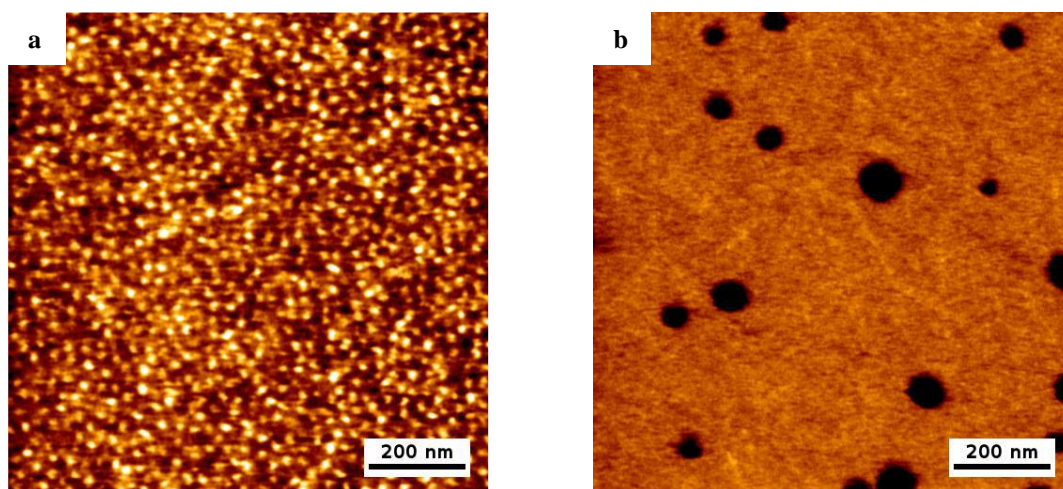


Figure 60: (a)Phase mode atomic force image of RE-140; (b) phase mode atomic force image of A-E-RE-55

Thus, figures 59 and 60 clearly demonstrate the differences generated in the blends morphology for HMPSAs produced with styrenic block copolymers and olefinic block copolymers.

4.4.3 Adhesion and adhesive performance of poly(ethylene-co-1-octene) block copolymer based blends as hot melt pressure sensitive adhesives

Adhesion and adhesive performance of the EOBC blends were investigated by means of contact angle measurements, peel strength, loop tack and holding power.

Figure 61 presents surface energy of the HMPSAs based on EOBC and the different tackifiers measured by means of the contact angle method.

It is observed that for blends where a better compatibility between EOBC and resin was detected, the surface energy of the blend was lower. To achieve good adhesion, it is known that the surface energy of the adhesive should be lower than the surface adhesion of the substrate. Stainless steel plates were used as a substrate and its surface energy was measured to be 45 mN/m. Metals are considered high surface energy substrates. All the samples presented some adhesion against stainless steel as shown in figure 61. It can also be observed that as the blends surface energy increased, peel strength decreased. This suggests that intrinsic adhesion term plays a relevant role in the adhesion fracture strength of EOBC based HMPSAs blends. This behavior was not identified for SIS based HMPSAs blends. Probably thermodynamic caused adhesion mechanism is at least one of the mechanisms responsible for adhesion in EOBC based HMPSAs.

Figure 62 is a schematic picture that attempts to explain the surface energy measured by means of contact angle method for blends employing EOBC. In comparison to the blends employing SIS as the thermoplastic elastomer, the measured values for the total surface energy were higher, varying from 30 mN/m to 40 mN/m, while for SIS based blends, the values ranged from 20 mN/m to 30 mN/m. Considering that surface energy values can be used as an indication of compatibility between the phases,¹⁷¹ this shows poorer interaction between EOBC and the tackifiers in comparison to the SIS based systems.

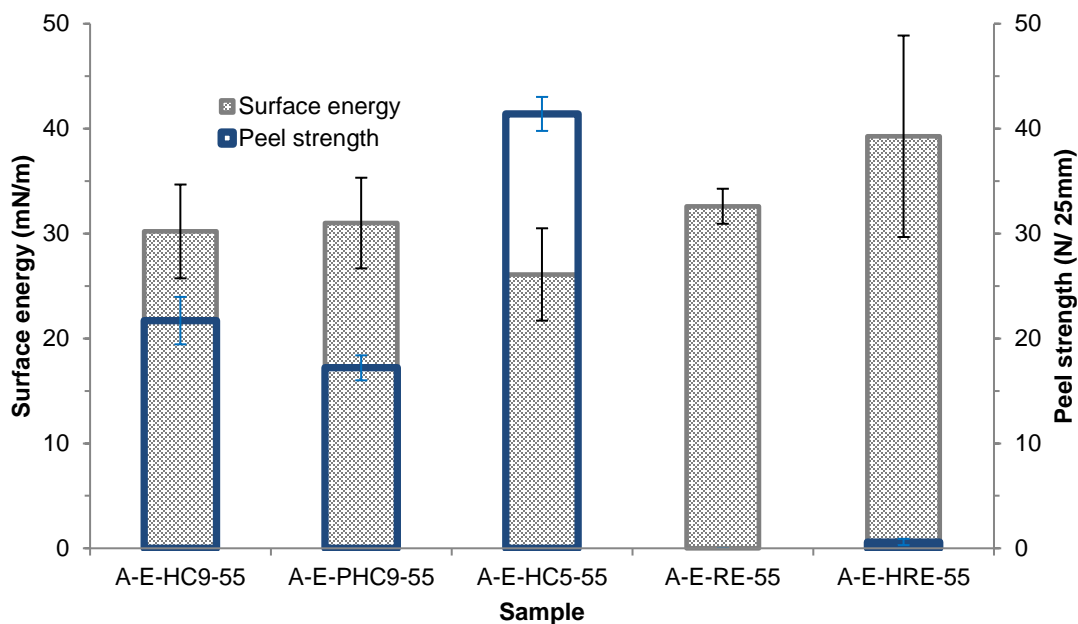


Figure 61: Surface energy and peel strength results for hot melt pressure sensitive adhesive blends containing 55 wt% of resin an based on poly(ethylene-co-1-octene) blends.

According to figure 62, coarser dispersed particles are expected to be identified in such blends due to this poor interaction among the phases. Since the phases are less interacted and understanding that lower molecular weight polymer chains have the trend to come to the surface layer due to reduction of conformational entropic penalty,¹⁷¹ it is expected that the tackifier is preferentially located on the surface.

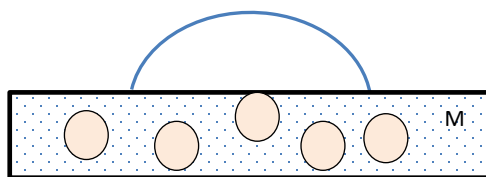


Figure 62: Schematic representation of film being measured by contact angle method. The orange spheres represent the dispersed phase and the blue dots represent the matrix phase.

Considering that the dispersed component is an indication of interaction between the phases in the blend,¹⁷¹ poor interactions are perceived for such blends and especially for the natural resins based ones. This is in congruence with the DMA results.

From the SAFT results displayed in figure 63, it is observed that all values were higher when EOBC was employed in comparison to the analogous SIS based blend.

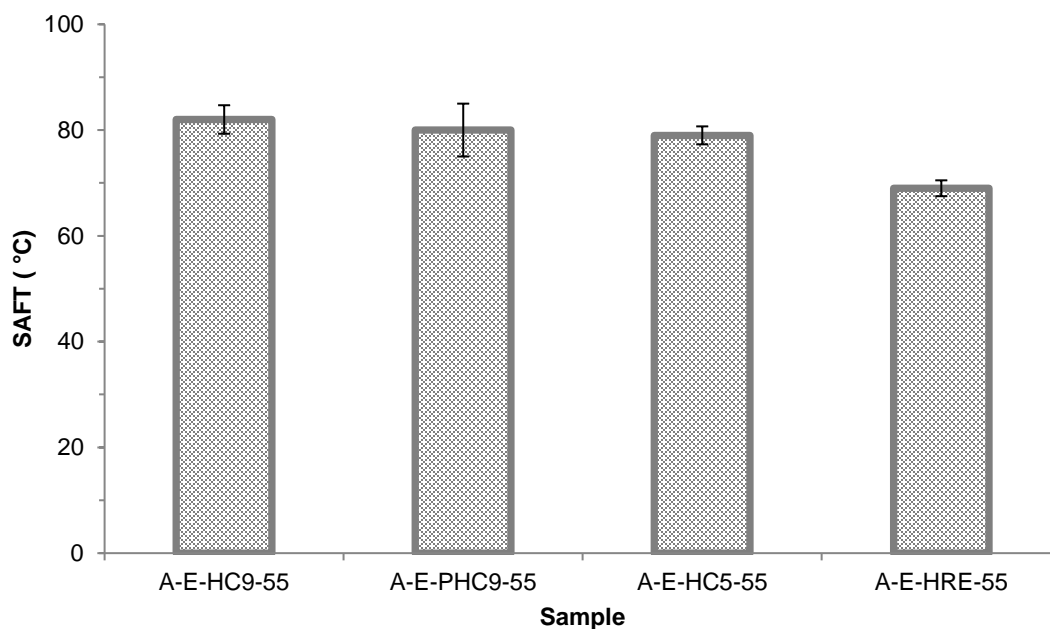


Figure 63: Shear adhesion holding power and shear adhesion failure temperature (SAFT) results for hot melt pressure sensitive adhesive blends containing 55 wt% of resin an based on poly(ethylene-co-1-octene) blends.

Two factors might be possibly related to this result which are the storage modulus of the neat polymers and the melt temperature of EOBC based blends. As stated by Brien et al.¹⁵, SAFT values are related to the transition from the elastic to the viscous region. Further investigation would be needed to better understand the crystals melting influence on cohesion.

5 Assessment of future applications of new poly(ethylene-co-1-octene) block copolymer based pressure sensitive adhesives

The influence of tackifiers employed in polymer blends for producing hot melt pressure sensitive adhesives on viscoelastic behavior, morphology, surface properties and adhesive performance were evaluated in this work for HMPSAs based on classical poly(styrene-*block*-isoprene-*block*-styrene), which is currently the state of the art.

Due to new developments on catalyst field, olefin block copolymers are currently able to be economically synthesized.¹⁷³ It is reported that OBC has excellent elastomeric properties even at high temperatures.¹⁷³ Hence, it can be used as an alternative for classical styrenic block copolymers.

An investigation of the influence of poly(ethylene-co-1-octene) block copolymer on viscoelastic behavior, morphology, surface properties as well as adhesive performance in polymer blends employed as HMPSA was conducted. The same formulations were prepared. However, SIS was exchanged by EOBC.

It could be demonstrated that although SIS and EOBC presented similar viscoelastic behavior, the polymer blends presented chemical and morphological differences, which affected the adhesive performance. Thus, the formulation employed was certainly not the optimized one for OBC's based HMPSA. Based on these results, poly(ethylene-co-1-octene) block copolymer is suitable to be used as HMPSA, however, a fine-tuning on the blends composition must be carried out. The results obtained in the current study can support in such optimization.

The adhesive industry focuses its efforts in developing environment friendly materials, which are just as effective as, or even better than solvent based systems. In transportation segment, for example, the original motivation for application of adhesives is still the driving force for new developments, namely, replacement of mechanical fastening.¹⁷⁴ Pressure sensitive adhesives can be employed in different areas and regarding end-use industry, electronics, medical and automotive are those with highest expectation of growth for specialty PSA tapes market.¹⁷⁵

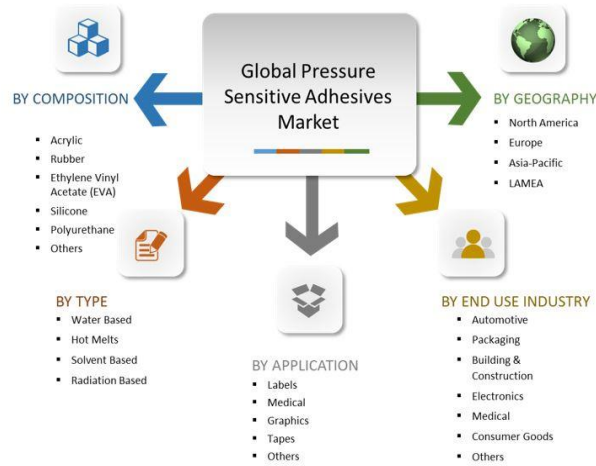


Figure 64: Global market segments for pressure sensitive adhesives according to composition, type, application, end-use industry and geography.¹⁷⁶

Electronics are present in several areas of modern life. As displayed in figure 65, all the red marked areas are parts employing adhesives for assembling a smartphone.

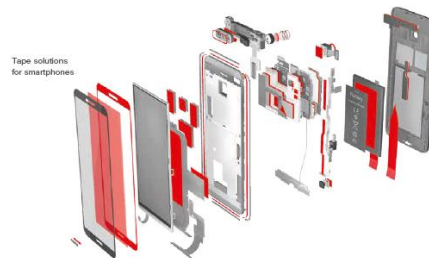


Figure 65: Schematic representation of a disassembled smartphone. Red marked areas are parts employing adhesives during assembly.¹⁷⁷

The importance of electronic pieces in automotive industry has also increased considerably, e.g. with the demand coming from electric car manufacturers.

Another trend for pressure sensitive adhesives is the so-called radio frequency identification (RFID).¹⁷⁸

Hot melt pressure sensitive adhesives are unique. Processing occurs at elevated temperature. This must be at a rheologically suitable range, in order to allow the coating to be accomplished in the molten state. However, during utilization, the adhesive stiffness increases, despite being still in a fluid state.¹⁶ Thus, the viscoelastic properties of the bulk

adhesive must be carefully selected, so the adhesive will be able to properly contact the substrate and remain cohesive. Styrenic block copolymers are thermoplastic elastomers, thus they are suitable to be used as hot melt adhesives. Due to physical crosslink, formed by styrene domains, they can achieve adequate mechanical properties even though they are not chemically crosslinked. Nevertheless, for some applications aromatic components are not suitable or undesired. Further on, it was demonstrated in this study that process temperature influences hot melt pressure sensitive adhesive performance, since thermo-mechanical degradation occurs mainly due to the presence of unsaturation in the polymer chain.

OBCs are also thermoplastic elastomers; however, in contrast to SBCs, neither aromatic rings nor unsaturation are present in the polymer chain. Thus, promising applications for OBCs are, for example, in food, hygiene or medical fields.

The use of OBCs has been reported in transposable pressure sensitive adhesives, i.e. adhesive which changes state or properties under variations in environment, for example under heating.¹⁷⁹

Also concerning its chemical structure, OBCs have pronounced affinity with low surface energy substrates, since most of them are based on olefins. Adhesion to low surface energy substrates are challenging, however, development in such field has been achieved by optimized OBCs HMPSA formulation.¹⁸⁰

As reported by Raja⁷², blends containing OBC are suitable for application in hygiene products. Not only adhesive performance could be attained in contrast to styrenic block copolymers blends, but also OBC based blends showed advantages in processing in comparison to SBC based blends. Due to the viscosity of the reported blend being lower than that of the compared formulation, the material can be adequately processed at lower temperatures.

Hot melt adhesives are environment friendly adhesives, since only heat is required for their processing.⁷ A combination with olefin block copolymer is of advantage. Not only due to the absence of styrene but also due to a rheological motivation. Since EOBC is comprised of ethylene and octene segments, i.e. both olefins, a homogenous melt is obtained during

processing. Further on, oxidative breakdown during process is not expected, as the polymer lacks unsaturation.

It could be observed that blends based on cycloaliphatic or aliphatic hydrocarbon resins presented better HMPSA performance than those based on partially hydrogenated C9 resin or natural resins. This result suggests further development on HMPSA's blends fully committed to environment friendly products.

The arguments exposed demonstrate the potential use of OBCs in HMPSAs, especially in growing demanding areas. It has to be considered that an optimization of the blend is necessary; nevertheless, there are significant advantages in using newly developed olefinic block copolymer in comparison to the classical styrenic block copolymers.

6 Summary and outlook

The aim of this work was to understand polymer blends structure-properties relationships, which are the state of the art for mixtures employed as hot melt pressure sensitive adhesives and compare these results with polymer blends produced by replacing classical polymer by newly developed polymers. These polymers are olefinic block copolymers synthesized via chain shuttling polymerization, which is reported to be an economically feasible route.¹⁷³

The specific goals of the present work was to investigate polymer blends as models of hot melt pressure sensitive adhesives employing five chemically different tackifying resins varying their concentrations. Hot melt pressure sensitive adhesives are environment friendly glues since only heat is needed to process them avoiding the use of solvents or chemically reactive substances. The chosen thermoplastic elastomer was SIS, since styrenic block copolymers are the state of the art in HMPSA.

The realization of the goals was achieved by investigating the compatibility of the main materials employed in a HMPSA blend, namely, tackifiers, thermoplastic elastomer and plasticizing oil whereas polymer blend compatibility among its components influences final properties; by assessing the influence of chemically different tackifiers on viscoelastic, morphological, surface properties in connection to adhesive performance of SIS based HMPSA as well as OBC based ones and by evaluating the influence of temperature as a process parameter, which affects mixing and coating steps, on the aforementioned properties.

For the compatibility investigation, blends of SIS and the selected tackifiers (hydrogenated C9 hydrocarbon resin, partially hydrogenated C9 hydrocarbon resin, hydrogenated C5 hydrocarbon resin, pentaerythritol rosin ester resin and hydrogenated rosin ester resin) were mixed using a stirrer at elevated temperature and concentrations ranging from 70 wt% to 30 wt%. Polymer blends of EOBC and the selected tackifiers were mixed using the same stirrer and a concentration of 50 wt%. The compatibility degree was evaluated by means of dynamic mechanical analysis.

For the model HMPSA, polymer blends containing SIS (from 16 wt% to 64 wt%) and the selected tackifiers (from 64 wt% to 16 wt%) as well as paraffinic oil (19 wt%) and anti-

oxidant (1 wt%) were mixed using a sigma blade kneader (internal mixer). Blends containing EOBC, the previously mentioned tackifiers and paraffinic oil as well as antioxidant were mixed in a proportion of 25 wt% / 55 wt% / 19 wt% / 1 wt%. The samples were coated using a laboratory melt coater and a slot die technology. Viscoelastic behavior was evaluated by means of dynamic mechanical analysis, surface properties were assessed via contact angle measurements, morphology was investigated by optical as well as atomic force microscopy and adhesive performance was measured by means of typical industrial methods, i.e., 180° peel strength, loop tack, holding power and shear adhesion failure temperature.

It could be observed that the chemical structure of the tackifiers influences the adhesive performance of the HMPSAs. Their compatibility with the elastomeric part of the polymer has a high impact on the viscoelastic properties. No blends were thermodynamically miscible but a degree of compatibility was detected. Natural resins also showed a more pronounced association with polystyrene domains.

For HMPSAs, adhesion strength is very much dependent on blends viscoelastic properties, nevertheless, it was also noticed that surface energy of the blends were minimized in comparison to neat materials. This gives a contribution to the blend intrinsic adhesion. Lower values of surface energy were measured for hydrocarbon based resins. It was observed that shear resistance is related to tackifiers association with styrenic domains. Natural resins presented a higher association degree with polystyrene domains than hydrocarbon resins. Thus, glass transition temperature of the polystyrene was shifted to lower temperatures leading to a lower resistance against shear forces when natural resins were employed.

The influence of processing temperature when mixing and coating the polymer blends could be observed and this was reflected on the adhesive performance. Higher mixing and processing temperatures led to thermomechanical degradation of the thermoplastic elastomer. Rheological properties of the molten HMPSA changed and consequently different mixing degrees of the polymer blend occurred at different processing temperatures. This could be evaluated by surface energy results.

Viscoelastic properties of HMPSAs based on poly(ethylene-co-1-octene) were similar to those based on SIS. However, from the compatibility investigation it could be seen that especially for natural resins, the association degree was not as strong as to the hydrocarbon resins. Consequently, different adhesive performance in comparison to SIS based blends was observed. Natural resins produced highly incompatible mixtures.

Viscoelastic properties of the HMPSAs are well known to play an important role in the final adhesive performance and this could be demonstrated through this work. However, it was interesting to show that when another thermoplastic elastomer, namely EOBC, was used to prepare a model HMPSA, although similarities in viscoelastic properties were observed in the polymer blends, significant morphological differences were identified as well as complete different adhesive performance. It is important to highlight that the SIS used is an amorphous polymer while OBCs are semi-crystalline polymers.

The differences observed in chemical and morphological properties of polymer blends produced with OBC when compared to SIS contribute to further development of OBC based HMPSA. It could be perceived that blends based on cycloaliphatic or aliphatic hydrocarbon resins presented better HMPSA performance than those based on partially hydrogenated C9 resin or natural resins. This pathway should be further investigated in order to achieve polymer blend with optimized adhesive performance. Based on these results, poly(ethylene-co-1-octene) block copolymer is of advantage in applications, in which aromatic components are not suitable or undesired, for example, food, hygiene or medical fields.

References

1. Mildenberg R, Zander M, Collin G. *Hydrocarbon Resins*. Weinheim: VCH; 1997.
2. Wang C, Han W, Tang X, Zhang H. Evaluation of drug release profile from patches based on styrene – isoprene – styrene block copolymer : the effect of block structure and plasticizer. *AAPS PharmSciTech*. 2012;13(2):556-567. doi:10.1208/s12249-012-9778-3
3. Rana A, Kaur V, Kaushal S. A review on transdermal drug delivery system. *World Journal of Pharmaceutical Research*. 2018;7(11):229-235. doi:10.20959/wjpr201811-12360
4. Yang HWH, Chang E-P. The role of viscoelastic properties in the design of pressure-sensitive adhesives. *Trends in Polymer Science*. 1997;5(11):380-384.
5. Raja PR, Hagood AG, Peters MA, Croll SG. Evaluation of natural rubber latex-based PSAs containing aliphatic hydrocarbon tackifier dispersions with different softening points — Adhesive properties at different conditions. *International Journal of Adhesion and Adhesives*. 2013;41:160-170. doi:10.1016/j.ijadhadh.2012.11.009
6. Raja PR, Wilson JK, Peters MA, Croll SG. Evaluation of olefinic block copolymer blends with amorphous polyolefins-effect of different unsaturated and saturated hydrocarbon tackifier resins on blend miscibility. *Journal of Applied Polymer Science*. 2013:1-21. doi:10.1002/APP.39450
7. Chabert F, Tournilhac F, Sajot N, Tence-Girault S, Leibler L. Supramolecular polymer for enhancement of adhesion and processability of hot melt polyamides. *International Journal of Adhesion and Adhesives*. 2010;30:696-705. doi:10.1016/j.ijadhadh.2010.08.003
8. IUPAC. *Compendium of Chemical Terminology*.; 1997. doi:10.1351/goldbook.I03352
9. Sasaki M, Adachi M, Kato Y, Fujii S, Nakamura Y, Urahama Y, Sakurai S. Adhesion property and morphology of styrene triblock/diblock copolymer blends. *Journal of Applied Polymer Science*. 2010;118:1766-1773. doi:10.1002/app.32490
10. Nakamura Y, Adachi M, Ito K, Kato Y, Fujii S, Sasaki M, Urahama Y, Sakurai S. Effects of compatibility between tackifier and polymer on adhesion property and phase structure : Tackifier-added polystyrene-based triblock / diblock copolymer blend system. *Journal of Applied Polymer Science*. 2011;120:2251-2260. doi:10.1002/app.33442
11. Aubrey DW, Sherriff M, College N. Viscoelasticity of rubber-resin mixtures. *Journal of Applied Polymer Science : Polymer Chemistry Edition*. 1978;16:2631-2643.
12. O'Connor AE, Macosko CW. Melt versus solvent coating: Structure and properties of block-copolymer-based pressure-sensitive adhesives. *Journal of Applied Polymer*

Science. 2002;86(13):3355-3367. doi:10.1002/app.11300

13. Class JB, Chu SG. The viscoelastic properties of rubber-resin blends. I. The effect of resin structure. *Journal of Applied Polymer Science*. 1985;30(2):805-814. doi:10.1002/app.1985.070300230
14. Class JB, Chu SG. The viscoelastic properties of rubber-resin blends. II. The effect of resin molecular weight. *Journal of Applied Polymer Science*. 1985;30(2):815-824. doi:10.1002/app.1985.070300230
15. O'Brien EP, Germinario LT, Robe GR, Williams T, Atkins DG, Moroney DA, Peters MA. Fundamentals of hot-melt pressure-sensitive adhesive tapes: The effect of tackifier aromaticity. *Journal of Adhesion Science and Technology*. 2007;21(7):637-661. doi:10.1163/156856107781192328
16. Benedek I, Heymans LJ. *Pressure Sensitive Adhesives Technology*. CRC Press Inc; 1997.
17. Ryu DY, Kim JK. The aromatic hydrocarbon resins with various hydrogenation degrees part 2. The adhesion and viscoelastic properties of the mixtures of resins and block copolymers. *Polymer*. 2000;41(14):5207-5218. doi:10.1016/S0032-3861(99)00811-3
18. Kim JK, Ryu DY, Lee KH. The aromatic hydrocarbon resins with various hydrogenation degrees part 1. The phase behavior and miscibility with polybutadiene and with polystyrene. *Polymer*. 2000;41(14):5195-5205. doi:10.1016/S0032-3861(99)00614-X
19. Sasaki M, Fujita K, Adachi M, Fujii S, Nakamura Y, Urahama Y. The effect of tackifier on phase structure and peel adhesion of a triblock copolymer pressure-sensitive adhesive. *International Journal of Adhesion and Adhesives*. 2008;28(7):372-381. doi:10.1016/j.ijadhadh.2007.11.002
20. Llevot A, Grau E, Carlotti S, Grelier S, Cramail H. Dimerization of abietic acid for the design of renewable polymers by ADMET. *European Polymer Journal*. 2015;67:409-417. doi:10.1016/j.eurpolymj.2014.10.021
21. Zheng Y, Yao K, Lee J, Chandler D, Wang J, Wang C, Chu F, Tang C. Well-defined renewable polymers derived from gum rosin. *Macromolecules*. 2010;43(14):5922-5924. doi:10.1021/ma101071p
22. Kajiyama M, Ono H, Mizumachi H, Zufu Z. Miscibility and pressure-sensitive adhesive performances of acrylic copolymer and hydrogenated rosin systems. *Journal of Applied Polymer Science*. 1999;71:651-663.
23. Pocius A V. *Adhesion and Adhesives Technology: An Introduction*. München: Carl Hanser Verlag; 1997.
24. Kim SH, Kim BG. Ink composition for roll printing process and method of fabricating pattern on substrate using the same. Patent US 20100126959A1. 2010.
25. Kraus G, Jones FB, Marrs OL, Rollmann KW. Morphology and viscoelastic

- behavior of styrene-diene block copolymers in pressure sensitive adhesives. *The Journal of Adhesion*. 1977;8(3):235-258. doi:10.1080/00218467608075086
26. Baldan A. Adhesively-bonded joints and repairs in metallic alloys, polymers and composite materials: Adhesives, adhesion theories and surface pretreatment. *Journal of Materials Science*. 2004;39(1):1-49. doi:10.1023/B:JMISC.0000007726.58758.e4
 27. *The Global Adhesive and Sealant Industry*. Frankfurt, Germany; 1998.
 28. Kenney JF, Haddock TH, Sun RL, Parreira HC. Medical-grade acrylic adhesives for skin contact. *Journal of Applied Polymer Science*. 1992;45:355-361.
 29. Ho KY, Dodou K. Rheological studies on pressure-sensitive silicone adhesives and drug-in-adhesive layers as a means to characterise adhesive performance. *International Journal of Pharmaceutics*. 2007;333:24-33. doi:10.1016/j.ijpharm.2006.09.043
 30. Padding, J. T.; Mohite, L. V.; Auhl, D.; Schweizer, T.; Briels, W. J.; Bailly C. Quantitative mesoscale modeling of the oscillatory and transient shear rheology and the extensional rheology of pressure sensitive adhesives. *Soft Matter*. 2012;8:7967-7981.
 31. Paris J. Adhesives for paper, board and foils. *International Journal of Adhesion and Adhesives*. 2000;20:89-90.
 32. Moyano MA, París R, Martín-martínez JM. Viscoelastic and adhesion properties of hot-melts made with blends of ethylene-co-n-butyl acrylate (EBA) and ethylene-co-vinyl acetate (EVA) copolymers. *International Journal of Adhesion and Adhesives*. 2019;88:34-42. doi:10.1016/j.ijadhadh.2018.11.001
 33. Daoulas KC, Theodorou DN, Roos A, Creton C. Experimental and self-consistent-field theoretical study of styrene block copolymer self-adhesive materials. *Macromolecules*. 2004;37(13):5093-5109. doi:10.1021/ma035383a
 34. Diethert A, Körstgens V, Magerl D, Ecker K, Perlich J, Roth S V, Müller-Buschbaum P. Structure and macroscopic tackiness of ultrathin pressure sensitive adhesive films. *Applied Materials & Interfaces*. 2012;4:3951-3958. doi:10.1021/am300774b
 35. Peykova Y, Lebedeva O V., Diethert A, Muller-Buschbaum P, Willenbacher N. Adhesive properties of acrylate copolymers: effect of the nature of the substrate and copolymer functionality. *International Journal of Adhesion and Adhesives*. 2012;34:107-116. doi:10.1016/j.ijadhadh.2011.12.001
 36. Fujita M, Takemura A, Ono H, Kajiyama M, Hayashi S, Mizumachi H. Effects of miscibility and viscoelasticity on shear creep resistance of natural-rubber-based pressure-sensitive adhesives. *Journal of Applied Polymer Science*. 2000;75(12):1535-1545. doi:10.1002/(SICI)1097-4628(20000321)75:12<1535::AID-APP12>3.0.CO;2-1

37. Zosel A. Adhesion and tack of polymers: Influence of mechanical properties and surface tensions. *Colloid & Polymer Science*. 1985;263(7):541-553. doi:10.1007/BF01421887
38. Jeusette M, Peeterbroeck S, Simal F, Cossement D, Roose P, Leclère P, Dubois P, Hecq M, Lazzaroni R. Microscopic morphology of blends between a new “all-acrylate” radial block copolymer and a rosin ester resin for pressure sensitive adhesives. *European Polymer Journal*. 2008;44(12):3931-3940. doi:10.1016/j.eurpolymj.2008.09.003
39. Kano Y, Kawahara S, Akiyama S. Pressure sensitive adhesive properties and miscibility in blends of Poly(vinyl ethylene-co-1,4-butadiene) with hydrogenated terpene resin. *The Journal of Adhesion*. 1993;42:25-37. doi:10.1080/00218469308026568
40. Yuan B, McGlinchey C, Pearce EM. Explanation of tackifier effect on the viscoelastic properties of polyolefin-based pressure sensitive adhesives. *Journal of Applied Polymer Science*. 2006;99(5):2408-2413. doi:10.1002/app.22820
41. Habenicht G. *Kleben: Grundlagen, Technologie, Anwendungen*. 3rd ed. Berlin Heidelberg: Springer-Verlag; 1997.
42. Dixit N, Pape A, Rong L, Joseph E, Martin SM. Isothermal microphase separation kinetics in blends of asymmetric styrene-isoprene block copolymers. *Macromolecules*. 2015;48(4):1144-1151. doi:10.1021/ma501988u
43. Sperling LH. *Introduction to Physical Polymer Science*. 4th ed. John Wiley & Sons, Hoboken, Inc; 2006.
44. Bates FS, Fredrickson GH. Block copolymer thermodynamics: theory and experiment. *Annual Review of Physical Chemistry*. 1990;41:525-557.
45. Mai SM, Mingvanish W, Turner SC, Chaibundit C, Fairclough JPA, Heatley F, Matsen MW, Ryan AJ, Booth C. Microphase-separation behavior of triblock copolymer melts. Comparison with diblock copolymer melts. *Macromolecules*. 2000;33(14):5124-5130. doi:10.1021/ma000154z
46. Kane L, Norman DA, White SA, Matsen MW, Satkowski MM, Smith SD, Spontak RJ. Molecular, nanostructural and mechanical characteristics of lamellar triblock copolymer blends: Effects of molecular weight and constraint. *Macromolecular Rapid Communications*. 2001;22(5):281-296. doi:10.1002/1521-3927(20010301)22:5<281::AID-MARC281>3.0.CO;2-G
47. Tureau MS, Rong L, Hsiao BS, Epps TH. Phase behavior of neat triblock copolymers and copolymer/homopolymer blends near network phase windows. *Macromolecules*. 2010;43(21):9039-9048. doi:10.1021/ma100783y
48. Bates FS. Polymer-Polymer Phase Behavior. *Science*. 1991;251(4996):898-905. doi:10.1126/science.251.4996.898
49. Dixit N. Microphase separation studies in styrene-diene block copolymer-based hot-

- melt pressure-sensitive adhesives. PhD Thesis, Virginia Polytechnic Institute and State University Blacksburg/USA. 2014.
50. Nakajima N, Babrowicz R, Harrell ER. Rheology, composition, and peel-mechanism of block copolymer-tackifier-based pressure sensitive adhesives. *Journal of Applied Polymer Science*. 1992;44(8):1437-1456. doi:10.1002/app.1992.070440814
 51. Roos A, Creton C. Effect of the presence of diblock copolymer on the nonlinear elastic and viscoelastic properties of elastomeric triblock copolymers. *Macromolecules*. 2005;38:7807-7818. doi:10.1021/ma050322t
 52. Roos A, Creton C. Linear viscoelasticity and non-linear elasticity of block copolymer blends used as soft adhesives. *Macromolecular Symposia*. 2004;214:147-156. doi:10.1002/masy.200451011
 53. Berglund CA, McKay KW. Viscoelastic properties of a styrene-isoprene-styrene triblock copolymer and its blends with polyisoprene homo polymer and styrene-isoprene diblock copolymer. *Polymer Engineering and Science*. 1993;33(18):1195-1203.
 54. Gibert FX, Marin G, Derail C, Allal A, Lechat J. Rheological properties of hot melt pressure-sensitive adhesives based on styrene— isoprene copolymers. Part 1: a rheological model for [SIS-Si] Formulations. *The Journal of Adhesion*. 2003;79:825-852. doi:10.1080=00218460390233333
 55. Honeker CC, Thomas EL. Impact of morphological orientation in determining mechanical properties in triblock copolymer systems. *Chemistry of Materials*. 1996;8(8):1702-1714. doi:10.1021/cm960146q
 56. Laurer JH, Hajduk DA, Dreckötter S, Smith SD, Spontak RJ. Bicontinuous morphologies in homologous multiblock copolymers and their homopolymer blends. *Macromolecules*. 1998;31(21):7546-7549. doi:10.1021/ma9807872
 57. Auriemma F, Rosa C De, Scoti M, Girolamo R Di, Malafronte A, Alterio MCD, Boggioni L, Losio S, Boccia AC, Tritto I. Structure and mechanical properties of ethylene/1-octene multiblock copolymers from chain shuttling technology. *Macromolecules*. 2019;52:2669-2680. doi:10.1021/acs.macromol.8b02470
 58. Auriemma F, Rosa C De, Scoti M, Girolamo R Di, Malafronte A, Galotto GN. Structural investigation at nanometric length scale of ethylene/1-octene multiblock copolymers from chain-shuttling technology. *Macromolecules*. 2018;51:9613-9625. doi:10.1021/acs.macromol.8b01947
 59. Lin Y, Marchand GR, Hiltner A, Baer E. Adhesion of olefin block copolymers to polypropylene and high density polyethylene and their effectiveness as compatibilizers in blends. *Polymer*. 2011;52(7):1635-1644. doi:10.1016/j.polymer.2011.02.012
 60. Kamdar AR, Wang H, Khariwala DU, Chum SP, Chen HY, Hiltner A, Baer E. Miscibility of novel block copolymers. *Proceedings of ANTEC*. 2007.

61. Wang HP, Khariwala DU, Cheung W, Chum SP, Hiltner A, Baer E. Characterization of some new olefinic block copolymers. *Macromolecules*. 2007;40(8):2852-2862. doi:10.1021/ma061680e
62. Zuo F, Mao Y, Li X, Burger C, Hsiao BS, Chen H, Marchand GR. Effects of block architecture on structure and mechanical properties of olefin block copolymers under uniaxial deformation. *Macromolecules*. 2011. doi:10.1021/ma102512p
63. Chum PS, Swogger KW. Olefin polymer technologies-History and recent progress at The Dow Chemical Company. *Progress in Polymer Science*. 2008;33(8):797-819. doi:10.1016/j.progpolymsci.2008.05.003
64. Rojas G, Inci B, Wei Y, Wagener KB. Precision polyethylene: Changes in morphology as a function of alkyl branch size. *Journal of the American Chemical Society*. 2009;131(47):17376-17386. doi:10.1021/ja907521p
65. Simanke AG, Galland GB, Freitas L, Da Jornada JAH, Quijada R, Mauler RS. Influence of the comonomer content on the thermal and dynamic mechanical properties of metallocene ethylene/1-octene copolymers. *Polymer*. 1999. doi:10.1016/S0032-3861(98)00771-X
66. Kalyon DM, Moy FH. Ultimate properties of blown films of linear low density polyethylene resins as affected by alpha-olefin comonomers. *Polymer Engineering & Science*. 1988;28(23):1551-1558. doi:10.1002/pen.760282305
67. Mirabella FM. Crystallization and melting of polyethylene copolymers: differential scanning calorimetry and atomic force microscopy studies. *Journal of Polymer Science Part B: Polymer Physics*. 2006;44:2369-2388. doi:10.1002/polb
68. Wilfong DL, Knight GW. Crystallization mechanisms for LLDPE and its fractions. *Journal of Polymer Science Part B: Polymer Physics*. 1990;28(6):861-870. doi:10.1002/polb.1990.090280605
69. Hamley IW. *The Physics of Block Copolymer*. Oxford university press; 1998.
70. Hiltner A, Wang H, Khariwala D, Cheung W, Chum S, Baer E. Solid state structure and properties of novel olefin block copolymers. *Proceedings of ANTEC*. 2006:1-16.
71. Shan CLP, Yalvac S, Diehl C, Marchand G, Rickey C, Karjala T. Development of olefin block copolymers for pressure sensitive adhesives. In: *PSTC Technical Seminar 30*. ; 2007.
72. Raja PR, Jones CM, Seo KS, Peters MA, Croll SG. Evaluation of disposable diaper construction hot melt pressure-sensitive adhesives using blends of olefinic block copolymer and amorphous polyolefin polymers - Adhesive performance, sprayability, and viscoelastic characteristics. *Journal of Applied Polymer Science*. 2013;130(5):3311-3318. doi:10.1002/app.39586
73. Laurer JH, Mulling JF, Khan SA, Spontak RJ, Bukovnik R. Thermoplastic elastomer gels. I. Effects of composition and processing on morphology and gel

- behavior. *Journal of Polymer Science Part B: Polymer Physics*. 1998;36(14):2379-2391.
74. Flosenzier LS, Torkelson JM. Influence of molecular weight and composition on the morphology and mechanical properties of SBS-polystyrene-mineral oil blends. *Macromolecules*. 1992;25(2):735-742. doi:10.1021/ma00028a036
75. Laurer JH, Khan SA, Spontak RJ, Satkowski MM, Grothaus JT, Smith SD, Lin JS. Morphology and rheology of SIS and SEPS triblock copolymers in the presence of a midblock-selective solvent. *Langmuir*. 1999;15(23):7947-7955. doi:10.1021/la981441n
76. Galán C, Sierra CA, Gómez Fatou JM, Delgado JA. A hot-melt pressure-sensitive adhesive based on styrene-butadiene-styrene rubber. The effect of adhesive composition on the properties. *Journal of Applied Polymer Science*. 1996;62:1263-1275.
77. Herzog B, Gardner DJ, Lopez-Anido R, Goodell B. Glass-transition temperature based on dynamic mechanical thermal analysis techniques as an indicator of the adhesive performance of vinyl ester Resin. *Journal of Applied Polymer Science*. 2005;97:2221-2229. doi:10.1002/app.21868
78. Cohen MH, Turnbull D. Molecular transport in liquids and glasses. *The Journal of Chemical Physics*. 1959;31(5):1164-1168. doi:10.1063/1.371053
79. Turnbull D. Free-volume model of the amorphous phase: Glass Transition. *The Journal of Chemical Physics*. 1961;120(34):120-125.
80. Sherriff M, Knibbs RW, Langley PG. Mechanism for the action of tackifying resins in pressure-sensitive adhesives. *Journal of Applied Polymer Science*. 1973;17:3423-3438.
81. Tobing SD, Klein A. Molecular parameters and their relation to the adhesive performance of acrylic pressure-sensitive adhesives. *Journal of Applied Polymer Science*. 2001;79:2230-2244.
82. Utracki LA, Shi ZH. Development of polymer blend morphology during compounding in a twin-screw extruder. Part I: droplet dispersion and coalescence-a review. *Polymer Engineering and Science*. 1992;32(24):1824-1833.
83. Shih H, Hamed GR. Peel adhesion and viscoelasticity of poly(ethylene-co-vinyl acetate)-based hot melt adhesives. I. The effect of tackifier compatibility. *Journal of Applied Polymer Science*. 1997;63:323-331.
84. Lim DH, Do HS, Kim HJ. PSA performances and viscoelastic properties of SIS-based PSA blends with H-DCPD tackifiers. *Journal of Applied Polymer Science*. 2006;102(3):2839-2846. doi:10.1002/app.24571
85. Turreda LD, Sekiguchi Y, Takemoto M, Kajiyama M, Hatano Y, Mizumachi H. Rheological study on the adhesion properties of the blends of ethylene vinyl acetate / terpene phenol adhesives. *Journal of Applied Polymer Science*. 1998;70:409-418.

86. Tse MF. Studies of triblock copolymer-tackifying resin interactions by viscoelasticity and adhesive performance. *Journal of Adhesion Science and Technology*. 1989;3:551-570. doi:10.1163/156856189X00407
87. Chang EP. Viscoelastic properties of pressure-sensitive adhesives. *The Journal of Adhesion*. 1997;60:233-248. doi:10.1080/00218469708014421
88. Chang EP. Viscoelastic windows of pressure-sensitive adhesives. *The Journal of Adhesion*. 1991;34:189-200. doi:10.1080/00218469108026513
89. Derail C, Allal A, Marin G, Tordjeman P. Relationship between viscoelastic and peeling properties of model adhesives. part 2. The interfacial fracture domains. *The Journal of Adhesion*. 1998;68:203-228.
90. Derail C, Allal A, Marin G, Tordjeman P. Relationship between viscoelastic and peeling properties of model adhesives. Part 1. Cohesive fracture. *The Journal of Adhesion*. 1997;61:123-157.
91. Marin G, Vandermaesen P, Komornicki J. Rheological properties of hot-melt adhesives: A model for describing the effects of resin content. *The Journal of Adhesion*. 1991;35(1):23-37. doi:10.1080/00218469108030433
92. Sun S, Li M, Liu A. A review on mechanical properties of pressure sensitive adhesives. *International Journal of Adhesion and Adhesives*. 2013;41:98-106. doi:10.1016/j.ijadhadh.2012.10.011
93. Park Y, Joo H, Kim H, Lee Y. Adhesion and rheological properties of EVA-based hot-melt adhesives. *International Journal of Adhesion & Adhesives*. 2006;26:571-576. doi:10.1016/j.ijadhadh.2005.09.004
94. Creton C, Hooker J, Shull KR. Bulk and interfacial contributions to the debonding mechanisms of soft adhesives : extension to large strains. *Langmuir*. 2001;(11):4948-4954. doi:10.1021/la010117g
95. Krecneski MA, Johnson JF, Temin SC. Chemical and physical factors affecting performance of pressure-sensitive adhesives. *Journal of Macromolecular Science, Part C: Polymer Reviews*. 1986;26(1):143-182. doi:10.1080/07366578608081971
96. Derks D, Lindner A, Creton C, Bonn D. Cohesive failure of thin layers of soft model adhesives under tension. *Journal of Applied Physics*. 2003;93(3):1557. doi:10.1063/1.1533095
97. Class JB, Chu SG. The viscoelastic properties of rubber-resin blends. III. The effect of resin concentration. *Journal of Applied Polymer Science*. 1985;30(2):825-842. doi:10.1002/app.1985.070300230
98. Kraus G, Rollmann KW. The entanglement plateau in the dynamic modulus of rubbery styrene-diene block copolymes. Significance to pressure-sensitive adhesive formulations. *Journal of Applied Polymer Science*. 1977;21:3311-3318.
99. Tackifiers for adhesives. Kraton brochure. KRATON corporation. 2018.

100. Mickiewicz RA, Ntoukas E, Avgeropoulos A, Thomas EL. Phase behavior of binary blends of high molecular weight diblock copolymers with a low molecular weight triblock. *Macromolecules*. 2008;41:5785-5792.
101. Hadziioannou G, Skoulios A. Structural study of mixtures of styrene/isoprene two- and three-block copolymers. *Macromolecules*. 1982;15(1):267-271.
102. Saad ALG, El-Sabbagh S. Compatibility studies on some polymer blend systems by electrical and mechanical techniques. *Journal of Applied Polymer Science*. 2000;9(79):60-71.
103. Oderkerk J, Groeninckx G. Morphology development by reactive compatibilisation and dynamic vulcanisation of nylon6/EPDM blends with a high rubber fraction. *Polymer*. 2002;43(8):2219-2228. doi:10.1016/S0032-3861(01)00816-3
104. Han CD, Chuang HK. Criteria for rheological compatibility of polymer blends. *Journal of Applied Polymer Science*. 1985;30(11):4431-4454. doi:10.1002/app.1985.070301118
105. Robeson LM. *Polymer Blends: A Comprehensive Review*. Carl Hanser Verlag, Munich; 2007.
106. Utracki LA. *Polymers Alloys and Blends. Thermodynamics and Rheology*. Munich Vienna New York: Hanser Publishers; 1989.
107. Cantor AS. Glass transition temperatures of hydrocarbon blends: adhesives measured by differential scanning calorimetry and dynamic mechanical analysis. *Journal of Applied Polymer Science*. 2000;77(4):826-832. doi:10.1002/(SICI)1097-4628(20000725)77:4<826::AID-APP16>3.0.CO;2-7
108. Patterson D. Polymer compatibility with and without a solvent. *Polymer Engineering & Science*. 1982;22(2):64-73. doi:10.1002/pen.760220204
109. Flory PJ. Thermodynamics of high polymer solutions. *The Journal of Chemical Physics*. 1942;10(51).
110. Huggins L. Some properties of solutions of long-chain compounds. *The Journal of Physical Chemistry*. 1942;46(1):151-158.
111. Huggins ML. Theory of solutions of high polymers. *Journal of the American Chemical Society*. 1942;64(7):1712-1719. doi:10.1021/ja01259a068
112. Krause S. Polymer-polymer miscibility. *Pure and Applied Chemistry*. 1986;58(12):1553-1560.
113. Belmares M, Blanco M, Goddard WA, Ross RB, Caldwell G, Chou S, Pham J, Olofson PM, Thomas C. Hildebrand and Hansen solubility parameters from molecular dynamics with applications to electronic nose polymer sensors. *Journal of Computational Chemistry*. 2004;25(15):1814-1826. doi:10.1002/jcc.20098
114. Koenhen DM, Smolders CA. The determination of solubility parameters of solvents and polymers by means of correlations with other physical quantities. *Journal of*

Applied Polymer Science. 1975;19(4):1163-1179. doi:10.1002/app.1975.070190423

115. Akiyama S, Kobori Y, Sugisaki A, Koyama T, Akiba I. Phase behavior and pressure sensitive adhesive properties in blends of poly(styrene-*b*-isoprene-*b*-styrene) with tackifier resin. *Polymer*. 2000;41(11):4021-4027. doi:10.1016/S0032-3861(99)00585-6
116. Utracki LA, ed. *Polymer Blends Handbook Vol 1*. Dordrecht: Kluwer Academic Publishers; 2002.
117. Kawahara S, Akiyama S. Adhesive property and phase separation of poly(vinyl ethylene-co-1,4-butadiene) with rosin resin mixtures. *Polymer Journal*. 1991;23(1):47-54.
118. Han CD, Kim J, Baek DM, Chu SG. Viscoelastic behavior, order-disorder transition, and phase equilibria in mixtures of a block copolymer and an endblock-associating resin. *Journal of Polymer Science Part B: Polymer Physics*. 1990;28(3):315-341. doi:10.1002/polb.1990.090280306
119. Ho R-M, Adedeji A, Giles DW, Hajduk DA, Macosko CW, Bates FS. Microstructure of triblock copolymers in asphalt oligomers. *Journal of Polymer Science, Part B: Polymer Physics*. 1997;35:2857-2877.
120. Favis BD, Willis JM. Phase size / composition dependence in immiscible blends: experimental and theoretical considerations. *Journal of Polymer Science Part B: Polymer Physics*. 1990;28:2259-2269.
121. Doshev P, Lohse G, Henning S, Krumova M, Heuvelsland A, Michler G, Radusch HJ. Phase interactions and structure evolution of heterophasic ethylene-propylene copolymers as a function of system composition. *Journal of Applied Polymer Science*. 2006;101(5):2825-2837. doi:10.1002/app.22921
122. Ohlsson B, Hassander H, Törnell B. Blends and thermoplastic interpenetrating polymer networks of polypropylene and polystyrene-block-poly(ethylene-stat-butylene)-block-polystyrene triblock copolymer. 1: Morphology and structure-related properties. *Polymer Engineering and Science*. 1996;36(4):501-510. doi:10.1002/pen.10436
123. Jordhamo GM, Manson JA, Sperling LH. Phase continuity and inversion in simultaneous interpenetrating networks of castor-oil based polyesters and polystyrene. *Polymer Engineering and Science*. 1984;25(1):148. doi:10.1002/pen.760260802
124. Sundararaj U, Macosko CW. Drop breakup and coalescence in polymer blends: the effects of concentration and compatibilization. *Macromolecules*. 1995;28(8):2647-2657. doi:10.1021/ma00112a009
125. Manas-Zloczower. I, Tadmor Z. *Mixing and Compounding of Polymers. Theory and Practice*. Munich, Vienna, New York: Hanser Publishers; 1994.
126. Bretas RES, d'Ávila MA. *Reologia Dos Polimeros Fundidos*. 2nd ed. Sao Carlos:

Edufscar; 2005.

127. Favis BD. The Effect of processing parameters on the morphology of an immiscible binary blend. *Journal of Applied Polymer Science*. 1990;39:285-300.
128. Ema MK, Dryer B, Balakrishnan N, Bigio DI, Brown C, Flanagan F, Yang F. Mechanism of the operating conditions on dispersive mixing and humidity of polymer in a twin screw extrusion process. *Annual Technical Conference - ANTEC, Conference Proceedings*. 2017;2017-May:1107-1111.
129. Sundararaj U, Macosko CW, Shih CK. Evidence for inversion of phase continuity during morphology development in polymer blending. *Polymer Engineering and Science*. 1996;36(13):1769-1781. doi:10.1002/pen.10572
130. Clarke N. Effect of shear flow on polymer blends. In: *Phase Behaviour of Polymer Blends. Advances in Polymer Science*. Berlin, Heidelberg: Springer-Verlag; 2005:127-173. doi:10.1007/b135884
131. Taylor GI. The viscosity of a fluid containing small drops of another fluid. *Proceedings of the Royal Society*. 1932;138(834):41-48.
132. Wu S. Formation of dispersed phase in incompatible polymer blends: interfacial and rheological effects. *Polymer Engineering and Science*. 1987;27(5):335-343.
133. Favis BD, Chalifoux JP. The effect of viscosity ratio on the morphology of polypropylene-polycarbonate blends during processing. *Polymer Engineering and Science*. 1987;27(20):1591-1600.
134. Sundararaj U, Macosko CW, Rolando RJ, Chan HT. Morphology development in polymer blends. *Polymer Engineering and Science*. 1992;32(24):1814-1823.
135. Hock CW. The morphology of pressure-sensitive adhesive films. *Journal of Polymer Science Part C: Polymer Symposia*. 1963;3(1):139-149. doi:10.1002/polc.5070030117
136. Nakamura Y, Sakai Y, Imamura K, Ito K, Fujii S, Urahama Y. Effects of the compatibility of a polyacrylic block copolymer / tackifier blend on the phase structure and tack of a pressure-sensitive adhesive. *Journal of Applied Polymer Science*. 2012;123:2883-2893. doi:10.1002/app.34883
137. Dee GT, Sauer BB. The surface tension of polymer blends: theory and experiment. *Macromolecules*. 1993;26(11):2771-2778. doi:10.1021/ma00063a021
138. Nakamura Y, Kanbe M, Takekuni E, Lida T. Effect of interfacial adhesion on the mechanical properties of poly(vinyl chloride) modified with cross-linked poly(methyl methacrylate) particles prepared by seeded emulsion polymerization. *Colloid and Polymer Science*. 2001;279:368-375.
139. Palierne JF. Linear rheology of viscoelastic emulsions with interfacial tension. *Rheologica Acta*. 1990;29(3):204-214. doi:10.1007/BF01331356
140. Geoghegan M, Krausch G. Wetting at polymer surfaces and interfaces. *Progress in*

- Polymer Science*. 2003;28:261-302. doi:10.1016/S0079-6700(02)00080-1
141. Lee JH, Balsara NP, Chakraborty AK, Krishnamoorti R, Hammouda B. Thermodynamics and phase behavior of block copolymer / homopolymer blends with attractive and repulsive interactions. *Macromolecules*. 2002;7748-7757.
 142. Harkins WD, Feldman A. Films. The spreading of liquids and the spreading coefficient. *Journal of the American Chemical Society*. 1922;44(12):2665-2685. doi:10.1021/ja01433a001
 143. Ravati S, Favis BD. Morphological states for a ternary polymer blend demonstrating complete wetting. *Polymer*. 2010;51(20):4547-4561. doi:10.1016/j.polymer.2010.07.014
 144. Bateup BO. Surface chemistry and adhesion. *International Journal of Adhesion and Adhesives*. 1981;1(5):23-239. doi:10.1016/0143-7496(81)90071-3
 145. Marshall SJ, Bayne SC, Baier R, Tomsia AP, Marshall GW. A review of adhesion science. *Dental Materials*. 2010;26:11-16. doi:10.1016/j.dental.2009.11.157
 146. Tse MF, Jacob L. Pressure sensitive adhesives based on vector SIS polymers I. Rheological model and adhesive design pathways. *The Journal of Adhesion*. 1996;56(1):79-95. doi:10.1080/00218469608010500
 147. Maurer E. Strukturuntersuchungen an Haftklebstoffen beim mechanischen Tack-Test auf makroskopischer und mikroskopischer Längenskala. PhD Thesis, Technische Universität München. 2006.
 148. Baldan A. Adhesion phenomena in bonded joints. *International Journal of Adhesion and Adhesives*. 2012;38:95-116. doi:10.1016/j.ijadhadh.2012.04.007
 149. Burnett DJ, Thielmann F, Ryntz RA. Correlating thermodynamic and mechanical adhesion phenomena for thermoplastic polyolefins. *Journal of Coatings Technology Research*. 2007;4(2):211-215. doi:10.1007/s11998-007-9017-0
 150. Leite FL, Bueno CC, Da Róz AL, Ziemath EC, Oliveira ON. Theoretical models for surface forces and adhesion and their measurement using atomic force microscopy. *International Journal of Molecular Sciences*. 2012;13(10):12773-12856. doi:10.3390/ijms131012773
 151. Shanahan MER, Garré A. Viscoelastic dissipation in wetting and adhesion phenomena. *Langmuir*. 1995;11(4):1396-1402. doi:10.1021/la00004a055
 152. Severtson SJ, Wang XP, Kroll MS. Development of environmentally benign pressure sensitive adhesive systems via modification of substrate properties. *Industrial & Engineering Chemistry Research*. 2002;41:5668-5675. doi:10.1021/ie0204383
 153. Awaja F, Gilbert M, Kelly G, Fox B, Pigram PJ. Adhesion of polymers. *Progress in Polymer Science*. 2009;34:948-968. doi:10.1016/j.progpolymsci.2009.04.007
 154. Owens DK, Wendt RC. Estimation of the surface free energy of polymers. *Journal of Applied Polymer Science*. 1969;13:1741-1747.

155. Gourianova S, Willenbacher N, Kutschera M. Chemical force microscopy study of adhesive properties of polypropylene films: influence of surface polarity and medium. *Langmuir*. 2005;21(12):5429-5438. doi:10.1021/la0501379
156. Oss CJ V, Chaudhury MK, Good RJ. Interfacial Lifshitz-van der Waals and polar interactions in macroscopic systems. *Chemical Reviews*. 1988;88:927-941. doi:10.1021/cr00088a006
157. Gibert FX, Allal A, Marin G, Derail C. Effect of the rheological properties of industrial hot-melt and pressure-sensitive adhesives on the peel behavior. *Journal of Adhesion Science and Technology*. 1999;13(9):1029-1044. doi:10.1163/156856199X00497
158. Erath J, Schmidt S, Fery A. Characterization of adhesion phenomena and contact of surfaces by soft colloidal probe AFM. *Soft Matter*. 2010;6(7):1432-1437. doi:10.1039/b923540j
159. Kaelble DH, Cirlin EH. Dispersion and polar contributions to surface tension of poly(methylene oxide) and Na-treated polytetrafluoroethylene. *Journal of Polymer Science: Part A-2*. 1971;9:363-368.
160. Mittal KL. The role of the interface in adhesion phenomena. *Polymer Engineering & Science*. 1977;17(7):467-473. doi:10.1002/pen.760170709
161. Bikerman JJ. *The Science of Adhesive Joints*. Second Edi. New York: Academic Press; 1968.
162. Wu P, Qi S, Liu N, Deng K, Nie H. Investigation of thermodynamic properties of SIS, SEBS and naphthenic oil by inverse gas chromatography. *Journal of Elastomers and Plastics*. 2011;43(4):369-386. doi:10.1177/0095244311405000
163. Menard KP. *Dynamic Mechanical Analysis: A Practical Introduction*. 2nd ed. Boca raton: CRC Press; 2008.
164. *Test Methods for Pressure Sensitive Adhesive Tapes*. 15th ed. Northbrook, IL: Pressure Sensitive Tape Council; 2007.
165. Kamagata K, Kosaka H, Hino K, Toyama M. On the internal structure of pressure-sensitive adhesives. *Journal of Applied Polymer Science*. 1971;15(2):483-500. doi:10.1002/app.1971.070150222
166. Flory PJ. Thermodynamics of crystallization in high polymers. IV. A theory of crystalline states and fusion in polymers, copolymers, and their mixtures with diluents. *The Journal of Chemical Physics*. 1949;17(3):1-10. doi:10.1063/1.1747230
167. Keller A, Hikosaka M, Rastogi S, Toda A, Barham PJ, Goldbeck-Wood G. An approach to the formation and growth of new phases with application to polymer crystallization: effect of finite size, metastability, and Ostwald's rule of stages. *Journal of Materials Science*. 1994;29(10):2579-2604.
168. Carvagno TR, O'Brien E, Rigby S. The effect of base oil composition on pressure sensitive adhesive properties. In: *PSTC Technical Seminar 33*. ; 2010.

169. Debier I, De Keyzer N. The use of rheometry to evaluate the compatibility of thermoplastic rubber based adhesives. In: *16th Munich Adhesive and Finishing Seminar.* ; 1991:107-116.
170. Dahlquist CA, Patrick RL. *Treatise on Adhesion and Adhesives, Vol. 2.* New York: Dekker; 1969.
171. Siročić AP, Hrnjak-Murčić Z, Jelenčić J. The surface energy as an indicator of miscibility of SAN/EDPM polymer blends. *Journal of Adhesion Science and Technology.* 2013;27(24):2615-2628. doi:10.1080/01694243.2013.796279
172. Sosson F, Chateauminois A, Creton C. Investigation of shear failure mechanisms of pressure-sensitive adhesives. *Journal of Polymer Science, Part B: Polymer Physics.* 2005;43(22):3316-3330. doi:10.1002/polb.20619
173. Arriola DJ, Carnahan EM, Hustad PD, Kuhlman RL, Wenzel TT. Catalytic production of olefin block copolymers via chain shuttling polymerization. *Science.* 2006;312(5774):714-719. doi:10.1126/science.1125268
174. *The Worldwide Hydrocarbon Resin Report. Technical Report Argus DeWitt.* Houston; 2013.
175. Reardon C. PSA tape and specialty tape market data and trends : 2019 AWA preliminary study results update. <https://www.fera.com/technical-centre/market-research/exclusive-market-insight-organisational-branding-and-self-medication-applications-to-intensify-demand-for-duct-tapes/>. Published 2019. Accessed June 25, 2019.
176. Sinha B. Pressure sensitive adhesives market by chemical composition (acrylic, rubber, ethylene vinyl acetate (EVA), silicone, polyurethane, and others), type (water based, hot melts, solvent based, and radiation based), application (labels, medical, graphics, tap. <https://www.alliedmarketresearch.com/pressure-sensitive-adhesives-market>. Published 2017. Accessed June 25, 2019.
177. Manifold tape solutions in electronic devices. <https://www.tesa.com/en/industry/electronics/devices>. Published 2019. Accessed June 25, 2019.
178. Schuh C, Krawinkel T. Adhesive tape for encapsulating electronic constructions. US20190161648 A1. 2019;1.
179. Bartholomew EL, Heimbach KR, Kohler CE, Zajackowski M. Transposable pressure sensitive adhesives, articles and related methods. US20170128615A1. 2017.
180. Wang SJ, Seth J, Ma J, Bharti V, Bany SW. Olefin block copolymer based pressure sensitive adhesives. EP2794795B1. 2018.
181. Rulison C. Models for surface free energy calculation. *Technical note.* 1999.

Appendices

Appendix A –Composition of blends prepared

Table A-1: Blends formulations for studying interactions between base polymer and resins.

Sample	Polymer	Amount Polymer(parts)	Resin	Amount Resin (parts)	Amount AO(parts)
S-HC9-80	SIS	20	Hydrogenated C9 hydrocarbon resin	80	1
S-HC9-70	SIS	30	Hydrogenated C9 hydrocarbon resin	70	1
S-HC9-50	SIS	50	Hydrogenated C9 hydrocarbon resin	50	1
S-HC9-30	SIS	70	Hydrogenated C9 hydrocarbon resin	30	1
S-PHC9-80	SIS	20	Partially Hydrogenated C9 hydrocarbon resin	80	1
S-PHC9-70	SIS	30	Partially Hydrogenated C9 hydrocarbon resin	70	1
S-PHC9-50	SIS	50	Partially Hydrogenated C9 hydrocarbon resin	50	1
S-PHC9-30	SIS	70	Partially Hydrogenated C9 hydrocarbon resin	30	1
S-HC5-80	SIS	20	Hydrogenated C5 hydrocarbon resin	80	1
S-HC5-70	SIS	30	Hydrogenated C5 hydrocarbon resin	70	1
S-HC5-50	SIS	50	Hydrogenated C5 hydrocarbon resin	50	1
S-HC5-30	SIS	70	Hydrogenated C5 hydrocarbon resin	30	1
S-RE-80	SIS	20	Rosin Ester	80	1
S-RE-70	SIS	30	Rosin Ester	70	1
S-RE-50	SIS	50	Rosin Ester	50	1
S-RE-30	SIS	70	Rosin Ester	30	1
S-HRE-80	SIS	20	Hydrogenated Rosin Ester	80	1
S-HRE-70	SIS	30	Hydrogenated Rosin Ester	70	1
S-HRE-50	SIS	50	Hydrogenated Rosin Ester	50	1
S-HRE-30	SIS	70	Hydrogenated Rosin Ester	30	1
E-HC9-50	EOBC	50	Hydrogenated C9 hydrocarbon resin	50	1
E-PHC9-50	EOBC	50	Partially Hydrogenated C9 hydrocarbon resin	50	1
E-HC5-50	EOBC	50	Hydrogenated C5 hydrocarbon resin	50	1
E-RE-50	EOBC	50	Rosin Ester	50	1
E-HRE-50	EOBC	50	Hydrogenated Rosin Ester	50	1

Table A-2: Blends formulations for studying interactions between base polymer and oils.

Sample	Polymer	Amount Polymer(%)	Oil	Amount Oil(%)	Amount AO(%)
S-P-80	SIS	80	Paraffinic	19	1
S-N-80	SIS	80	Naphthenic	19	1
E-P-80	EOBC	80	Paraffinic	19	1
E-N-80	EOBC	80	Naphthenic	19	1

Table A-3: Blends formulations for studying interactions between tackifiers and oils.

Sample	Resin	Amount Resin (parts)	Oil	Amount Oil(parts)	Amount AO(parts)
P-HC9-70	Hydrogenated C9 hydrocarbon resin	70	Paraffinic	30	1
P-PHC9-70	Partially Hydrogenated C9 hydrocarbon resin	70	Paraffinic	30	1
P-HC5-70	Hydrogenated C5 hydrocarbon resin	70	Paraffinic	30	1
P-RE-70	Rosin Ester	70	Paraffinic	30	1
P-HRE-70	Hydrogenated Rosin Ester	70	Paraffinic	30	1

Table A-4: Hot melt pressure sensitive adhesives blends formulations.

Sample	Polymer	Amount Polymer (%)	Resin	Amount Resin (%)	Oil	Amount Oil (%)	Amount AO(%)
A-S-HC9-16	SIS	64	Hydrogenated C9 hydrocarbon resin	16	Paraffinic	19	1
A-S-HC9-55	SIS	25	Hydrogenated C9 hydrocarbon resin	55	Paraffinic	19	1
A-S-HC9-64	SIS	16	Hydrogenated C9 hydrocarbon resin	64	Paraffinic	19	1
A-S-PHC9-16	SIS	64	Partially Hydrogenated C9 hydrocarbon resin	16	Paraffinic	19	1
A-S-PHC9-55	SIS	25	Partially Hydrogenated C9 hydrocarbon resin	55	Paraffinic	19	1
A-S-PHC9-64	SIS	16	Partially Hydrogenated C9 hydrocarbon resin	64	Paraffinic	19	1
A-S-HC5-16	SIS	64	Hydrogenated C5 hydrocarbon resin	16	Paraffinic	19	1
A-S-HC5-55	SIS	25	Hydrogenated C5 hydrocarbon resin	55	Paraffinic	19	1
A-S-HC5-64	SIS	16	Hydrogenated C5 hydrocarbon resin	64	Paraffinic	19	1
A-S-RE-16	SIS	64	Rosin Ester	16	Paraffinic	19	1
A-S-RE-55	SIS	25	Rosin Ester	55	Paraffinic	19	1
A-S-RE-64	SIS	16	Rosin Ester	64	Paraffinic	19	1
A-S-HRE-16	SIS	64	Hydrogenated Rosin Ester	16	Paraffinic	19	1
A-S-HRE-55	SIS	25	Hydrogenated Rosin Ester	55	Paraffinic	19	1
A-S-HRE-64	SIS	16	Hydrogenated Rosin Ester	64	Paraffinic	19	1
A-E-HC9-55	EOBC	25	Hydrogenated C9 hydrocarbon resin	55	Paraffinic	19	1
A-E-PHC9-55	EOBC	25	Partially Hydrogenated C9 hydrocarbon resin	55	Paraffinic	19	1
A-E-HC5-55	EOBC	25	Hydrogenated C5 hydrocarbon resin	55	Paraffinic	19	1
A-E-RE-55	EOBC	25	Rosin Ester	55	Paraffinic	19	1
A-E-HRE-55	EOBC	25	Hydrogenated Rosin Ester	55	Paraffinic	19	1

Table A-5: Hot melt pressure sensitive adhesives blends formulations for process investigation.

Sample	Polymer	Amount Polymer (%)	Resin	Amount Resin (%)	Oil	Amount Oil (%)	Amount AO (%)	Process Temp. (°C)
HC9-140	SIS	25	Hydrogenated C9 hydrocarbon resin	55	Paraffinic	19	1	140
HC9-165	SIS	25	Hydrogenated C9 hydrocarbon resin	55	Paraffinic	19	1	165
PHC9-140	SIS	25	Partially Hydrogenated C9 hydrocarbon resin	55	Paraffinic	19	1	140
PHC9-165	SIS	25	Partially Hydrogenated C9 hydrocarbon resin	55	Paraffinic	19	1	165
HC5-140	SIS	25	Hydrogenated C5 hydrocarbon resin	55	Paraffinic	19	1	140
HC5-165	SIS	25	Hydrogenated C5 hydrocarbon resin	55	Paraffinic	19	1	165
RE-140	SIS	25	Rosin Ester	55	Paraffinic	19	1	140
RE-165	SIS	25	Rosin Ester	55	Paraffinic	19	1	165
HRE-140	SIS	25	Hydrogenated Rosin Ester	55	Paraffinic	19	1	140
HRE-165	SIS	25	Hydrogenated Rosin Ester	55	Paraffinic	19	1	165

Appendix B – Contact angle data analysis

The contact angle results were obtained by means of the sessile drop measurement applying the equation proposed by Owens, Wendt and Rabel, also known as the geometric mean theory (equation 16).^{154,155}

Equation 15 can be expressed in a linear form (equation B-1):¹⁸¹

$$y = mx + b \quad (\text{B-1})$$

Where:

$$y = \frac{\gamma_L(1+\cos\theta)}{2\sqrt{\gamma_L^d}} \quad ; \quad m = \sqrt{\gamma_S^p} \quad ; \quad x = \frac{\sqrt{\gamma_L^p}}{\sqrt{\gamma_L^d}} \quad ; \quad b = \sqrt{\gamma_S^d}$$

The slope (m) of the linearized equation is used to calculate the polar component of the surface energy of the solid. The intercept (b) is used to calculate the dispersive component of the surface energy of the solid.

Prior to applying this linearized equation for determining m and b , the polar and dispersive component of each probe liquid must be determined. It was done by using a standard reference, namely (poly(tetrafluoroethylene)). Pure poly(tetrafluoroethylene) is assumed to have no polar type interactions (polar component is zero). Thus, the total surface energy for poly(tetrafluoroethylene) is equal to its dispersive surface energy.¹⁸¹

The polar surface energy component for the liquid is obtained by the difference between the liquid total surface energy and its dispersive component.

Figure B-1 presents an example of a graph obtained using the DSA4 software employing the OWRK method for obtaining the surface energy of the analyzed solids.

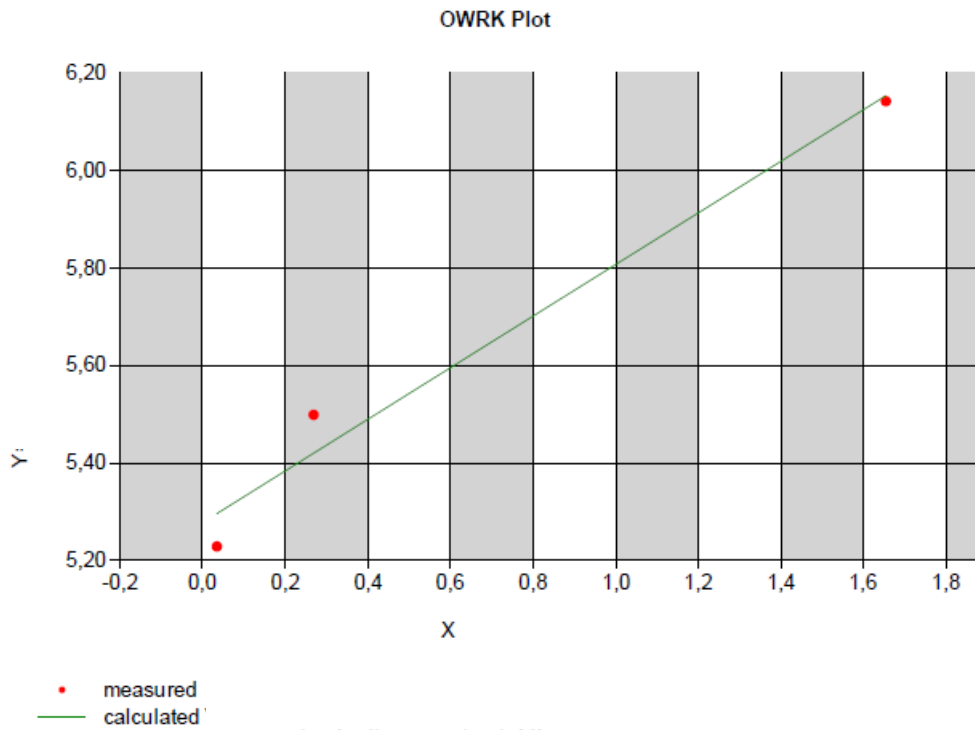


Figure B-1: Example of measurement for the calculation of surface energy employing the method proposed by Owens, Wendt and Rabel.

Appendix C – Description of data

Table C-1: Viscoelastic, surface and adhesive properties for HMPSAs blends comprising 55wt% of tackifier.

Sample	tan δ Temp. (G'=G'') (°C)	Log G'' at 100 rad/s 25 °C (Pa)	Surface Energy dispers. (mN/m)	Surface Energy polar (mN/m)	Surface Energy Total (mN/m)	Peel Strength Steel (N/25mm)	Loop Tack (N)	Holding power at 60 °C (min)	SAFT (°C)
A-S-HC9-55	93	5.37	20.07	0.01	20.08	32.8	18.8	27	78
A-S-PHC9-55	84	5.28	24.50	0.00	24.50	26.7	17.2	9	74
A-S-HC5-55	92	5.23	22.90	0.00	22.90	23.3	15.4	24	75
A-S-RE-55	66	5.77	27.80	0.20	28.00	33.6	23.7	74 (40 °C)	61
A-S-HRE-55	62	4.82	27.40	0.30	27.70	20.5	15.0	15 (40 °C)	54

Table C-2: Rheological, viscoelastic, mechanical, surface properties and adhesive performance of HMPSAs blends processed at 140 °C and at 165°C.

Sample	Brook. Viscosity at 140 °C (mPas)	G' at 25 °C (Pa)	σ max (N/mm ²)	Surface Energy dispers. (mN/m)	Surface Energy polar (mN/m)	Surface Energy total (mN/m)	Peel Strength (steel) (N/25mm)	Holding Power 60 °C (min)
HC9-140	16715	3.53E+04	1.29	22.27	0.22	22.48	25.2	22
HC9-165	15127	2.73E+04	1.23	23.50	0.30	23.90	27.8	17
PHC9-140	17309	3.47E+04	1.43	23.90	0.00	23.90	25.1	13
PHC9-165	15778	3.33E+04	1.39	25.13	0.13	25.26	29.6	13
HC5-140	17552	3.83E+04	1.12	23.00	0.00	23.00	19.9	31
HC5-165	14814	2.97E+04	0.81	21.30	0.00	21.30	20.5	13
RE-140	15590	6.09E+04	0.97	27.20	0.00	27.20	30.4	8
RE-165	15361	5.36E+04	0.82	29.50	0.10	29.60	31.4	4
HRE-140	9092	2.52E+04	0.65	24.00	0.40	24.40	20.3	5 (40 °C)
HRE-165	8030	2.68E+04	0.62	25.00	0.20	25.20	22.1	4 (40 °C)

Table C-3: Viscoelastic, surface properties as well as adhesive performance for EOBC based blends as HMPSAs.

Sample	Log G'' at 100rad/s 25 °C (Pa)	Surface energy dispers. (mN/m)	Surface energy polar (mN/m)	Surface energy total (mN/m)	Peel Strength Steel(N/25 mm)	Loop Tack (N)	Holding power at 60 °C (min)	SAFT (°C)
A-E-HC9-55	6.04	29.90	0.30	30.20	21.7	0.0	18	82
A-E-PHC9-55	6.03	30.80	0.20	31.00	17.2	0.0	13	80
A-E-HC5-55	5.69	25.70	0.40	26.10	41.4	11.9	10	79
A-E-RE-55	6.09	31.90	0.80	32.60	NA	NA	NA	NA
A-E-HRE-55	6.03	38.60	0.60	39.27	0.6	0.0	6	69

Appendix D – Viscoelastic properties of hot melt pressure sensitive adhesives blends prepared with different resin amount

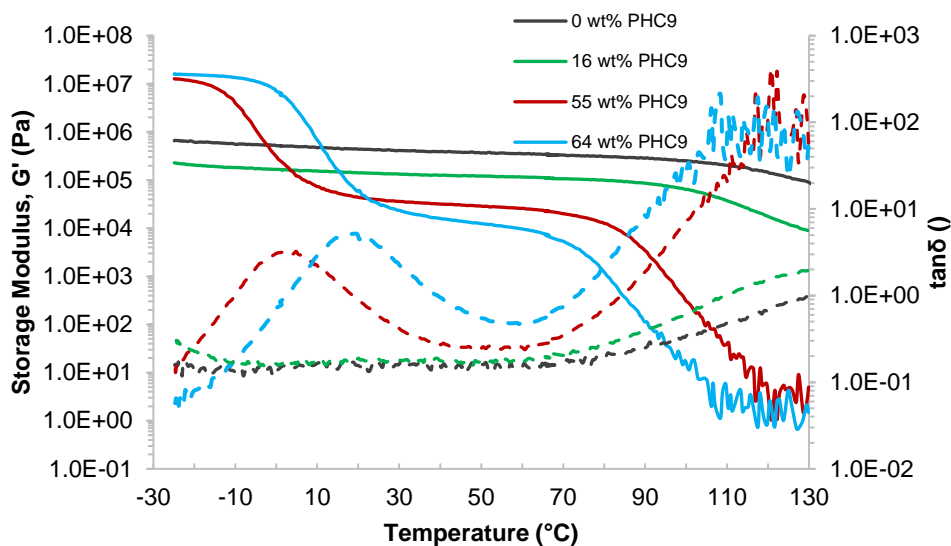


Figure D-1: Storage modulus (full lines) and loss factor curves (dashed lines) for pure SIS (black curves), and 16 wt% resin (green curves), 55 wt% resin (red curves) and 64 wt% resin (blue curves) for blends comprising partially hydrogenated C9 resin (A-S-PHC9).

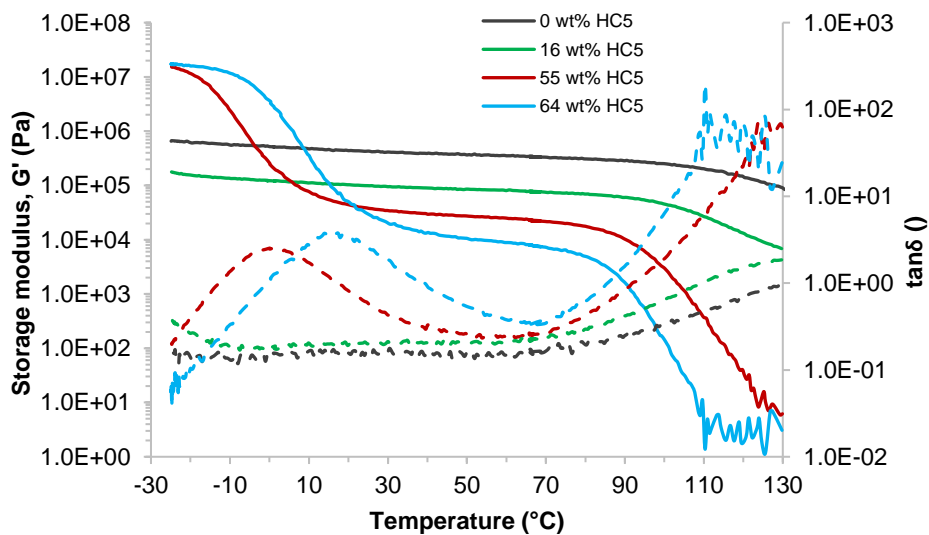


Figure D-2: Storage modulus (full lines) and loss factor (dashed lines) curves for pure SIS (black curves), and 16 wt% resin (green curves), 55 wt% resin (red curves) and 64 wt% resin (blue curves) for blends comprising hydrogenated C5 resin (A-S-HC5).

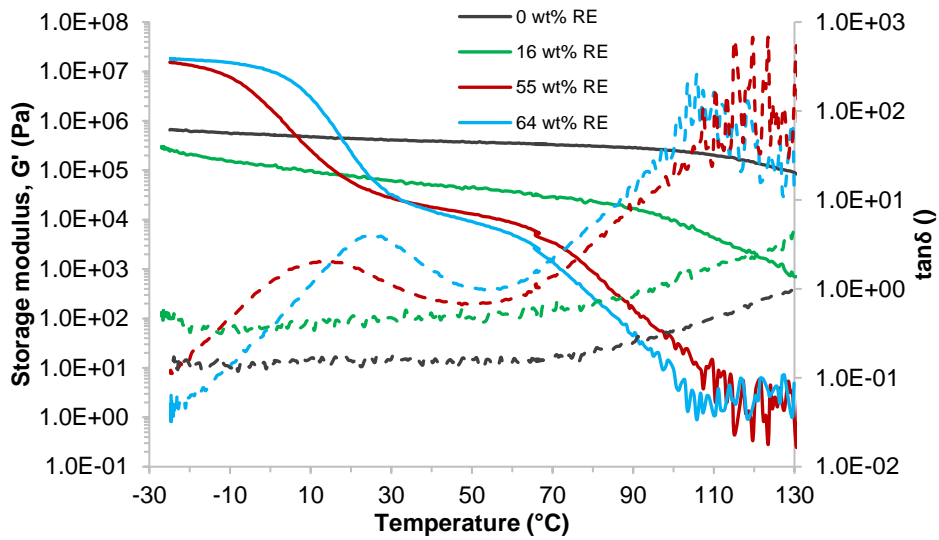


Figure D-3: Storage modulus (full lines) and loss factor (dashed lines) curves for pure SIS (black curves), and 16 wt% resin (green curves), 55 wt% resin (red curves) and 64 wt% resin (blue curves) for blends comprising pentaerithritol rosin ester resin (A-S-RE).

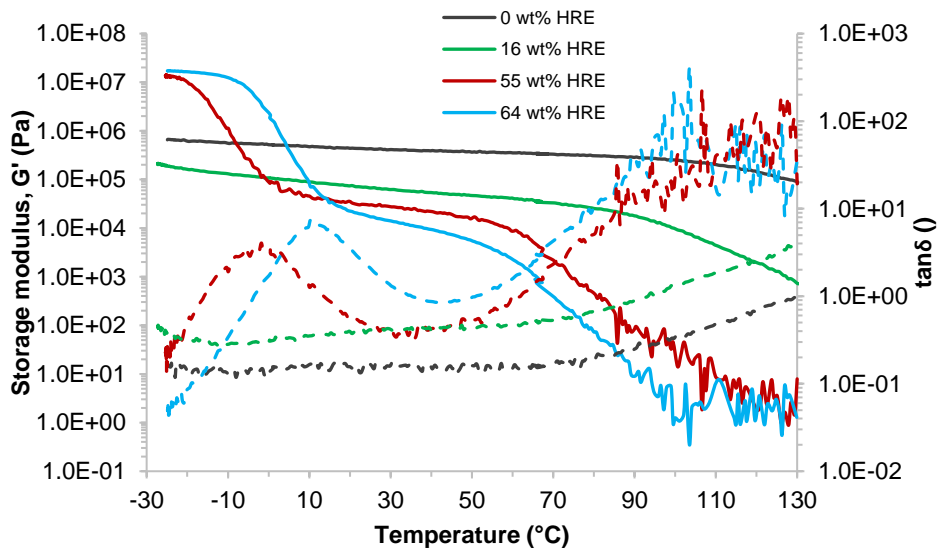


Figure D-4: Storage modulus (full lines) and loss factor (dashed lines) curves for pure SIS (black curves), and 16 wt% resin (green curves), 55 wt% resin (red curves) and 64 wt% resin (blue curves) for blends comprising hydrogenated rosin ester (A-S-HRE).

Acknowledgments

The accomplishment of this PhD work would not have been possible without the help and support of great people along the last years.

I am deeply thankful to Prof. Hans-Jachim Radusch for accepting me as a PhD student. His guidance and discussions really encouraged me to keep forward through the correct pathway. I will never forget him reminding me that I am the driving force of my work. I am also thankful to Dr. Wutzler, who also inspired me with his pieces of advice and discussions as well as his patience during the practical work in the lab. I would like to thank Prof. Thomas Groth for accepting me as a PhD student as well. By our discussions, he made me see the whole work from a different point of view, which challenged me even more to show the importance of this investigation.

I am very thankful to Arakawa Europe GmbH as well as Arakawa Chemical Industries, Ltd for supporting the accomplishment of this investigation. I am very thankful to all my colleagues in AREG and ACIJ. In particular, I am deeply thankful to Dr. Katsuhiko Tahara not only for approving the accomplishment of this work but for truly believing it would be possible. I am also very thankful to Mr. Kondo and Mr. Ishimoto for taking their time in giving extremely valuable comments in my work. I have no words to express my gratitude to Ms. Ilona Dannenberg. Not only supporting me with practical tasks, even when we were miles and miles away but especially for teaching me with so much patience and kindness a lot of what I learned to conclude this PhD study. I may be forever in debt with her.

I am deeply thankful to my parents for providing me the basis to be able to accomplish this work. I am thankful to my beloved husband, Frederico Moraes, for never letting me give up on my dreams, always encouraging me to try and for having so much patience. I am also very thankful to my mother-in-law, Maria Luiza Moraes, for never letting me give up, especially in very adverse times. I will never forget all her energy and positive attitude.

Curriculum Vitae

Tâmara Abboud

Personal Data

Date of Birth: 19/Dec/1981
Marital Status: Married
Nationality: Brazilian/ Italian
Address: Marthastraße 3
06108 Halle/Saale Germany
E-mail: abtamara@yahoo.com.br

Education

10/2005-05/2008 M.Sc. Applied polymer science
Martin-Luther-University Halle-Wittenberg, Germany
Thesis Title: "Viscoelastic Properties of Hot Melt Adhesives and their
Relationship with Adhesive Performance"

04/1999-12/2004 Universidade Federal de Santa Catarina, UFSC, Florianopolis, Brazil
Graduation in Chemical Engineering

02/1996-12/1998 High school

Work Experience

04/2012 – Present 1. Arakawa Europe GmbH
Technical Service & Development

11/2008 – 02/2012 2. Pirelli Pneus
Materials Development Engineer

Project work

11/2006 – 03/2007 1. Institute of Pharmaceutical Technology and Biopharmacy –
Department of Pharmacy
Application of Benchtop MRI in a polymer based drug delivery
system. Characterization of floating tablets coated with very flexible
polymers.

Other Skills

Language Skills

Portuguese (Native language); English: Fluent, TOEFL – 250
(Computer based test, April 2005); German: Intermediate written,
intermediate oral comprehension; Spanish: Basic written, basic oral
comprehension; Italian: Basic written, basic oral comprehension

Publications

1. Strübing, S., Abboud, T., Contri, R. V., Metz, H. and Mäder, K. New insights on poly(vinyl acetate)-based coated floating tablets: Characterisation of hydration and CO₂ generation by benchtop MRI and its relation to drug release and floating strength. *Eur. J. Pharm. Biopharm.* **69**, (2008).
2. Abboud T, Wutzler A, Radosch H-J. Tackifying resins and their polymer blends properties - application in hot melt pressure sensitive adhesives. In: *44. Munich Adhesives and Finishing Symposium 2019* ; 2019.
3. Abboud T, Wutzler A, Radosch H-J. Effect of viscoelastic and surface properties on tack, peel and shear adhesion of polymer blends applied as hot melt pressure sensitive adhesive models. *Express Polymer Letters.* **14**(8), (2020).
4. Abboud T, Wutzler A, Groth, T., Radosch H-J., Evaluation of polymer blends comprising tackifying resins and thermoplastic elastomers for application as hot melt pressure sensitive adhesives, PolyMerTec 2020. (*Submitted*).

Erklärung

Hiermit erkläre ich, Tâmara Abboud, dass ich die vorliegende Dissertation selbstständig und nur unter Zuhilfenahme der ausgewiesenen Hilfsmittel angefertigt habe. Sämtliche Stellen der Arbeit, die im Wortlaut oder dem Sinn nach gedruckten oder anderweitig veröffentlichten Werken entnommen sind, habe ich durch genaue Quellenangaben kenntlich gemacht. Diese Dissertation wurde an keiner anderen Universität oder Hochschule vorgelegt.

Halle(Saale), 23.10.2019

Tâmara Abboud